

2

NAVAL POSTGRADUATE SCHOOL Monterey, California

AD-A261 719



DTIC
ELECTE
MAR 24 1993
S C D

THESIS

A CLIMATOLOGY OF POLAR LOW
OCCURRENCES IN THE NORDIC SEAS
AND AN EXAMINATION OF KATABATIC
WINDS AS A TRIGGERING MECHANISM

by

Kenneth A. Vos

December 1992

Thesis Advisor

K.L. Davidson

Approved for public release; distribution is unlimited.

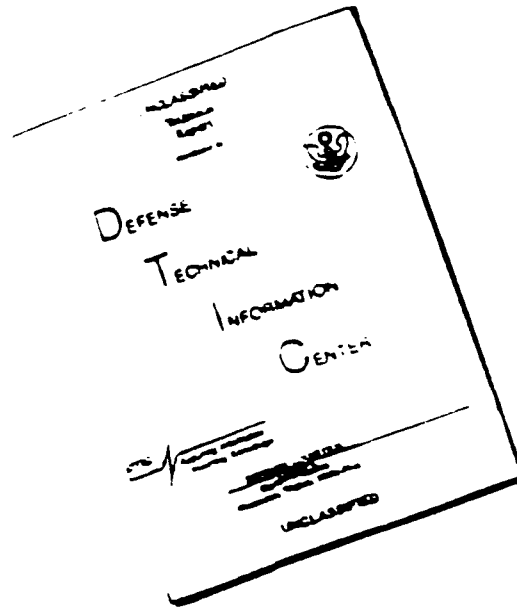
93-05968



15301

93 3 23 013

DISCLAIMER NOTICE



THIS DOCUMENT IS BEST
QUALITY AVAILABLE. THE COPY
FURNISHED TO DTIC CONTAINED
A SIGNIFICANT NUMBER OF
PAGES WHICH DO NOT
REPRODUCE LEGIBLY.

Unclassified

security classification of this page

REPORT DOCUMENTATION PAGE				
1a Report Security Classification: Unclassified			1b Restrictive Markings	
2a Security Classification Authority			3 Distribution Availability of Report	
2b Declassification Downgrading Schedule			Approved for public release; distribution is unlimited.	
4 Performing Organization Report Number(s)			5 Monitoring Organization Report Number(s)	
6a Name of Performing Organization Naval Postgraduate School		6b Office Symbol (if applicable): 35	7a Name of Monitoring Organization Naval Postgraduate School	
6c Address (city, state, and ZIP code) Monterey, CA 93943-5000			7b Address (city, state, and ZIP code) Monterey, CA 93943-5000	
8a Name of Funding Sponsoring Organization		8b Office Symbol (if applicable):	9 Procurement Instrument Identification Number	
8c Address (city, state, and ZIP code)			10 Source of Funding Numbers	
			Program Element No	Project No
			Task No	Work Unit Accounting No
11 Title (include security classification): A CLIMATOLOGY OF POLAR LOW OCCURRENCES IN THE NORDIC SEAS AND AN EXAMINATION OF KATABATIC WINDS AS A TRIGGERING MECHANISM				
12 Personal Author(s): Kenneth A. Wos				
13a Type of Report Master's Thesis		13b Time Covered From To		14 Date of Report (year, month, day) December 1992
15 Page Count 154				
16 Supplementary Notation: The views expressed in this thesis are those of the author and do not reflect the official policy or position of the Department of Defense or the U.S. Government.				
17 Cosat: Codes			18 Subject Terms (continue on reverse if necessary and identify by block number)	
Field	Group	Subgroup	Polar lows, Arctic Meteorology, Greenland, Katabatic.	
19 Abstract (continue on reverse if necessary and identify by block number)				
<p>Existing polar low climatologies for the region from Cape Farewell, Greenland east to Novaya Zemlya, Russia are incomplete. They primarily address storms affecting a particular geographic area or a limited time period. This study examines polar low formation frequency, origin region and storm tracks in the entire Nordic Sea region for a complete polar low season and identify the prevailing synoptic situation common to polar low formation. The number of polar lows detected through TIROS-N satellite imagery between September 1988 and May 1989 was significantly greater than one would expect from previous studies. No minimum wind speed requirement was applied to storm selection, as in some studies. Many polar lows were detected over the land areas of Greenland, Iceland and Svalbard away from a direct surface heat source. The storms detected over Greenland generally formed at the outflows of glacial valleys. Due to 12 hour or greater gaps in satellite imagery each day, storm detection positions were not necessarily those of formation. To determine probable formation areas, polar lows were linearly backtracked along the reciprocal of their storm tracks. A significant number were backtracked to glacier outflows along the Greenland coast. These formation locations suggest a katabatic influence on storm formation, possibly due to vortex stretching, or the enhancement and distortion of an over-ice or over-land boundary layer baroclinic zone. Katabatic flows were examined by analyzing one month of regional surface synoptic observations and NOGAPS 1000 mb height gradients. To develop aids to enhance polar low forecasting, monthly mean 1000 and 500 mb fields for chart times closest to polar low detection, or time backtracked to Northern, Central and Southern Greenland, were calculated from archived NOGAPS 12 hourly analyses and compared to the monthly averaged climatology fields of height and temperature. The overall monthly synoptic patterns for polar lows detected over and backtracked to the three geographic areas were very similar to those for polar lows detected there. There was also significant agreement between the months for the three geographic areas. Both over-land and backtracked storms form in regions of stronger than normal off-shore 1000 mb height gradients. At 500 mb, polar lows forming north of 68 North generally formed under ridges while those south of 68 North formed under troughs.</p>				
20 Distribution Availability of Abstract			21 Abstract Security Classification	
<input checked="" type="checkbox"/> unclassified unlimited <input type="checkbox"/> same as report <input type="checkbox"/> DTIC users			Unclassified	
22a Name of Responsible Individual K. L. Davidson			22b Telephone (include Area code) (408) 656-2563	22c Office Symbol MR Ds

DD FORM 1473, 84 MAR

83 APR edition may be used until exhausted
All other editions are obsolete

security classification of this page

Unclassified

Approved for public release; distribution is unlimited.

A Climatology of Polar Low
Occurrences in the Nordic Seas
and an Examination of Katabatic
Winds as a Triggering Mechanism

by

Kenneth A. Vos
Lieutenant Commander, United States Navy
B.S., State University of New York, College at Oswego, 1979

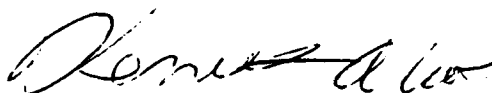
Submitted in partial fulfillment of the
requirements for the degree of

MASTER OF SCIENCE IN METEOROLOGY AND PHYSICAL
OCEANOGRAPHY

from the

NAVAL POSTGRADUATE SCHOOL
December 1992

Author:

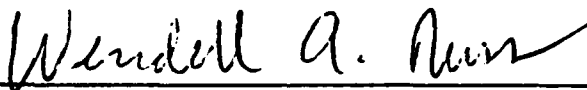


Kenneth A. Vos

Approved by:



K.L. Davidson, Thesis Advisor



W.A. Nuss, Second Reader



Robert L. Haney, Chairman,
Department of Meteorology

ABSTRACT

Existing polar low climatologies for the region from Cape Farewell, Greenland east to Novaya Zemlya, Russia are incomplete. They primarily address storms affecting a particular geographic area or a limited time period. This study examines polar low formation frequency, origin region and storm tracks in the entire Nordic Sea region for a complete polar low season and identifies the prevailing synoptic situation common to polar low formation. The number of polar lows detected through TIROS-N satellite imagery between September 1988 and May 1989 was significantly greater than one would expect from previous studies. No minimum wind speed requirement was applied to storm selection, as in some studies. Many polar lows were detected over the land areas of Greenland, Iceland and Svalbard away from a direct surface heat source. The storms detected over Greenland generally formed at the outflows of glacial valleys. Due to 12 hour or greater gaps in satellite imagery each day, storm detection positions were not necessarily those of formation. To determine probable formation areas, polar lows were linearly backtracked along the reciprocal of their storm tracks. A significant number were backtracked to glacier outflows along the Greenland coast. These formation locations suggest a katabatic influence on storm formation, possibly due to vortex stretching, or the enhancement and distortion of an over-ice or over-land boundary layer baroclinic zone. Katabatic flows were examined by analyzing one month of regional surface synoptic observations and NOGAPS 1000 mb height gradients. To develop aids to enhance polar low forecasting, monthly mean 1000 and 500 mb fields for chart times closest to polar low detection, or time backtracked to Northern, Central and Southern Greenland, were calculated from archived NOGAPS 12 hourly analyses and compared to the monthly averaged climatology fields of height and temperature. The overall monthly synoptic patterns for polar lows detected over and backtracked to the three geographic areas were very similar to those for polar lows detected there. There was also significant agreement between the months for the three geographic areas. Both over-land and backtracked storms form in regions of stronger than normal off-shore 1000 mb height gradients. At 500 mb, polar lows forming north of 68 North generally formed under ridges while those south of 68 North formed under troughs.

in For	
CRA&I	<input checked="" type="checkbox"/>
TAB	<input type="checkbox"/>
Unannounced Justification	
By _____	
Distribution /	
Availability Codes	
Dist	Avail and/or Special
A-1	

TABLE OF CONTENTS

I. INTRODUCTION	1
II. BACKGROUND	5
A. POLAR LOW DEFINITION	5
B. CLASSIFICATION AND STRUCTURE OF POLAR LOWS	6
1. Short-Wave Jet Streak Type	6
2. Arctic Front Type	7
3. Cold Low Type	7
4. Scope of This Study	8
C. POLAR LOW CLIMATOLOGY	8
III. ANALYSIS PROCEDURES	14
A. POLAR LOW DETECTION FROM SATELLITE DATA	14
1. Detection by Satellite Imagery	14
2. Other Satellite Detection Sources	15
B. DESCRIPTION OF GEOGRAPHIC AREA	16
C. ANALYSIS FIELDS	16
D. POLAR LOW TRIGGERING MECHANISM	17
1. BAROCLINIC INSTABILITY	17
2. VORTEX STRETCHING	18
3. LOW-LEVEL TROUGH	18
4. UPPER-LEVEL SHORT-WAVE	18
5. BAROTROPIC INSTABILITY	19
E. KATABATIC FLOWS	19
F. KATABATIC FLOWS AND POLAR LOW FORMATION	21
IV. CLIMATOLOGY OF NORDIC SEA POLAR LOWS	28
A. TOTAL POLAR LOW FREQUENCY	28
B. TOTAL POLAR LOW DETECTION DISTRIBUTION	29
C. LIKELY POLAR LOW ORIGIN REGIONS	30
D. CLIMATOLOGY OF KATABATIC INFLUENCES	32

V. SYNOPSIS INDICATORS OF POLAR LOW FORMATION	61
A. SEPTEMBER	63
1. Summary	63
2. Mean Structure	63
3. Greenland North of 72 N.	63
4. Scoresby Sound.	63
5. Greenland South of 68 N.	64
B. OCTOBER	64
1. Summary	64
2. Mean Structure	64
3. Greenland North of 72 N.	65
4. Scoresby Sound.	65
5. Greenland South of 68 N.	65
C. NOVEMBER	66
1. Summary.	66
2. Mean Structure	66
3. Greenland North of 72 N.	66
4. Scoresby Sound.	66
5. Greenland South of 68 N.	67
D. DECEMBER	67
1. Summary.	67
2. Mean Structure	67
3. Greenland North of 72 N.	68
4. Vicinity of Scoresby Sound.	68
5. Greenland South of 68 N.	68
E. JANUARY	69
1. Summary.	69
2. Mean Structure	69
3. Greenland north of 72 N.	69
4. Scoresby Sound.	70
5. Greenland South of 68 N.	70
F. FEBRUARY	70
1. Summary.	70
2. Mean Structure	71
3. Greenland North of 72 N.	71

4. Vicinity of Scoresby Sound.	71
5. Greenland South of 68 N.	71
G. MARCH	72
1. Summary.	72
2. Mean Structure	72
3. Greenland North of 72 N.	72
4. Scoresby Sound.	73
5. Greenland South of 68 N.	73
H. APRIL	74
1. Summary.	74
2. Mean Structure	74
3. Greenland North of 72 N.	74
4. Scoresby Sound.	74
5. Greenland South of 68 N.	75
I. MAY	75
1. Summary.	75
2. Mean Structure.	75
3. Greenland North of 72 N.	76
4. Scoresby Sound.	76
5. Greenland South of 68 N.	76
J. INTERPRETATIONS OF RESULTS	77
1. Northern Greenland	78
2. Scoresby Sound	81
3. Southern Greenland	82
4. Summary	84
VI. CONCLUSIONS	123
A. FORMATION FREQUENCY	123
B. LACK OF SENSIBLE HEAT SOURCE	123
C. POLAR LOW SYNOPTIC CONDITIONS	123
D. KATABATIC FLOW AS A TRIGGERING MECHANISM	124
E. RELATION TO CYCLOGENESIS THEORIES	124
VII. RECOMMENDATIONS	125
A. POLAR LOW FORMATION FREQUENCY	125

B. POLAR LOW WIND SPEED	125
C. DETECTION OF KATABATIC FLOW	125
D. REPEATABILITY	125
APPENDIX CYCLOGENESIS MECHANISMS	126
A. THERMAL INSTABILITY	126
B. BAROCLINIC INSTABILITY	126
C. CONVECTIVE INSTABILITY OF THE SECOND KIND	127
D. AIR-SEA INTERACTION INSTABILITY	128
E. BAROTROPIC INSTABILITY	129
REFERENCES	134
INITIAL DISTRIBUTION LIST	138

LIST OF TABLES

Table 1.	STORMS DETECTED OVER LAND	28
Table 2.	POLAR LOW DETECTION AREAS AND STORMS IMPACTING NORWAY	30
Table 3.	POLAR LOW LIFETIMES	31
Table 4.	STORMS BACKTRACKED TO LAND AREAS	31
Table 5.	STORMS BACKTRACKED UNDER 1000 KM TO GREENLAND, ICELAND AND SVALBARD	32
Table 6.	AVERAGE DISTANCE STORMS BACKTRACKED TO LAND ...	33
Table 7.	APRIL STORMS WITH KATABATIC INFLUENCES	34
Table 8.	STORMS ORIGINATING OVER OR BACKTRACKED TO GREENLAND	62
Table 9.	STORMS DETECTED OVER NORTHERN GREENLAND	78
Table 10.	NORTHERN GREENLAND HEIGHT GRADIENTS	79
Table 11.	STORMS BACKTRACKED TO NORTHERN GREENLAND	80
Table 12.	SCORESBY SOUND HEIGHT GRADIENTS	81
Table 13.	STORMS DETECTED OVER SCORESBY SOUND	82
Table 14.	STORMS BACKTRACKED TO SCORESBY SOUND	83
Table 15.	STORMS DETECTED OVER SOUTHERN GREENLAND	84
Table 16.	SOUTHERN GREENLAND HEIGHT GRADIENTS	121
Table 17.	STORMS BACKTRACKED TO SOUTHERN GREENLAND	122

LIST OF FIGURES

Figure 1.	TIROS-N satellite image of a polar low (Rasmussen 1989).	4
Figure 2.	Relation of comma-cloud type polar lows to an extra-tropical cyclone (Businger and Reed 1989).	11
Figure 3.	Polar lows forming in reverse (top) and forward shear (bottom) (Businger and Reed 1989).	12
Figure 4.	Frequency distribution of gale producing polar lows near Norway for 1971-1982 (Wilhelmsen 1985).	12
Figure 5.	Polar lows trajectories for 1978 - 1982 (Lystad 1986).	13
Figure 6.	Significant Nordic Sea location names.	22
Figure 7.	Topography of Southern Greenland (in meters) from SEASAT imagery (Bindschadler et al. 1989).	23
Figure 8.	Direction of maximum slope and lines of converging flow along glacial topography (Bindschadler et al.	24
Figure 9.	Vertical potential temperature (θ) distribution in katabatic flows (Munzenberg et al. 1992).	25
Figure 10.	Wind shear in katabatic flows associated with a) offshore baroclinic zones b) flow distorted over-ice baroclinic zones.	26
Figure 11.	Vertical profiles of wind speed associated with katabatic flows (Parish et al. 1992).	27
Figure 12a.	September polar low detection points with ice edge (upper panel) and storm tracks (lower panel).	35
Figure 12b.	October polar low detection points with ice edge (upper panel) and storm tracks (lower panel).	36
Figure 12c.	November polar low detection points with ice edge (upper panel) and storm tracks (lower panel).	37
Figure 12d.	December polar low detection points with ice edge (upper panel) and storm tracks (lower panel).	38
Figure 12e.	January polar low detection points with ice edge (upper panel) and storm tracks (lower panel).	39
Figure 12f.	February polar low detection points with ice edge (upper panel) and storm tracks (lower panel).	40

Figure 12g. March polar low detection points with ice edge (upper panel) and storm tracks (lower panel).	41
Figure 12h. April polar low detection points with ice edge (upper panel) and storm tracks (lower panel).	42
Figure 12i. May polar low detection points with ice edge (upper panel) and storm tracks (lower panel).	43
Figure 13. Polar low detection points (upper) with storm tracks (lower) for the entire polar low season.	44
Figure 14a. Polar low formation areas in relation to Southern Greenland topography (Bindschadler 1989).	45
Figure 14b. Polar low formation areas in relation to Northern Greenland topography (Frstrup 1966).	46
Figure 15a. September backtracked formation areas and storm tracks with no distance limit (upper) and less than 1000 km (lower).	47
Figure 15b. October backtracked formation areas and storm tracks with no distance limit (upper) and less than 1000 km (lower).	48
Figure 15c. November backtracked formation areas and storm tracks with no distance limit (upper) and less than 1000 km (lower).	49
Figure 15d. December backtracked formation areas and storm tracks with no distance limit (upper) and less than 1000 km (lower).	50
Figure 15e. January backtracked formation areas and storm tracks with no distance limit (upper) and less than 1000 km (lower).	51
Figure 15f. February backtracked formation areas and storm tracks with no distance limit (upper) and less than 1000 km (lower).	52
Figure 15g. March backtracked formation areas and storm tracks with no distance limit (upper) and less than 1000 km (lower).	53
Figure 15h. April backtracked formation areas and storm tracks with no distance limit (upper) and less than 1000 km (lower).	54
Figure 15i. May backtracked formation areas and storm tracks with no distance limit (upper) and less than 1000 km (lower).	55
Figure 16a. Combined storm tracks for polar lows detected over land, backtracked or not backtracked for Sep (upper) and Oct (lower).	56
Figure 16b. Combined storm tracks for polar lows detected over land, backtracked or not backtracked for Nov (upper) and Dec (lower).	57

Figure 16c. Combined storm tracks for polar lows detected over land, backtracked or not backtracked for Jan (upper) and Feb (lower).	58
Figure 16d. Combined storm tracks for polar lows detected over land, backtracked or not backtracked for Mar (upper) and Apr (lower).	59
Figure 16e. Combined storm tracks for polar lows detected over land, backtracked or not backtracked for May (upper).	60
Figure 17a. September climatological NOGAPS fields for 1000 mb (upper) and 500 mb (lower).	85
Figure 17b. September mean 1000 mb (upper) and 500 mb (lower) NOGAPS fields for polar lows detected over Northern Greenland.	86
Figure 17c. September mean 1000 mb (upper) and 500 mb (lower) NOGAPS fields for polar backtracked to the Scoresby Sound region.	87
Figure 17d. September mean 1000 mb (upper) and 500 mb (lower) NOGAPS fields for polar lows backtracked to Southern Greenland.	88
Figure 18a. October climatological NOGAPS fields for 1000 mb (upper) and 500 mb (lower).	89
Figure 18b. October mean 1000 mb (upper) and 500 mb (lower) NOGAPS fields for polar lows detected over Northern Greenland.	90
Figure 18c. October mean 1000 mb (upper) and 500 mb (lower) NOGAPS fields for polar lows detected over the Scoresby Sound region.	91
Figure 18d. October mean 1000 mb (upper) and 500 mb (lower) NOGAPS fields for polar lows backtracked to Southern Greenland.	92
Figure 19a. November climatological NOGAPS fields for 1000 mb (upper) and 500 mb (lower).	93
Figure 19b. November mean 1000 mb (upper) and 500 mb (lower) NOGAPS fields for polar lows detected over Northern Greenland.	94
Figure 19c. November mean 1000 mb (upper) and 500 mb (lower) NOGAPS fields for polar lows detected over the Scoresby Sound region.	95
Figure 19d. November mean 1000 mb (upper) and 500 mb (lower) NOGAPS fields for polar lows detected over Southern Greenland.	96
Figure 20a. December climatological NOGAPS fields for 1000 mb (upper) and 500 mb (lower).	97
Figure 20b. December mean 1000 mb (upper) and 500 mb (lower) NOGAPS fields for polar lows detected over Northern Greenland.	98

Figure 20c. December mean 1000 mb (upper) and 500 mb (lower) NOGAPS fields for polar lows detected over the Scoresby Sound region.	99
Figure 20d. December mean 1000 mb (upper) and 500 mb (lower) NOGAPS fields for polar lows detected over Southern Greenland.	100
Figure 21a. January climatological NOGAPS fields for 1000 mb (upper) and 500 mb (lower).	101
Figure 21b. January mean 1000 mb (upper) and 500 mb (lower) NOGAPS fields for polar lows detected over Northern Greenland.	102
Figure 21c. January mean 1000 mb (upper) and 500 mb (lower) NOGAPS fields for polar lows detected over the Scoresby Sound region.	103
Figure 21d. January mean 1000 mb (upper) and 500 mb (lower) NOGAPS fields for polar lows detected over Southern Greenland.	104
Figure 22a. February climatological NOGAPS fields for 1000 mb (upper) and 500 mb (lower).	105
Figure 22b. February mean 1000 mb (upper) and 500 mb (lower) NOGAPS fields for polar lows detected over Northern Greenland.	106
Figure 22c. February mean 1000 mb (upper) and 500 mb (lower) NOGAPS fields for polar lows detected over the Scoresby Sound region.	107
Figure 22d. February mean 1000 mb (upper) and 500 mb (lower) NOGAPS fields for polar lows detected over Southern Greenland.	108
Figure 23a. March climatological NOGAPS fields for 1000 mb (upper) and 500 mb (lower).	109
Figure 23b. March mean 1000 mb (upper) and 500 mb (lower) NOGAPS fields for polar lows detected over Northern Greenland.	110
Figure 23c. March mean 1000 mb (upper) and 500 mb (lower) NOGAPS fields for polar lows detected over the Scoresby Sound region.	111
Figure 23d. March mean 1000 mb (upper) and 500 mb (lower) NOGAPS fields for polar lows detected over Southern Greenland.	112
Figure 24a. April climatological NOGAPS fields for 1000 mb (upper) and 500 mb (lower).	113
Figure 24b. April mean 1000 mb (upper) and 500 mb (lower) NOGAPS fields for polar lows detected over Northern Greenland.	114
Figure 24c. April mean 1000 mb (upper) and 500 mb (lower) NOGAPS fields for polar lows detected over the Scoresby Sound region.	115

Figure 24d. April mean 1000 mb (upper) and 500 mb (lower) NOGAPS fields for polar lows detected over Southern Greenland.	116
Figure 25a. May climatological NOGAPS fields for 1000 mb (upper) and 500 mb (lower).	117
Figure 25b. May mean 1000 mb (upper) and 500 mb (lower) NOGAPS fields for polar lows detected over Northern Greenland.	118
Figure 25c. May mean 1000 mb (upper) and 500 mb (lower) NOGAPS fields for polar lows detected over the Scoresby Sound region.	119
Figure 25d. May mean 1000 mb (upper) and 500 mb (lower) NOGAPS fields for polar lows detected over Southern Greenland.	120
Figure 26. Topography of polar low potential wetbulb temperature surfaces in km (Harrold and Browning 1969).	130
Figure 27. Flow relative to a polar low (numbers in arrows are in km) (Harrold and Browning 1969).	131
Figure 28. Vertical cross section of a CISK feedback loop (Rasmussen 1979). . . .	132
Figure 29. Integrated parcel path for ASI moisture advection (Emanuel and Rotunno 1989).	132
Figure 30. Equivalent barotropic atmosphere with geostrophic wind a) increasing and b) decreasing with height (Wallace and Hobbs 1977).	133

I. INTRODUCTION

Polar lows are short-lived, high latitude mesoscale cyclones that are generally thought to form and develop rapidly over the ocean near regions of strong baroclinity. A satellite image of a typical polar low appears in Fig. 1. Polar lows have short lifetimes compared to synoptic-scale storms, usually lasting 6 to 30 hours from formation to dissipation. They are generally associated with cold air outbreaks over warmer water and often result in severe weather conditions with surface winds above gale force and locally heavy precipitation, usually snow. Polar lows do not follow typical synoptic storm tracks, but their motions are not random, which indicates some larger-scale steering mechanisms. Polar lows are difficult to detect and forecast, because they exist in regions with limited observations and are too small to be resolved by all global and most regional numerical weather prediction models.

Polar lows can have devastating impacts on military and civilian operations at high latitudes. Strong wind, often of hurricane force, is the major factor that prevents aircraft operations and may cause damage or injury due to flying debris. High wind speeds generate rough seas that may cause shipboard damage and may lead to vessel icing in cold water regions. This is particularly serious in the Norwegian Sea, which is a productive fishing region. Each year, many small fishing boats are lost due to severe weather. The combination of strong winds and high seas can also damage coastal oil drilling platforms, which has lead the Norwegian oil industry to fund much polar low research. High winds and cold temperatures lead to dangerous wind chill conditions that prevents long-term outdoor work. Low-level wind shear, icing and low visibilities are dangerous to low flying helicopters or anti-submarine warfare (ASW) aircraft that had previously operated in the Nordic Seas during the cold war. The rapid movement of polar lows and their modifying influence on the lower troposphere may significantly change refractive conditions, and thus affect radar detection and counter-detection by military vessels and aircraft. Ice-edge deformation by polar lows may affect ship routing. SST cooling due to the large sensible and evaporative heat fluxes associated with polar lows leads to convective overturning of the water column, which affects the ocean sound velocity and impacts ASW operations.

While U.S. military requirements in the polar regions have diminished, the knowledge of mesoscale phenomena is still important to improve the safety of

commercial shipping, fishing vessels and petroleum industry operations. The Nordic Seas are situated at the northern edge of the major shipping route between North America and Europe, contain some of the world's most productive fishing grounds and contain significant petroleum reserves. The need for improved forecasting tools was made evident to the author during a tour of duty at Keflavik, Iceland which experienced several polar low passages and near misses. Because of the rapid storm movement, operational forces and local residents did not always have sufficient warning time to ensure proper safety.

Previous polar low studies in the Nordic Seas concentrated on storms that affected coastal Norway. The concentration on this area is understandable, since most of the researchers were Norwegian. Much of the research was funded by the Norwegian oil industry who sought to improve polar low forecasting to protect offshore oil operations (Lystad 1986). Wilhelmssen (1985) compiled the first climatology of polar lows in the Nordic Seas. Follow on studies by Businger (1985) and Eise et al. (1988) still concentrated on Norwegian storms, dealing with storm termination regions, rather than origin regions. Less research has been completed on storms in the vicinity of Greenland and Iceland which are the main focus of this thesis.

Polar low formation has been described as a two stage process by Harrold and Browning (1969), Rasmussen (1979) and Emanuel and Rotunno (1989). First, a "triggering mechanism", usually a low- to mid-level cyclonic vorticity disturbance destabilizes the normally stable arctic lower troposphere (Rasmussen 1985). As the initial disturbance passes over a strong baroclinic zone, such as one associated with the ice edge, cyclogenesis and rapid intensification occurs as a result of strong sensible heat flux from the relatively warm underlying water. Most polar low research has dealt with the cyclogenesis process rather than the initial triggering mechanism. The trigger was generally assumed to be an upper-level short-wave trough, but many polar lows were observed to form without upper level support. Recent research in Antarctica (Bromwich 1987, 1989 and 1991) has indicated that katabatic flows are a possible polar low triggering mechanism in that area. Greenland is similar to Antarctica; although on a smaller scale; so by extension, katabatic flows may be a polar low triggering mechanism in the Nordic Seas.

The primary objective of this thesis is to expand the polar low climatological data base for storms that form and propagate within the Nordic Sea region. A second, and equally important objective, is to relate polar low genesis areas and storm tracks to surface and upper-air features. The present polar low study uses satellite imagery.

surface and upper air charts and individual surface observations, which are the primary tools available to operational forecasters. This objective will contribute to the improvement of the ability to forecast polar low formation and movement. These forecasting aids are vital to improve the knowledge and predictability of polar lows in order to ensure the safety of naval, military and civilian operations at high latitudes. Visual and infra-red satellite imagery presents a two-dimensional view of the atmosphere, consequently the horizontal, rather than the vertical, polar low structure is emphasized in this study.



Figure 1. TIROS-N satellite image of a polar low (Rasmussen 1989).

II. BACKGROUND

Polar lows form poleward of the main polar front, have horizontal scales less than 1000 km, and usually less than 500 km, and have vertical scales of 1 to 5 km. They are thought to form over or rapidly intensify over the ocean and rapidly dissipate after landfall. Many storms have surface winds above gale force and usually produce heavy snow (Turner et al. 1991).

A. POLAR LOW DEFINITION

Polar lows have been studied in-depth since the early 1970's, but there is no "precise, unambiguous and widely accepted definition" of a polar low (Rasmussen 1992). Researchers also disagree over what to call polar lows, which are also known as arctic lows, arctic antarctic cyclones, comma clouds, arctic instability lows, meso-scale vortices, arctic hurricanes and vortices in the polar airstream. The term polar low has been used since the 1960's as a "catch-all" term to describe widely differing types of mesoscale arctic phenomena which are produced by varying formation mechanisms (Rasmussen 1992). Grouped together were storms with warm or cold cores, comma-cloud or spiral shaped, with sizes between 100 and 1000 km and formed by convective or baroclinic processes.

The first widely accepted polar low definition and description was offered by Reed (1979):

... form most often over the oceans in winter, organizing in regions of low-level heating and enhanced convection and acquiring a comma-shaped cloud pattern as they mature. They are associated with well-developed baroclinity throughout the troposphere and are located on the poleward side of the jet stream in a region marked by strong cyclonic wind shear and by conditional instability through a substantial depth of the troposphere.

A drawback to this comprehensive definition is that it excluded many types of polar lows, such as those with spiral cloud patterns and smaller scale storms confined to the boundary layer well away from the polar front without significant wind shear. Rasmussen (1989) broadened the generally accepted polar low definition to include almost all forms of polar lows:

Polar lows are small scale synoptic or sub-synoptic cyclones that form in the cold air mass poleward of the main baroclinic zone and/or major secondary fronts. They will often be of a convective nature but baroclinic effects may be important.

The drawbacks of this definition are that it did not specify storm size or intensity. Rasmussen (1992) recently presented the following "generic definition":

A polar low is a small, but fairly intense maritime cyclone which forms poleward of the main baroclinic zone (polar front). The horizontal scale of the polar low is approximately between 200 and 700 km, and the surface winds around gale force or above.

This later definition is still not all-encompassing, as it excludes very large- and small-scale storms and imposes a minimum speed requirement that is normally impossible to determine using only satellite imagery.

For the purposes of this study, polar lows are considered to be any closed mesoscale cyclonic circulation occurring poleward of the polar front. This differs from the previously stated definitions in that it imposes no minimum wind speed requirement and does not distinguish between the various polar low formation mechanisms. Mesoscale was considered to be between 100 and 1000 km to follow the common polar low size range.

B. CLASSIFICATION AND STRUCTURE OF POLAR LOWS

Polar lows exist in various forms, so they may be easier to describe than define. Businger and Reed (1989) identify three physically distinct classes of polar lows with differing degrees and distributions of baroclinity, static stability and surface latent and sensible heat fluxes.

1. Short-Wave/Jet Streak Type

The short-wave jet streak type is the largest polar low in size, and is characterized by large meso- or small synoptic-scale comma clouds up to 1000 km in diameter. They develop in regions of enhanced baroclinity just poleward of existing frontal boundaries (Fig. 2) where cold, continental air flows across warm ocean currents, such as off the east coast of Greenland. Storms form in areas of enhanced convection in the heated and moistened boundary layer under regions of strong mid-tropospheric positive vorticity advection (PVA), just ahead of an upper level short-wave or the left front exit region of a jet streak. If the PVA is strong enough, a low develops beneath the comma head and a surface front forms beneath the trough. There is weak to moderate baroclinity in the cold air mass throughout the troposphere. Cloud bands may develop as the comma matures. The bands are parallel to the wind shear vector and do not propagate with the mean flow.

If a comma cloud approaches an existing synoptic front, it may cause a wave to form on the front, but will not always interact with it. If the polar low merges with the front, it may form an "instant occlusion". The comma head provides the occlusion.

while the wave provides the warm and cold fronts. At this point, the system is reclassified as an occlusion, rather than a polar low. If a polar low is absorbed by an existing low on the polar front, extreme pressure falls of 25 mb in 12 hours may occur.

2. Arctic Front Type

Arctic front polar lows, also called boundary layer fronts (Fett, 1989), are small-scale, shallow, boundary layer features that usually form at the ice edge at extremely high latitudes, such as in the Fram Strait and near Svalbard. They are seldom analyzed on operational weather charts due to their small scale and lack of data. They tend to form below 850 mb, without significant PVA aloft, near regions of strong baroclinity where extremely cold air, originating over arctic landmasses or pack ice, flows over relatively warmer water. The storms develop as a result of the strong sensible heat flux. Arctic front polar lows can be detected in satellite imagery by observing the developing cloud streets in the boundary layer air. Strong short-wave jet streak appearing polar lows, with significant vertical development, may form at the southern ends of arctic front polar lows in regions with large relative and potential vorticity. Arctic front polar lows maintain their character when traveling over open water, often persisting from Svalbard to northern Norway.

Shapiro and Fedor (1989) examined an arctic front near the ice edge south of Svalbard in February 1984 using dropwindsondes. The arctic front polar low developed where cold air flowed from the pack ice over warmer open water, transferring sensible heat from the water to the lower atmosphere. Arctic front polar lows may also develop in areas of "reverse shear" where the storm motion is opposite of the thermal wind (Fig. 3), often where warm air is advected over cold pack ice. Polar lows combining short-wave and arctic front characteristics may develop as upper-level short-waves cross the marginal ice zone (MIZ). The amplifying effects of upper-level PVA and low-level baroclinity result in rapidly deepening polar lows with associated strong winds.

3. Cold Low Type

Cold low type polar lows develop within the inner cores of old occlusions or cold-core synoptic lows. They are generally associated with comma- or spiral shaped convective cloud pattern which are often symmetric around clear "eyes" (Businger and Reed 1989). The strongest winds are observed at the surface just outside the eye and decrease with height and radial distance. Deep convection precedes polar low formation and the associated rapid increase in surface vorticity. Cold low types may form in the Nordic seas, but are most often observed in the Mediterranean Sea.

4. Scope of This Study

This study will concentrate on the short-wave jet streak type of polar lows, the most common and most readily identifiable on satellite imagery. Cold-low types are rarely seen at high latitudes and are often difficult to differentiate from the short-wave jet streak type; and are not included here. Arctic front polar lows are shallow, boundary-layer phenomena and are usually detected through observing off-ice convective cloud streets on satellite imagery. Being low-level in nature, they are thought to be independent of upper-level support, so their inclusion in an upper-air climatology could distort results. These storms are only included if significant vertical development, as described by Businger and Reed (1989) and Fett (1989), occurs at the southern end of the arctic front polar low.

C. POLAR LOW CLIMATOLOGY

Nearly all Nordic Sea polar low climatological studies extend work by Wilhelmsen (1985) who presented monthly distributions of polar low formation and storm tracks, examining 71 gale strength storms between 1972 and 1982. The annual polar low season runs from September to April with occasional storms in May and June. Storm frequency is roughly constant in November, December, January and March, but with a distinct minimum in February (Fig. 4), thought to be due to the near-maximum southern sea ice extent and the minimum temperature contrast between the region near Svalbard and Northern Greenland. Wilhelmsen found that most storms originated near Svalbard or in the Barents Sea near strong SST gradients, then traveled at 8-13 m/s over water and 15-20 m/s over land. Storm tracks from 1978 to 1982 are depicted in Fig. 5. If land temperatures were less than -20°C , storms did not make landfall, but tracked parallel to the coast. A drawback to Wilhelmsen's study is that storms with wind speeds less than 15 m/s or storms not observed by Norwegian weather ships or coastal stations were not included.

Businger (1985) examined the synoptic situations involved in 52 of the polar lows studied by Wilhelmsen. Most, but not all, storms formed in areas of cold air advection from north of Svalbard after the passage of a synoptic occlusion through the Norwegian Sea. A strong surface high was located over Greenland. No polar lows were observed to form over land. Businger believed that a polar low triggering mechanism was cyclonic vorticity associated with an upper-level short-wave trough which caused cyclogenesis over the main baroclinic zone associated with the maximum SST gradient.

Using National Meteorological Center (NMC) gridded field data, Businger compiled the average deviations of 500 mb heights and temperatures from climatology for each polar low case and found that polar lows tended to form under areas of abnormally low geopotential heights and temperatures. A 500 mb low, 140 meters below climatology, was located over northern Norway with a long-wave trough extending to the west of Iceland. A 500 mb high, 110 meters above normal, was located in the Davis Strait. Temperatures at 500 mb were 5.5 ° C colder than normal with the minimum centered on an area near Bear Island. A 1000-500 mb thickness low was centered south of Franz Josef Land with a strong gradient over the Norwegian Sea.

Ese et al. (1988) also examined Wilhelmsen's storm cases and further expanded Businger's work. Different upper-level conditions were observed for polar lows forming east and west of 5 degrees East longitude. For the 43 western storms, a 500 mb low, 230 meters below climatology, was located west of Norway with troughs extending west to Scoresby Sound and southeast into the Baltic Sea. A 1000-500 mb thickness low, 162 meters below climatology, was centered over Iceland. For the 31 eastern storms, a 500 mb low, 179 meters below climatology, was centered at North Cape with troughs extending west northwest into the Fram Strait and southwest to east of Iceland. A 1000 - 500 mb thickness low, 124 meters below climatology, was centered west of Bear Island.

Kanestrom et al. (1988) examined surface pressure differences between the Greenland coast and the Norwegian Sea for 53 days of polar low occurrences, examining pressure differences between 20W and 5E along 70N and 20W and 15 E along 75N. For winter polar lows, there was a 20.7 mb surface pressure difference between both sets of points, compared with climatological values of 5.0 mb along 70N and 8.1 mb along 75N. Slightly smaller values were observed for fall and spring polar lows. This strong pressure gradient results in strong northerly geostrophic winds which advect cold air over the relatively warm Norwegian Sea.

Satellite Climatology Studies produce a somewhat different frequency of occurrence for polar lows. Lystad (1986) reports that 14.7 gale producing polar lows per year impacted the Norwegian coast when observed by polar orbiting satellites, compared to 6.4 storms per year reported by Wilhelmsen who relied on surface observations. Due to the short three year time period of the study, Lystad could not determine whether the increase was due to inter-annual variability or the increased detection capabilities of satellite imagery.

Carleton (1985) observed Northern Hemisphere mesoscale vorticies using 12 hour DMSP infra-red mosaic imagery for mid-season months (January, April, July and

October) and found that storm numbers peaked in January and were at a minimum in July. For January 1978 and 1979, 2.1 cyclogenetic, or forming polar lows and 0.8 mature storms were observed per image for the entire hemisphere. In 1978, there were 77 cyclogenetic storms in the North Atlantic region and 52 in 1979. Using the 2.1 to 0.8 ratio, there should be 29 and 20 mature storms respectively, per year. This suggests there were a total of 106 polar lows in January 1978 and 72 in January 1979. Carleton did not specify what bounded his "North Atlantic" region.

Carleton's results indicated that polar low formation frequency was far greater than previous studies indicated. Using only satellite imagery, Carleton did not employ a minimum speed requirement in his climatology as Wilhelmsen did. Carleton identified most North Pacific storms as comma shaped, indicating that moist baroclinic processes dominated in this region, but that spiral forms dominated in the North Atlantic, indicating CISK was the dominant process. Yarnel and Henderson (1989) examined North Pacific polar lows and found that spiral type polar lows tended to form near the land ice edge and comma clouds formed over open water.

Using satellite imagery, this study will examine polar low frequency of occurrence, formation areas and storm tracks in the Nordic Seas between Cape Farewell, Greenland and Novaya Zemlya, Russia for an entire polar low season (September 1988 - May 1989). A primary goal of this study is to build upon the large area scale, but time-limited study by Carleton (1985) and the small area, but seasonal scale study by Wilhelmsen (1985). Because satellite imagery is the primary detection tool, the 15 m/s minimum wind speed criteria used by Wilhelmsen (1985) is not applied to the storms detected here. The climatological results of this study are expected to differ from those of Businger (1985) and Eise et al. (1988) due to the different regions covered and storm selection criteria employed.

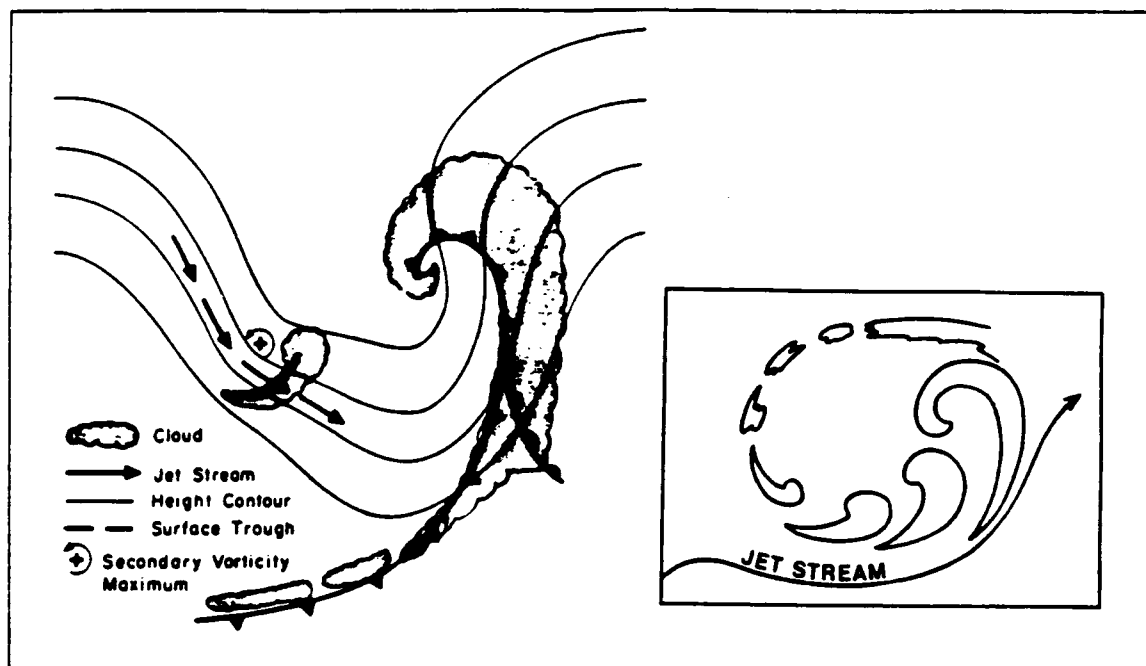


Figure 2. Relation of comma-cloud type polar lows to an extra-tropical cyclone (Businger and Reed 1989).

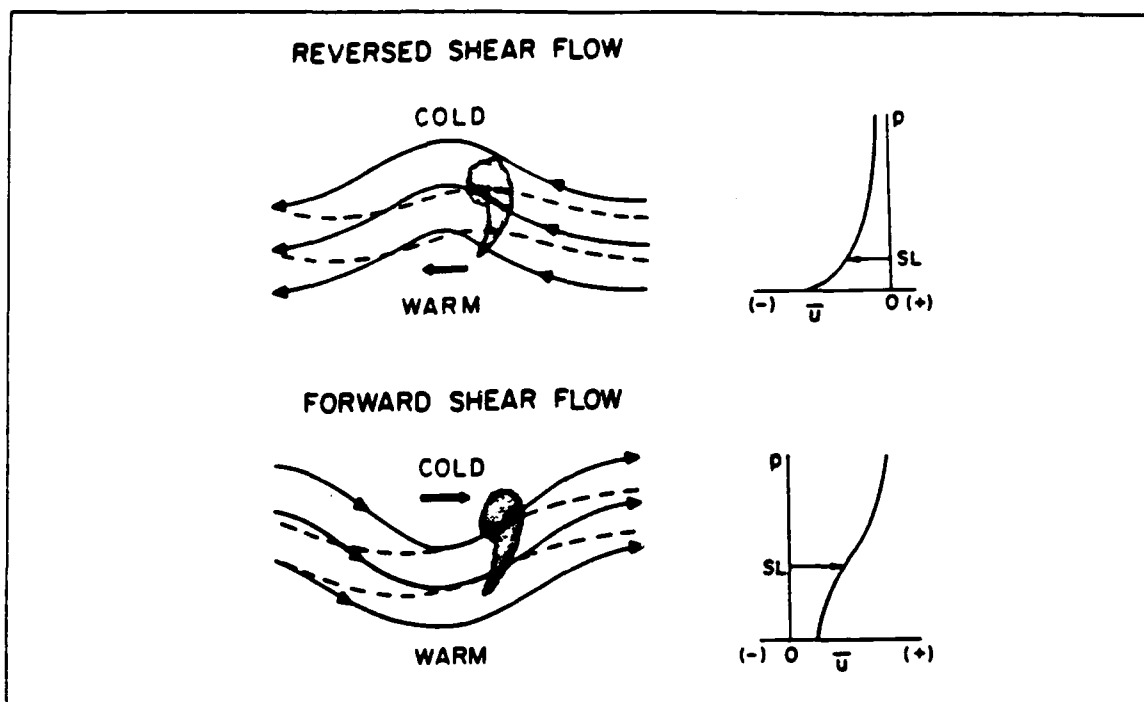


Figure 3. Polar lows forming in reverse (top) and forward shear (bottom) (Businger and Reed 1989).

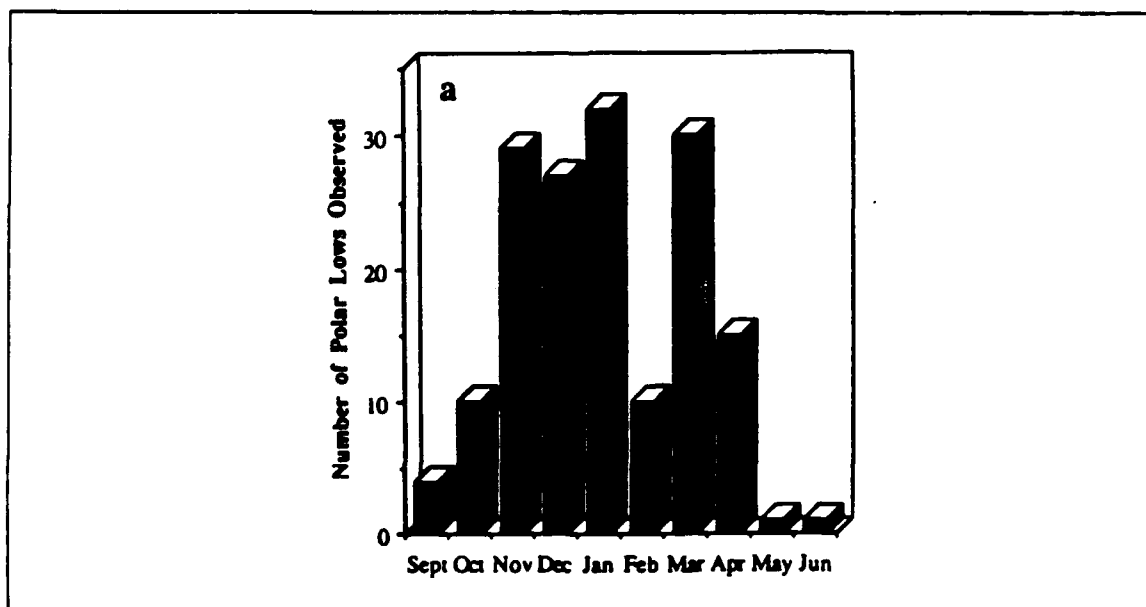


Figure 4. Frequency distribution of gale producing polar lows near Norway for 1971-1982 (Wilhelmsen 1985).

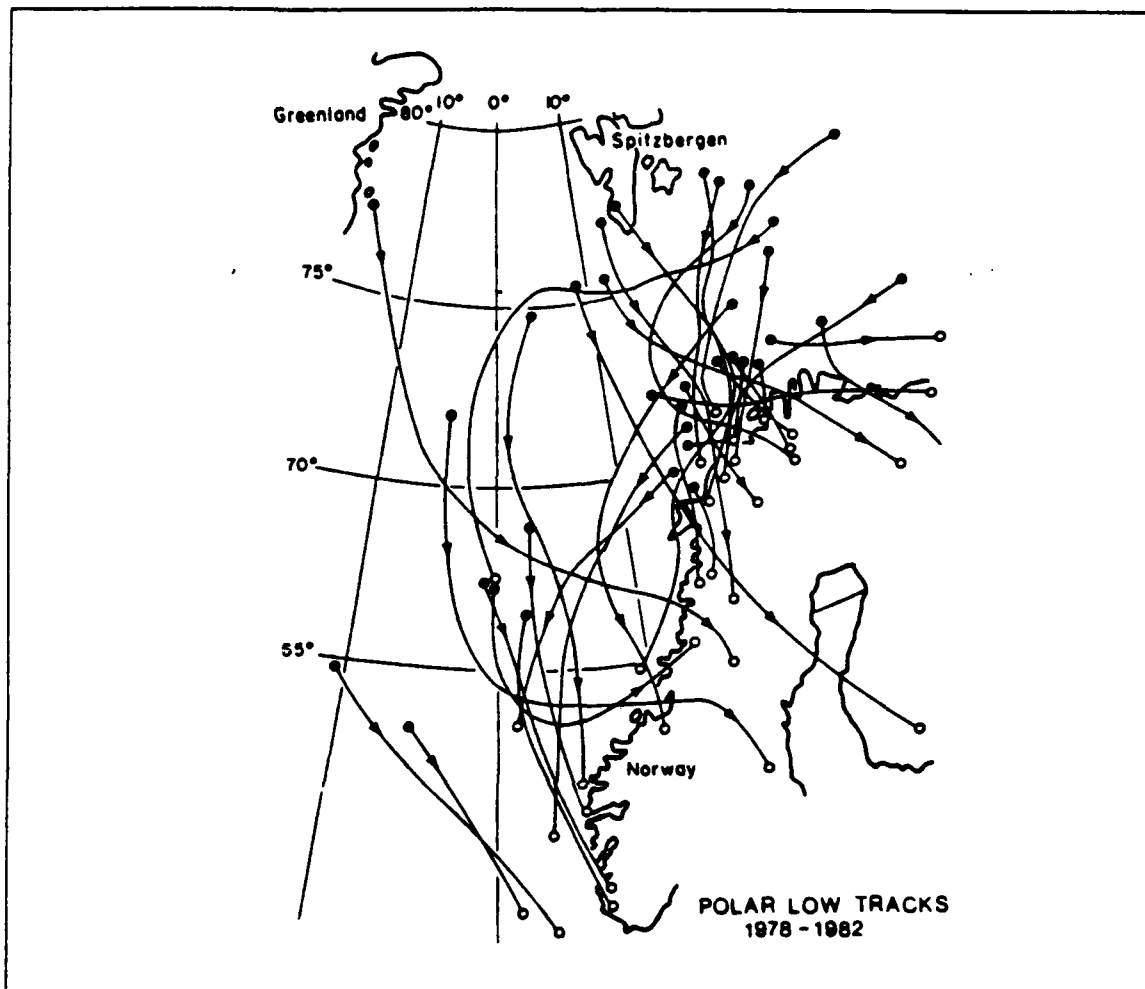


Figure 5. Polar lows trajectories for 1978 - 1982 (Lystad 1986).

III. ANALYSIS PROCEDURES

A. POLAR LOW DETECTION FROM SATELLITE DATA

Satellite imagery is crucial for studying polar low occurrences due to their mainly over-water lifetimes and the sparsity of data in the Nordic Seas (Lystad 1986). Surface and rawinsonde observation densities are not sufficient for the detailed analyses necessary for polar low detection (Rasmussen 1991). In the entire Nordic Sea region, there are 15 rawinsonde stations, 15 automated surface weather observing stations, less than 40 surface synoptic stations, approximately 20 ship reports and a handful of drifting buoys. Detection can be improved by increasing the number of drifting buoys and coastal radar stations. Most early climatological studies are based on storms detected by coastal or shipboard stations, but according to Kenestrom et al. (1988), the number of detected polar lows more than doubles when satellite imagery is used. Between September 1985 and April 1986, 44 gale producing polar lows impacted the Norwegian coast, but a total of 83 strong storms were detected by satellite imagery.

1. Detection by Satellite Imagery

Polar lows normally exist too far north for geostationary satellite coverage, so visual and particularly infrared imagery from polar orbiters is the best way to detect them (Lystad 1986). Real-time TIROS-N Advanced Very High Resolution Radiometer (AVHRR) imagery with 1.1 km resolution is most widely used by operational forecasters since Defense Meteorological Satellite Program (DMSP) imagery is encrypted, and not available to many receiving stations in real time. However, TIROS-N satellites only provide coverage between 0200Z and 1500Z, so storms may form, move and dissipate during the data gap. The two TIROS-N satellites currently operating are in sun-synchronous orbits which view the geographic point at the same time each day. One satellite is timed to provide a local early morning view and the other, a local late afternoon view. At the equator and in low latitudes, each satellite provides one overhead and two edge views per day, but at high latitudes, each provides up to six images per day. Between 1500Z and 0200Z, both satellites are viewing other points of the globe and are out of range of local receiving stations.

The primary satellite imagery was received and archived by the Satellite Receiving Station of the Department of Electrical Engineering, University of Dundee, Scotland, made available to the author by Rasmussen (1991). It consists of TIROS-N

AVHRR visual and infra-red imagery in a reduced scale "proof" format, commonly called the "Dundee Browsefile". Additional TIROS-N AVHRR imagery was received and archived at the Tromso Telemetrystation, Tromso, Norway. It consisted of infra-red imagery that was zoomed to improve coverage of Northeast Greenland, Fram Strait, Svalbard and the Northern Barents Sea.

Many polar low climatological studies employ 12 hour DMSP mosaics with 3.7 km resolution. This method is useful to detect the presence of polar lows, as it provides a large area view. However, it is not as useful for pinpointing storm origin points or establishing storm tracks. A succession of images from a single, or preferably, multiple receiving sites is preferred for detecting and tracking these rapidly forming and moving mesoscale storms.

2. Other Satellite Detection Sources

The combination of the TIROS Operational Vertical Sounder (TOVS), Special Sensor Microwave Imager (SSM I) and radar altimeter shows promise in detecting the early stages of polar low formation. Formation areas are frequently obscured by middle and high clouds which mask low-level disturbances from TIROS-N imagery (Claud et al. 1991). However, data from these sources are not normally available to operational users in real time. SSM I can resolve surface wind speeds to within 2 m s, integrated cloud liquid water and water vapor content and precipitation-sized ice particles in a 1400 km swath with 25-50 km resolution. Altimeters infer surface wind speeds to within 1.8 m s and significant wave heights to within 10 percent in a narrow 10 km footprint. TOVS measures temperature and humidity profiles and cloud top temperatures and pressures in a 2400 km footprint with 17-100 km resolution.

Detection ability is degraded over land or ice, since SSM I and altimeters only resolve wind speeds over open water. SSM I cannot detect wind speeds beneath precipitation or heavy cloud liquid water. Altimeters cannot accurately infer winds at the center of storms where seas are not fully developed. TOVS is also degraded in areas of precipitation.

Other systems, such as Synthetic Aperture Radar (SAR) which derives sea heights and measures sea ice deformation and scatterometers which can derive wind speeds and directions also show promise in detecting polar lows (Shuchman, 1992), but are not normally available to operational forecasters. The European Space Agency plans to provide ERS-1 scatterometer and radar-altimeter derived winds to subscribers within three hours of real time receipt.

B. DESCRIPTION OF GEOGRAPHIC AREA

The geographic area dealt with in this thesis corresponds to the area covered by the satellite coverage received at Dundee, Scotland and Tromso, Norway. The area extends from Cape Farewell, Greenland east to Novaya Zemlya, Russia and from Ireland, north to 85 degrees North latitude. Figure 6 depicts the areal coverage and assigns names to geographic features.

Greenland is an ice covered, sub-continental landmass with a maximum elevation of 3100 meters. Figure 7 depicts topography from SEASAT radar altimetry for south of 72 degrees North latitude. It shows broad, gradual sloping inland plateaus with steeply sloping margins. (Topography for north of 72 North will be included when the topographic maps for northern Greenland arrive from DMA.) Seventy five percent of Greenland is above 850 mb and 20 percent is above 700 mb. The margins are cut by steep glacial valleys. Figure 8 shows the direction of maximum slope.

C. ANALYSIS FIELDS

Knowledge of how the specific atmospheric conditions appearing in analyzed fields are related to polar low formation is vital if the ability to forecast storm genesis and movement is to be improved. Forecast aids that relate specific synoptic features to polar low formation are needed. To develop forecast aids, 12 hourly Navy Operational Global Prediction System (NOGAPS) analysis fields, received from the Fleet Numerical Oceanography Center, Monterey, CA (FNOC) were used. The resolution of the archived NOGAPS fields is approximately 320 km. This is not fine enough to resolve the mesoscale polar low circulation, but is sufficient to display the prevailing synoptic situation in which the polar low develops. Since polar lows are low level phenomena, the pressure levels of 1000, 925, 850, 700, 500 and 400 mb were chosen. Environmental parameters selected were ambient air temperatures, vector wind components and deviations from standard heights (D-values).

The raw NOGAPS data are archived in a 12 bit binary format for a 63 x 63 polar stereographic grid for the entire Northern Hemisphere. To convert the data to a usable ASCII format, it was transferred to the Naval Postgraduate School (NPS) IBM mainframe computer where it was transposed to a 8 bit format usable on the the NPS Meteorology Department Interactive Digital Environmental Analysis Laboratory (IDEA LAB) and was reduced to a 15 x 12 data point grid centered on the Nordic Sea region. The D-values were converted to geopotential heights and the wind vectors to

speeds and directions. These grids were used to generate synoptic descriptions as well as synoptic climatologies.

After conversion to the ASCII format, a fortran program summed the parameter values for each level on the 15 x 12 data point local grid and divided them by the number of NOGAPS charts. This resulted in monthly climatology values for each month of the polar low season. The climatology fields were then transferred from the IBM mainframe to the IDEALAB and printed out using the GEMPAK programs.

To develop forecasting aids, the average 1000 and 500 mb height and temperature fields were calculated on the IBM mainframe for polar lows detected over land or those that were backtracked to specific geographic areas. These monthly average polar low synoptic signatures were produced by averaging the data fields for the chart times closest to the time of detection over land or the likely time that a storm backtracked less than 1000 km was formed over land, assuming a constant storm speed of movement. After the average storm fields were calculated, they were transferred to the IDEALAB for display.

D. POLAR LOW TRIGGERING MECHANISM

Triggering mechanisms, the "basic mechanism for all polar low development", (Rasmussen 1985) have been studied less than, but are related to the cyclogenesis processes discussed in Appendix 1. A polar low triggering mechanism is any process that conditions the lower atmosphere so that one of the larger-scale cyclogenesis processes can take over and develop the localized vorticity center into an actual polar low (Fett 1989). Triggering mechanisms can be grouped into two process types:

- Boundary layer heating over a strong low-level baroclinic zone results in upward motion and an increase in low-level vorticity leading to spin-up.
- A localized positive vorticity source, usually low-level, but possibly an upper-level trough causes upward motion over a low-level baroclinic zone, which further increases vorticity, leading to spin-up.

Each of the following triggering mechanisms may provide the low-level cyclonic vorticity necessary for the initial development required by all polar low cyclogenesis theories.

1. BAROCLINIC INSTABILITY

Strong horizontal temperature gradients are often observed between the cold, dry continental air and warm, moist maritime air near the Marginal Ice Zone (MIZ) normally associated with polar low formation. The MIZ is the boundary between solid pack-ice and open water characterized by very strong horizontal temperature gradients

which lead to secondary vertical circulations with upward motion over the warmer water and downward over the colder pack ice. This process reduces the stability of the over-water boundary layer. The horizontal temperature gradients also result in changes in wind speed with height. This vertical wind shear also contributes to low-level baroclinic instability, a formation mechanism discussed by Harrold and Browning (1969).

2. VORTEX STRETCHING

Bromwich (1989) suggests that vertical vortex stretching, associated with katabatic flow in some regions, contributes to polar low formation by supplying the initial low-level cyclonic vorticity in the boundary layer baroclinic zone needed to initiate upward motion and cyclogenesis. Katabatic flows are restricted to lower levels by highly stable inversions aloft. Figure (9) depicts the vertical potential temperature (θ) pattern in a katabatic flow. Potential vorticity tends to be conserved on isentropic surfaces, so the katabatic column is bounded by the fixed θ surfaces, where

$$\text{Potential Vorticity} = (\zeta_0 + f) \frac{\partial \theta}{\partial p}. \quad (\text{Eq. 1})$$

As the katabatic flow descends from higher altitudes to sea level, the thickness of the katabatic layer increases and the θ gradient decreases. Since potential vorticity is fixed, the relative vorticity of the katabatic flow must increase. This increase in low-level cyclonic vorticity leads to polar low development. Munzenberg et al. (1992) modeled vortex stretching as a possible polar low triggering mechanism, but initial results were inconclusive.

3. LOW-LEVEL TROUGH

A low-level trough contains positive vorticity through the cyclonic turning of the wind. If the trough is over water and inverted, with lower pressure to the south, the onshore, reverse shear flow (Fig. 3) flow advects moisture, vorticity and generally warmer air onto the pack-ice. This process concentrates the low-level baroclinic zone and provides the vorticity necessary for storm development.

4. UPPER-LEVEL SHORT-WAVE

The positive vorticity advection (PVA) and warm-air advection ahead of an advancing short-wave trough may be a polar low triggering mechanism. The PVA aloft initiates upward motion over a low-level baroclinic zone that is generally less stable than the surrounding environment due to sensible heating from below. The resulting convergence increases low-level vorticity which tends to spin up a surface low. When the

atmosphere is weakly stratified, the vertical motion may generate moist convection, which causes latent heat release and enhances the development of the surface low.

5. BAROTROPIC INSTABILITY

Horizontal wind shear (Fig. 10a) on either side of an eastward flowing katabatic jet forms regions of cyclonic vorticity to the north of the flow and regions of anti-cyclonic vorticity to the south. This process may be associated with polar low development in some regions. If the sheared katabatic flow extends to a straight baroclinic zone and the shear is strong enough, then barotropic instability may cause a cyclonic vortex in the baroclinic zone. If the katabatic flow distorts the baroclinic zone (Fig. 10b), barotropic instability may generate a cyclonic vortex at the edge of the katabatic flow in the region of greatest shear and strongest thermal gradient.

E. KATABATIC FLOWS

Katabatic winds are boundary layer phenomena that form under a strong temperature inversion at higher, sloping elevations. As the near surface air temperature is reduced by radiational cooling, the denser air is accelerated downslope by gravity. This cold drainage wind is retarded by friction at the surface. Katabatic wind speeds depend on the terrain induced pressure gradient force (PGF) (Bromwich et al. 1992) which is proportional to the steepness of the terrain and the strength of the lower tropospheric inversion. The presence of clouds increases the downwelling long wave radiation, weakening the surface inversion and reducing the speed of the katabatic flow.

The katabatic PGF is directly related to the synoptic situation (Parish et al. 1992). Continental ice caps, such as over the Antarctic and Greenland, are dominated by high pressure where cold, dense air overlies colder ice. Regions of low pressure persist offshore, as observed in the belt of low pressure encircling Antarctica and the persistent Icelandic low in the Denmark Strait. The pressure gradient is generally perpendicular to the topographic slope (Mahrt 1982 and Macklin et al. 1988) and the overall geostrophic flow tends to parallel the coast. The katabatic flow is perpendicular to both the geostrophic flow and the pressure and temperature gradients. Strong katabatic winds are associated with strong geostrophic winds.

Katabatic flow are generally confined to the lowest 400 meters of the boundary layer (Parish et al. 1992). Figure 11 shows low level wind shears for selected wind speeds. At higher wind speeds, the maximum katabatic flow tends to be above the surface, as friction retards the surface flow.

Katabatic winds can be warmer ("Foehn") or cooler ("Bora") than the regions they flow into (Atkinson 1981). Both types are warmed by adiabatic compression, but the environments they flow into are markedly different. Foehn winds are cold mountain winds that warm adiabatically as they descend. They enter extremely cold continental plains, so they appear warmer than their new environment. Bora winds flow into maritime regions where the modifying influence of the water maintains a warm, moist environment. Although the Bora is warmed during descent, it is cooler than its new environment. Off-ice cap katabatic flows are generally of the Bora type, but this is not always apparent from observations.

Katabatic flows are caused by extremely cold, negatively buoyant air descending down glacial valleys. Katabatic flows may appear dark, or warmer than their surroundings on infra-red satellite imagery (Bromwich 1992b and Bromwich and Ganobcik 1992) after they propagate beyond the foot of the terrain slope. The apparent warming is caused by the turbulent mixing of the cold katabatic jet with the warmer air from above the inversion. This results in a band of high wind speed air that appears warmer, but is actually negatively buoyant with respect to the surrounding cold, stratified ice shelf air. These "Katabatic surge events" were observed at the outflow of valleys and glaciers across the Ross Ice Shelf, Antarctica and opened polynias up to 1000 km from their source. Surface warming was detected by automatic weather station (AWS) observations in the flow path. Cold katabatic surges were also observed by satellite imagery and AWS observations, where weak or no inversions were present (Atkinson 1981).

Streten (1963) examined one year of katabatic winds at Mawson, Station Antarctica, observing 118 cases of gravity flows. During the Antarctic summer, katabatic winds are diurnal, with maximum wind speeds corresponding to maximum radiational cooling. During winter, there is no diurnal variation because there is little temperature variation in low light periods. During winter, when strong inversions were present, katabatic flows were warmed by the downward turbulent mixing of warmer air aloft. During summer, with weak or no inversions, katabatic winds are cooler due to downward mixing of colder air aloft. Maximum wind speeds were at 200 meters, showing the effects of friction on the lower levels of these cold, dense gravity winds.

Katabatic flows have a large influence on the structure of boundary layers over glaciers (van den Broeke et al, 1992). Katabatic winds are strongest at night, corresponding to periods of maximum radiational cooling. Winds weaken or are reversed during the day when the maximum heating over the interior ice cap weakens the

downslope pressure gradient. In areas of shallow slope over dry snow fields, convection at maximum heating times causes a downward momentum exchange from the free atmosphere to the boundary layer, so maximum wind speeds are observed during the day.

F. KATABATIC FLOWS AND POLAR LOW FORMATION

Previous to this project, most studies linking katabatic winds to polar lows formation had been conducted by Bromwich, observing Antarctic storms. Bromwich (1987) observed that polar lows form soon after, and close to where strong katabatic winds with speeds of roughly 25 m/s flowed beyond the foot of steep, narrowing glacial valleys onto the Ross Ice Shelf.

Bromwich (1989) suggests that katabatic flows enhance "boundary layer baroclinity" through the convergence of warm, moist air advected onto ice-shelf from open water and the cold, dry continental air associated with katabatic flows. The temperature, moisture and pressure gradients associated with this baroclinic zone are normally parallel to the coast, but are distorted and enhanced by an intense katabatic event. Bromwich (1991) downplays the role of sensible and latent heat flux as major polar low formation mechanism in these storms, as there is little heat flux through the continental margins or the pack-ice. A polar low will form if a low- to mid-level vorticity source, such as a low-level trough, initiates upward motion over the concentrated baroclinic zone.

The majority of Antarctic polar lows formed without synoptic support. The offshore pressure gradient was enhanced by a weak, low pressure trough over open water, which is also the mechanism for onshore moist, warm-air advection. Cloud-free polar lows were also observed through the AWS network, indicating that dry baroclinic processes may also be important. Bromwich observed that upper-level support was not required for initial polar low formation. However, some mechanism, usually a short-wave trough, but often a ridge or divergent flow was needed for the upward motion necessary for full polar low cyclogenesis. Antarctic polar lows were usually observed with warm-air advection between 900 and 500 mb which produces upward vertical motion and enhances upper level divergence to deepen the surface low.

The Greenland Ice Sheet is one of the least studied areas of the Northern Hemisphere (Bromwich et al. 1992c) but Schwerdtfeger (1984) claims that the Greenland Ice Cap is very similar to the Antarctic continent with respect to gravity flows. Because of this, katabatic forces considered with Antarctic polar low formation may apply to storms forming near Greenland.

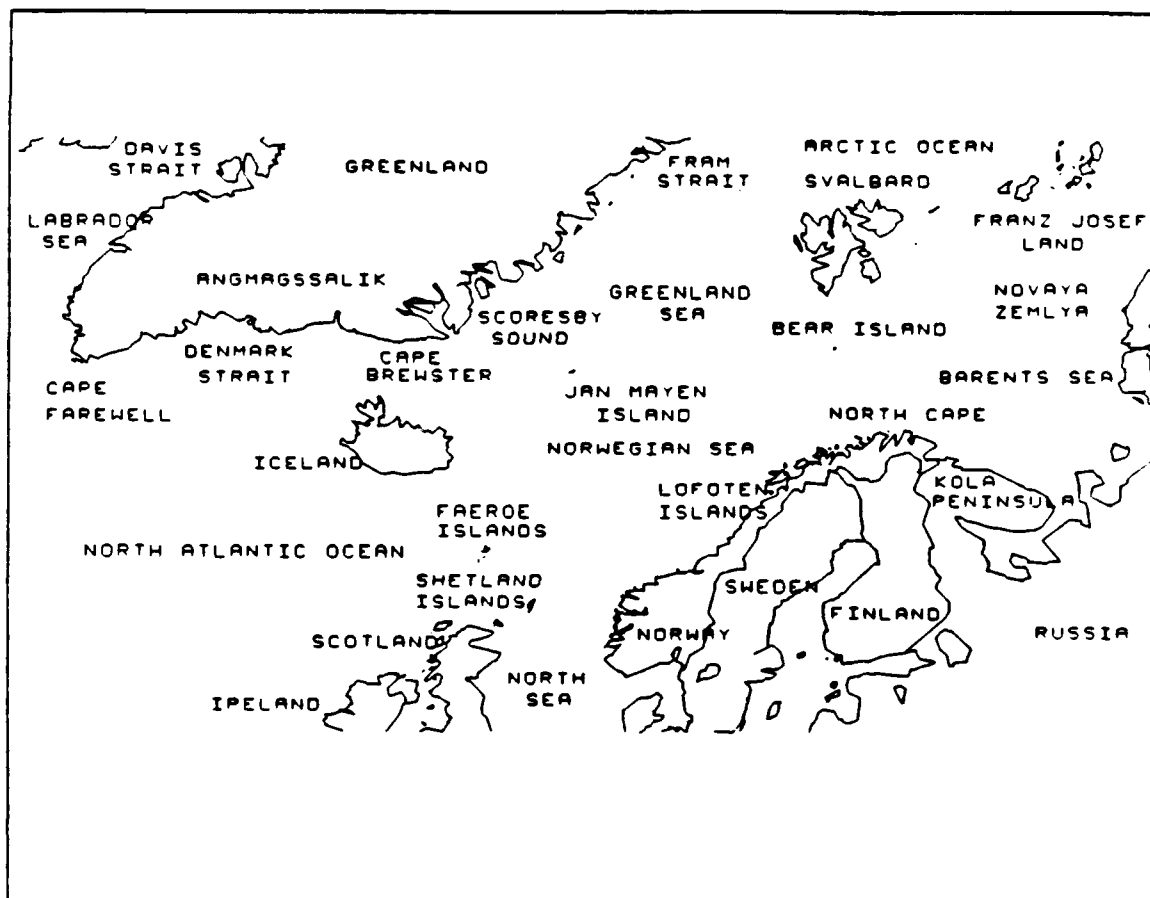


Figure 6. Significant Nordic Sea location names.

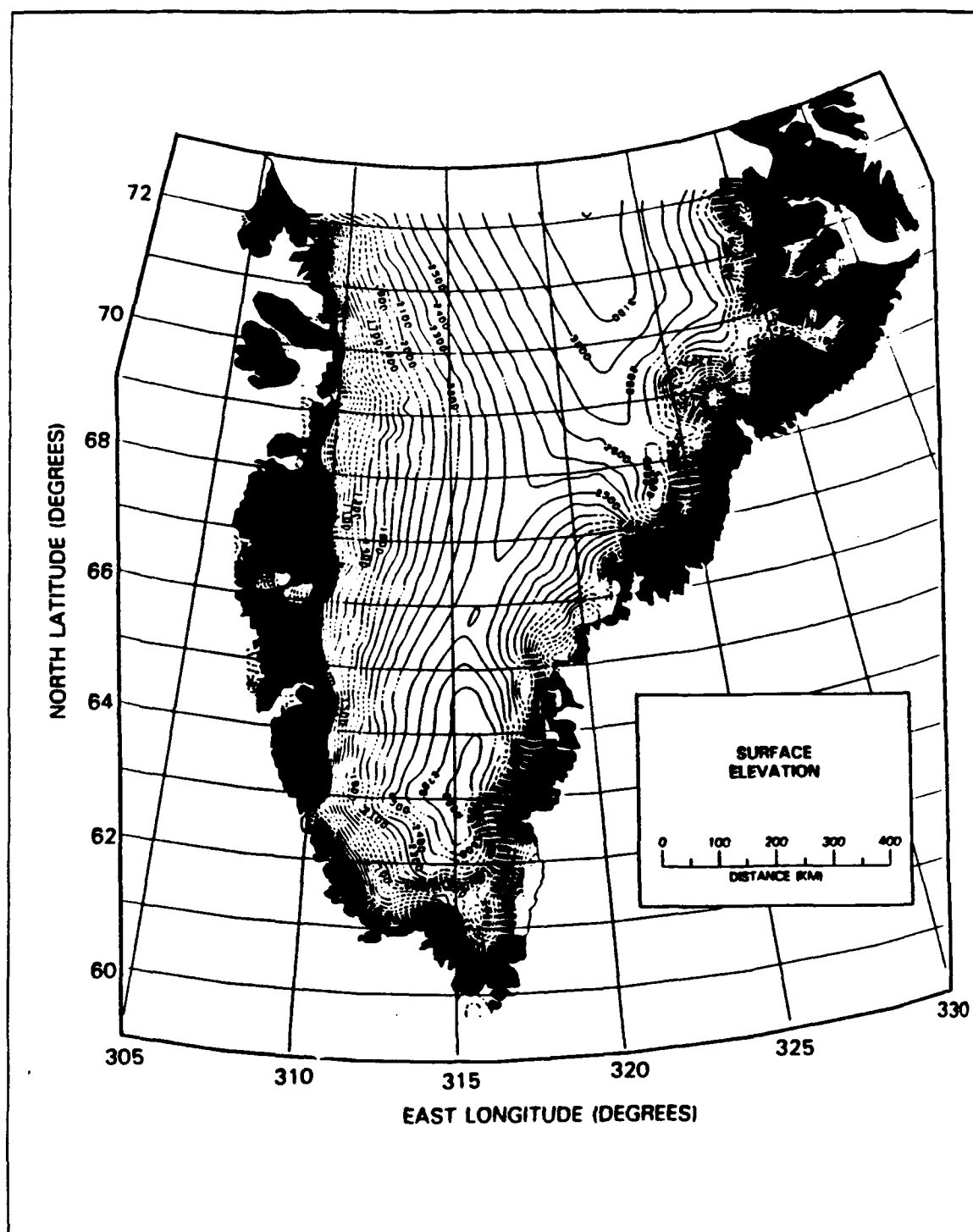


Figure 7. Topography of Southern Greenland (in meters) from SEASAT imagery (Bindschadler et al. 1989).

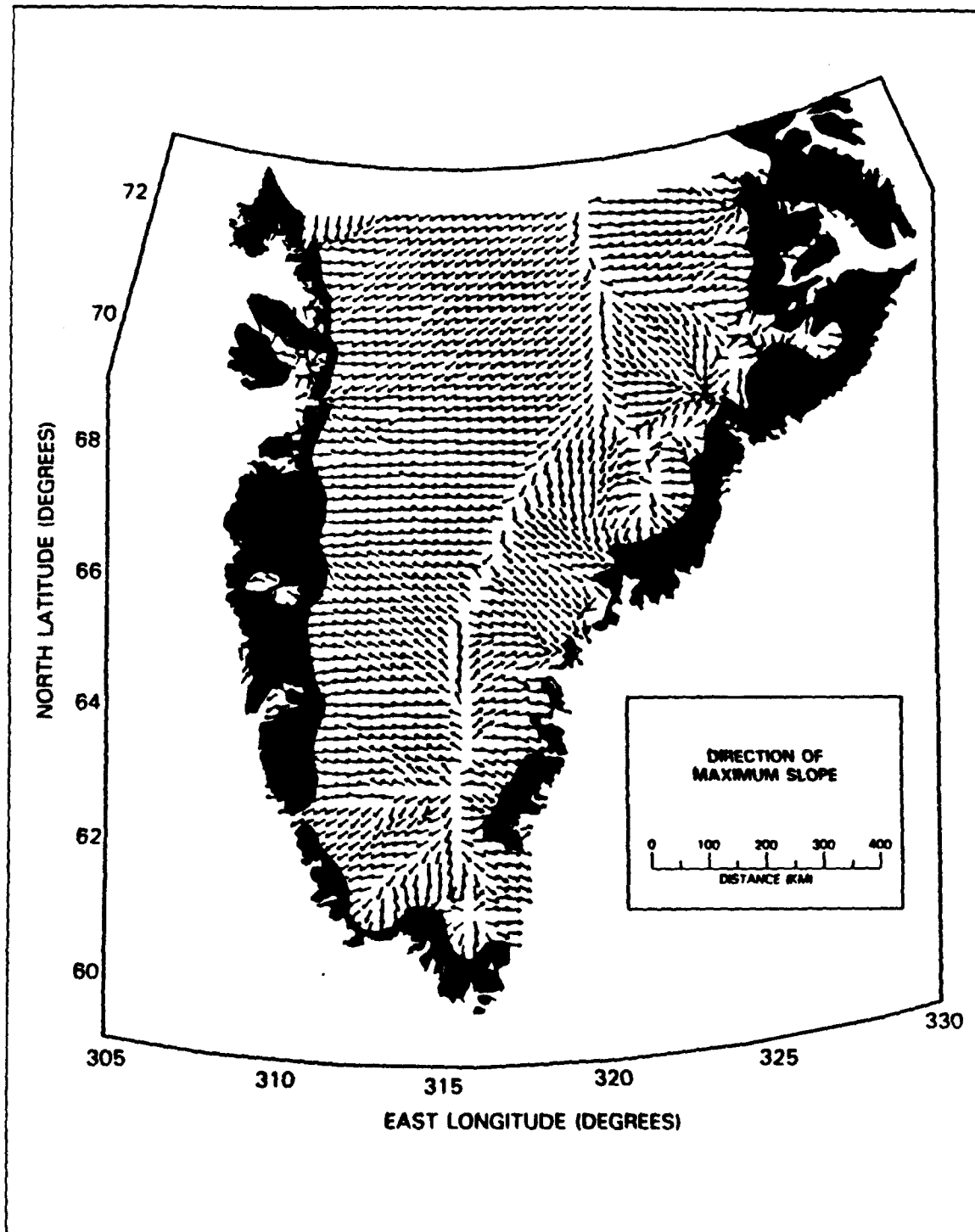


Figure 8. Direction of maximum slope and lines of converging flow along glacial topography (Bindshadler et al. 1989).

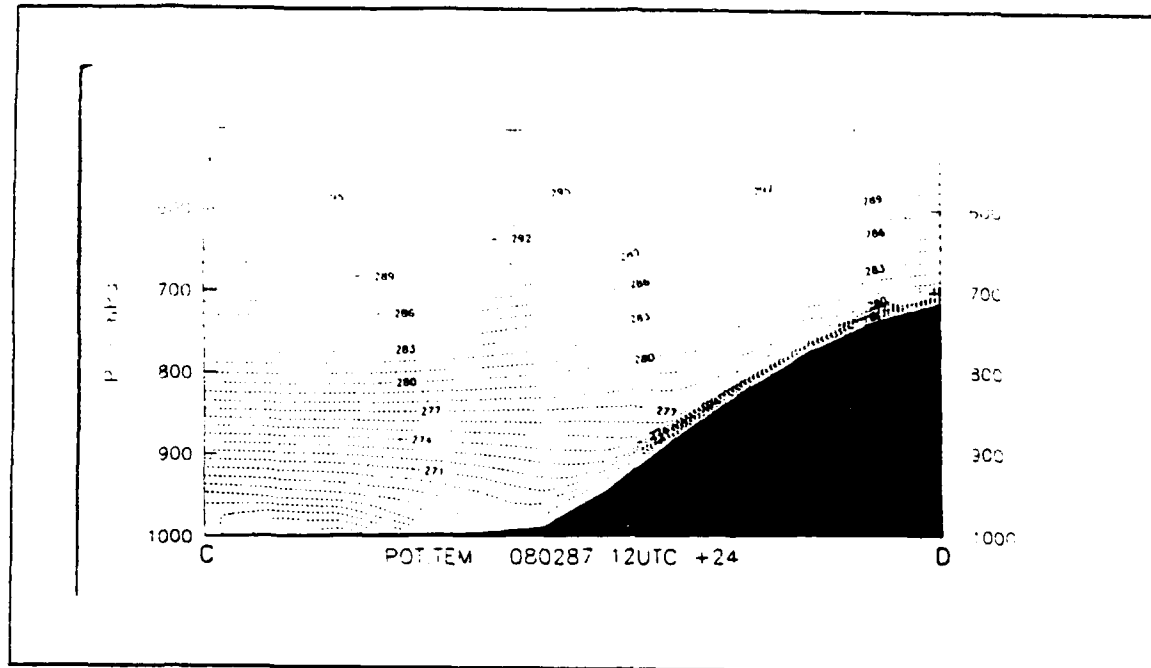


Figure 9. Vertical potential temperature (θ) distribution in katabatic flows (Munzenberg et al. 1992).

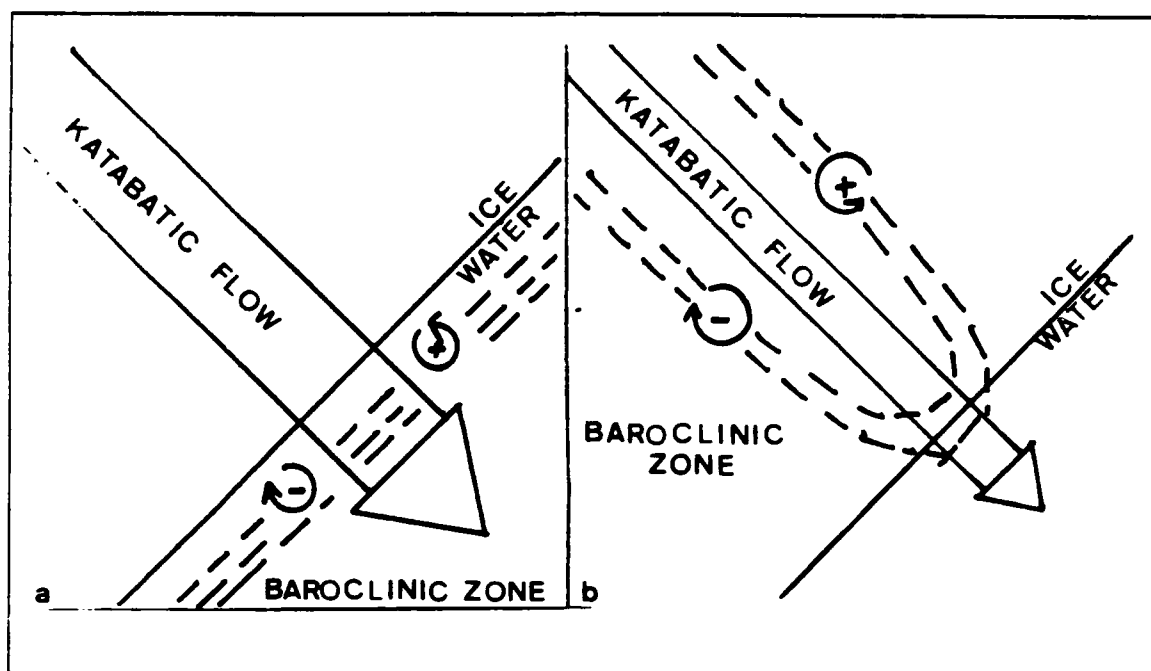


Figure 10. Wind shear in katabatic flows associated with a) offshore baroclinic zones
b) flow distorted over-ice baroclinic zones.

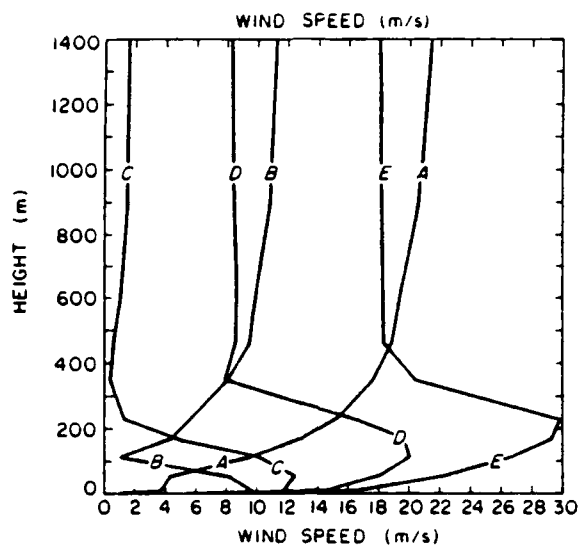
IV. CLIMATOLOGY OF NORDIC SEA POLAR LOWS

A. TOTAL POLAR LOW FREQUENCY

Using the TIROS-N visual and infrared satellite imagery received at Dundee, Scotland and Tromsø, Norway between September 1988 and May 1989, 941 mesoscale storms were detected in the Nordic Sea area of interest. Table 1 gives the total number of storms detected per month from September 1988 to May 1989. These storms were considered to be polar lows since they were all subsynoptic scale cyclonic circulations formed in the cold air poleward of the polar front. No effort was made to derive wind speeds or to determine the formation mechanism. Figures 12a - 12i (upper panel) show monthly detection points in relation to the calculated mean monthly ice edges (Naval Polar Oceanography Center 1988 and 1989). Polar low positions derived from satellite imagery were plotted on daily charts and the positions of the centers of the circulations connected to establish tracks for each storm. Storm tracks were composited by calendar month. Figures 12a - 12i (lower panel) depict monthly detection positions as indicated by each + mark and the subsequent storm tracks that were inferred by connecting the + marks for each storm.

Table 1. STORMS DETECTED OVER LAND

Month	Polar Lows		Origin Over Land		
	Total	Over Land	Greenland	Iceland	Svalbard
Sep	61	5	4	1	0
Oct	127	16	11	3	2
Nov	89	13	10	2	1
Dec	137	17	14	3	0
Jan	94	12	6	4	2
Feb	94	16	9	7	0
Mar	136	11	8	2	1
Apr	113	20	14	6	0
May	90	14	11	3	0
Total	941	124	87	31	6



A - Initial 20 m/s westerly wind, B - Initial 10 m/s westerly wind
 C - No initial pressure gradient, D - Initial 10 m/s easterly wind
 E - Initial 20 m/s easterly wind.

Figure 11. Vertical profiles of wind speed associated with katabatic flows (Parish et al. 1992).

The seasonal total of 941 polar lows is a significantly greater number of storms than expected. Previous studies by Wilhelmsen (1985) and Eise et al., (1988) only considered polar lows observed at Norwegian coastal stations and did not deal with origin regions (Fig. 4 and 5). Wilhelmsen's study also only considered storms with observed wind speeds greater than 15 m s. Wilhelmsen identified 71 polar low cases between 1972 and 1982, but did not include storms occurring over open water which were only detected by satellite imagery. Wilhelmsen's wind speed criteria for what constituted a polar low could not be used in this study because there is no way to consistently and accurately measure wind speeds with detection by satellite imagery.

Carleton (1985) detected 106 and 72 polar lows in the North Atlantic for January 1978 and January 1979 respectively, using only satellite imagery, but did not specify what constituted the "North Atlantic". These numbers compare favorably to the 94 storms detected in the Nordic Seas for this satellite study during January 1989.

B. TOTAL POLAR LOW DETECTION DISTRIBUTION

Several common polar low genesis regions were observed. As seen in Figs. 12a-12i, not all storms were detected near major baroclinic zones, such as the ice edge or over ocean fronts and currents, as was expected. Many polar lows were detected over land or pack ice before moving over open water and intensifying. Table 1 also gives the number of storms detected over glacial regions of Greenland, Iceland and Svalbard. Figure 13a depicts the initial positions of the 124 polar lows detected over land while Fig. 13b presents the subsequent storm tracks of these lows. The 87 polar lows that originated over Greenland were generally observed at the outflow of major glacial drainage basins (Fig. 14a and 14b), suggesting a katabatic formation mechanism. This is in contrast to Businger's (1985) observation that none of 52 gale producing polar lows formed over land.

Table 2 compares the number of polar lows detected over land, pack ice, the MIZ (within 100 km of the ice edge) and over open water. Table 2 also depicts the number of polar lows that either impacted Norway or were moving toward Norway when satellite imagery was not available. The 246 polar lows detected over Norway is a significantly greater number of storms than were detected by Wilhelmsen (1985). However, this study did not employ the 15 m/s minimum wind speed requirement. There were no common formation regions for the storms that impacted Norway. Polar lows that originated in the Fram Strait, Eastern Greenland and south of Iceland all tracked toward the Norwegian Coast.

Table 2. POLAR LOW DETECTION AREAS AND STORMS IMPACTING NORWAY

Month	Total	Storm Detection Areas				Storms Impacting Norway	
		Over Land	Over Ice	100 KM of Ice Edge	Over Open Water	Definite	Probable
Sep	61	5	12	13	31	7	1
Oct	127	16	18	16	77	32	6
Nov	89	13	23	22	31	29	5
Dec	137	17	23	50	47	11	5
Jan	94	12	26	23	33	31	10
Feb	94	16	22	27	29	35	5
Mar	136	11	18	36	71	37	9
Apr	113	20	16	31	46	17	5
May	90	14	12	29	35	17	6
Total	941	124	170	247	400	246	52

Table 3 depicts the lifetime frequency of the 941 detected polar lows. The bimodal nature of the lifetimes with peaks at 6-12 hours and 18-24 hours with a minimum at 12-18 hours is probably due to the interruption in satellite coverage between 1600Z and 0300Z. The majority of the polar lows had lifetimes within the 6-30 hour time frame given by Lystad (1986). Of the 941 detected polar lows, 414 had detected life times of less than 12 hours and 141 less than six hours. This suggests that polar formation frequency may be greater than indicated here since some storm lifetimes are less than the break in satellite coverage.

C. LIKELY POLAR LOW ORIGIN REGIONS

Due to gaps in satellite coverage between 1600 and 0300 Z, polar low detection points are not necessarily their formation points. To find probable formation regions, the storms were backtracked from their detection points along the reciprocal of their initial tracks. A total of 451 storms were linearly backtracked from their detection points to glacial areas on Greenland, Iceland and Svalbard. This suggests that up to 575 storms may have been formed due to katabatic influences. Table 4 depicts the number of polar

Table 3. POLAR LOW LIFETIMES

Mon	Tot	Polar Low Lifetimes In 6 Hourly Blocks									
		One View	< 6	6-12	12-18	18-24	24-30	30-36	36-42	42-48	> 48
Sep	61	6	13	24	0	5	8	4	1	0	0
Oct	127	7	15	43	8	14	21	9	5	3	3
Nov	89	4	9	13	2	18	15	11	4	7	6
Dec	137	6	17	48	5	24	14	12	5	5	1
Jan	94	2	3	23	4	25	15	12	2	4	5
Feb	94	2	12	26	1	25	20	15	6	10	2
Mar	136	6	12	33	1	28	18	18	4	18	7
Apr	113	0	12	21	2	16	22	20	5	13	2
May	90	6	9	22	0	20	6	10	1	12	4
Total	941	39	102	273	23	175	139	105	33	72	30

lows backtracked to land sources per month. Figures 15a - 15i (upper panel) depict likely storm formation areas and subsequent storm tracks.

Table 4. STORMS BACKTRACKED TO LAND AREAS

Month	Total	Number and Fraction Backtracked to Land			
		Total Back-tracked	Greenland	Iceland	Svalbard
Sep	61	38 (.62)	33 (.54)	2 (.03)	3 (.05)
Oct	127	74 (.57)	63 (.48)	5 (.04)	6 (.05)
Nov	89	60 (.67)	54 (.61)	4 (.05)	2 (.02)
Dec	137	84 (.61)	73 (.53)	8 (.06)	3 (.02)
Jan	94	57 (.61)	43 (.46)	7 (.07)	7 (.07)
Feb	94	71 (.75)	55 (.57)	13 (.14)	3 (.03)
Mar	136	73 (.53)	57 (.41)	11 (.08)	5 (.04)
Apr	113	68 (.60)	55 (.49)	11 (.10)	2 (.02)
May	90	50 (.59)	42 (.50)	8 (.81)	0 (.00)
Total	941	575 (.62)	457 (.51)	69 (.07)	31 (.03)

Some storms were linearly backtracked up to 1600 km. After considering Bromwich's evidence of katabatic influences extending up to 1000 km, all cases involving backtracking over 1000 km were rejected. This eliminated 41 of the 451 backtracked storms, leaving 410. Table 5 shows the monthly number of polar lows backtracked up to 1000 km to likely origin locations over Greenland, Iceland and Svalbard. Figures 15a - 15i (lower panel) depict likely storm formation regions and associated storm tracks for polar lows backtracked up to 1000 km. Table 6 depicts the average monthly backtracked distances. The average distance backtracked was 523 km for the unrestricted distance storms and 456 km for the polar lows limited to 1000 km. If storms detected over land are included, the average distance backtracked is reduced to 410 km.

Table 5. STORMS BACKTRACKED UNDER 1000 KM TO GREENLAND, ICELAND AND SVALBARD

Month	Total Lows	Total Lows Backtracked		Number Backtracked Under 1000 km to Land		
		Total	Under 1000 Km	Greenland	Iceland	Svalbard
Sep	61	38	36	31	2	3
Oct	127	74	71	60	5	6
Nov	89	60	57	51	4	2
Dec	137	84	71	65	8	3
Jan	94	57	54	40	7	7
Feb	94	71	65	55	13	3
Mar	136	73	67	51	11	5
Apr	113	68	64	52	11	2
May	90	50	49	41	8	0
Total	941	575	534	446	69	31

Figures 16a - 16i depict combined monthly storm tracks for polar lows detected over land, those backtracked to a likely land origin, as well as the remaining 366 storms that could not be backtracked to a definite land origin point. There is no limit to the backtracked distance in these figures.

D. CLIMATOLOGY OF KATABATIC INFLUENCES

To find evidence of katabatic winds, six hourly surface and ship observations along the East Greenland coast for April 1989 were plotted using the NPS IDEA LAB General

Table 6. AVERAGE DISTANCE STORMS BACKTRACKED TO LAND

Mon	Detected Polar Lows		Backtracked + Over land		Backtracked No Limit		Backtracked Up To 1000 KM	
	Total	Over Land	Num	Dist (Km)	Num	Dist (Km)	Num	Dist (Km)
Sep	61	5	38	416	33	480	31	444
Oct	127	16	74	350	58	447	55	413
Nov	89	12	60	360	48	450	45	404
Dec	137	18	84	536	66	682	53	551
Jan	94	12	57	408	45	517	42	472
Feb	94	16	71	405	55	423	50	442
Mar	136	12	73	460	61	550	55	466
Apr	113	20	68	376	48	532	44	476
May	90	13	50	326	37	440	36	425
Total	941	124	575	410 Km	451	523 Km	411	456 Km

Meteorology Package (GEMPAK) plotting program. Surface observing stations are generally located at the mouths of glacial valleys which open into deep-water fjords, so should indicate the presence of katabatic winds. The following criteria (Mahrt 1982) were used to determine if katabatic winds were coincident with polar low formation:

- Strong off-shore height gradient with synoptic scale geostrophic flow parallel to the coast.
- Low-level subsidence.
- Strong (15 kts or greater) off-shore winds perpendicular to the height gradient within 12 hours of storm detection (or likely formation in the case of backtracked storms).

The temperature of the flow was not used as a factor in determining if the flow was katabatic. Katabatic winds are warmed adiabatically during descent and also by mixing warmer air from above the inversion downward to the surface (Streten 1963), but cooled by heat loss to the underlying glacial ice and by evaporating surface moisture (van den Broeke et al. 1982). The likelihood of katabatic flows were assigned by the following:

- Probable - Offshore height gradient with overall cross-shore flow and subsidence and three strong off-shore wind observations within 12 hours of polar low formation.

- Possible - Offshore height gradient with overall cross-shore flow and subsidence and one observation of strong offshore winds with two or more observations missing.
- Not katabatic - No offshore height gradient, no cross-shore flow or no strong offshore winds with no missing data.
- Unknown - Offshore height gradient with overall cross-shore flow and subsidence, but missing observations.

Results of the katabatic wind examination are presented in Table 7. Of the 56 polar lows detected over or to backtracked Greenland in April 1989, only 17 cases showed probable or possible evidence of katabatic flow.

Table 7. APRIL STORMS WITH KATABATIC INFLUENCES

Location		Total	Probable Katabatic	Possible Katabatic	Not Katabatic	Unknown No Data
North of 72	Origin	5	1	2	2	0
	Backed	23	5	1	10	7
Scoresby Sound	Origin	6	0	0	5	1
	Backed	6	2	1	1	2
South of 68	Origin	10	3	0	5	2
	Backed	6	1	1	3	1

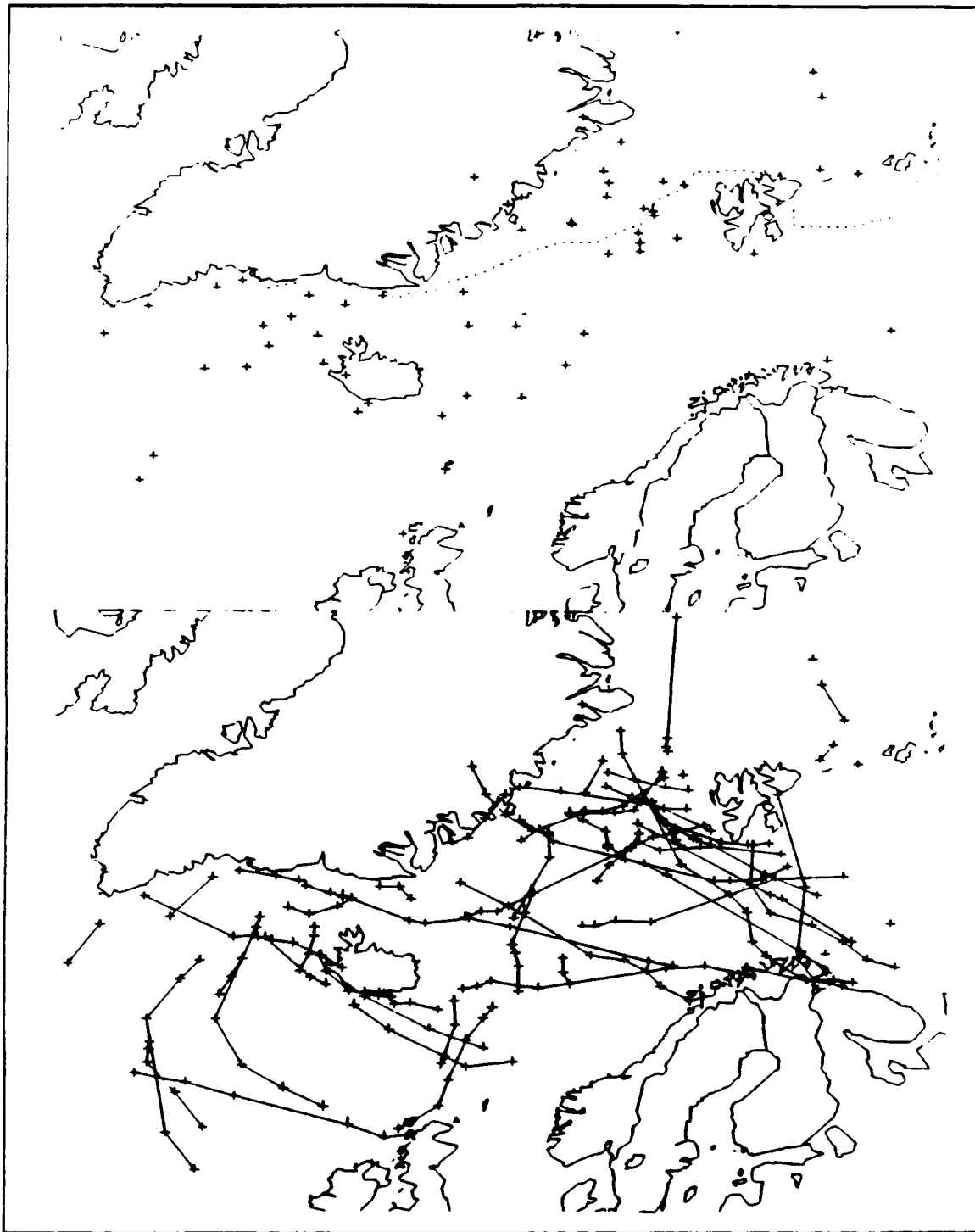


Figure 12a. September polar low detection points with ice edge (upper panel) and storm tracks (lower panel).

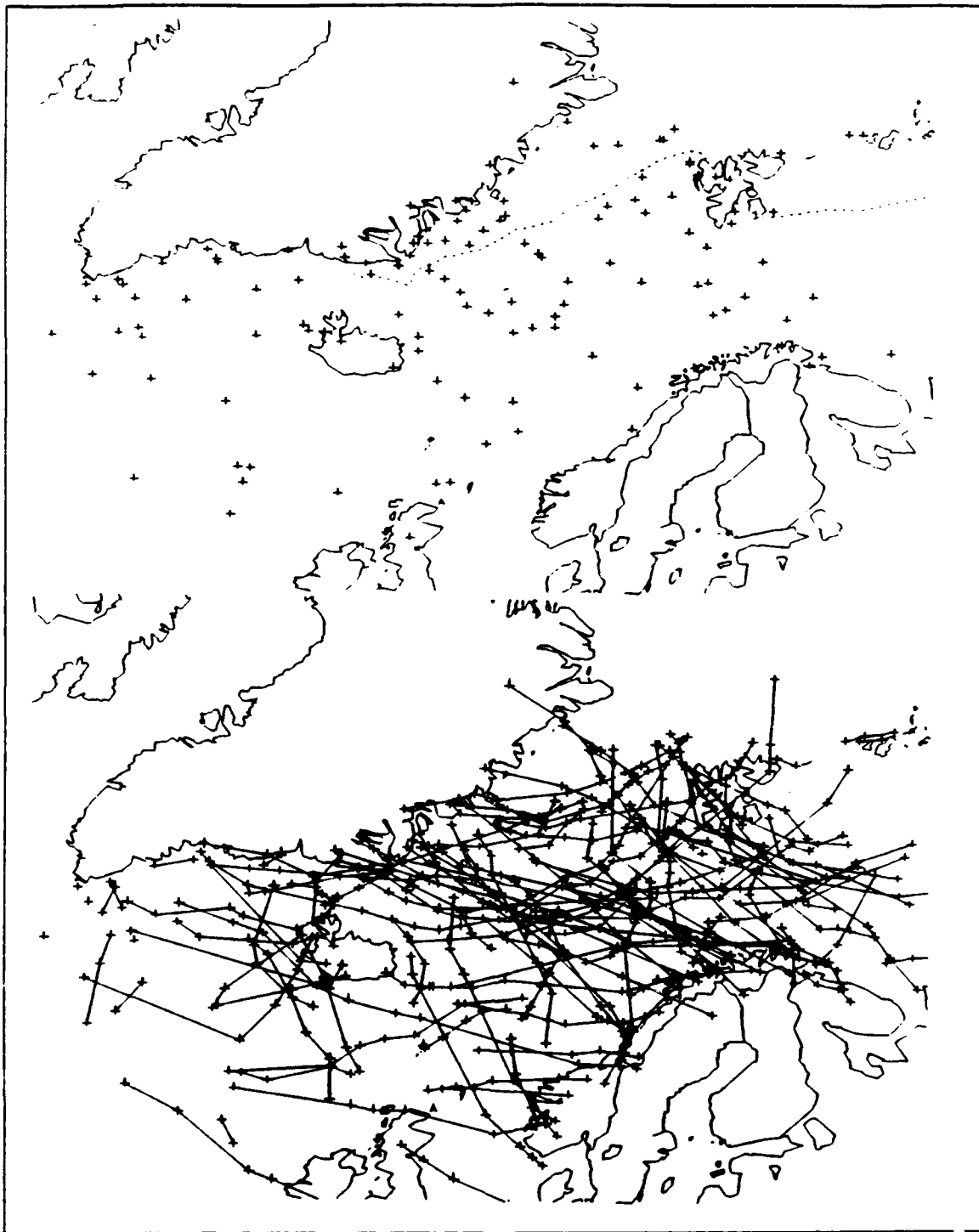


Figure 12b. October polar low detection points with ice edge (upper panel) and storm tracks (lower panel).

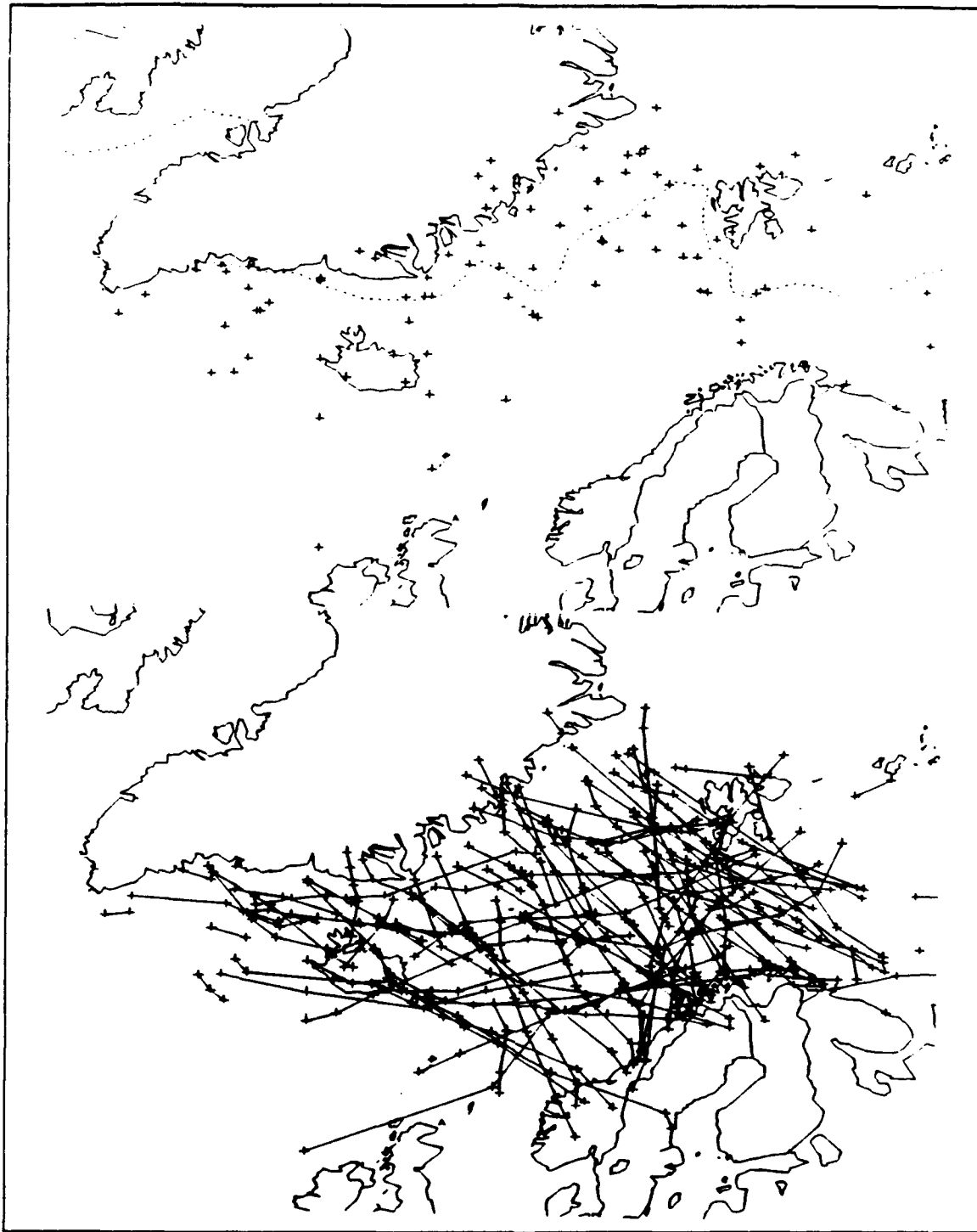


Figure 12c. November polar low detection points with ice edge (upper panel) and storm tracks (lower panel).

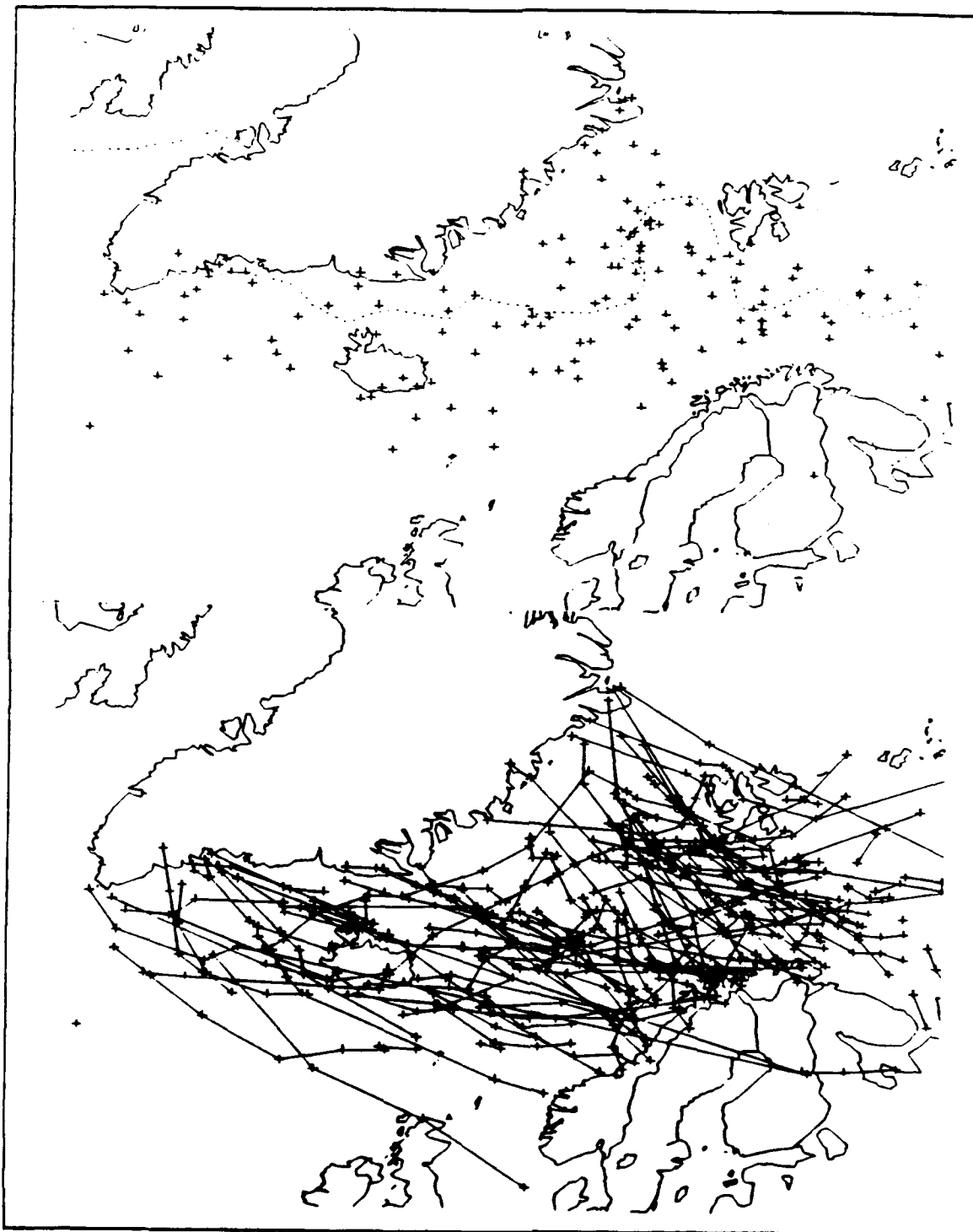


Figure 12d. December polar low detection points with ice edge (upper panel) and storm tracks (lower panel).

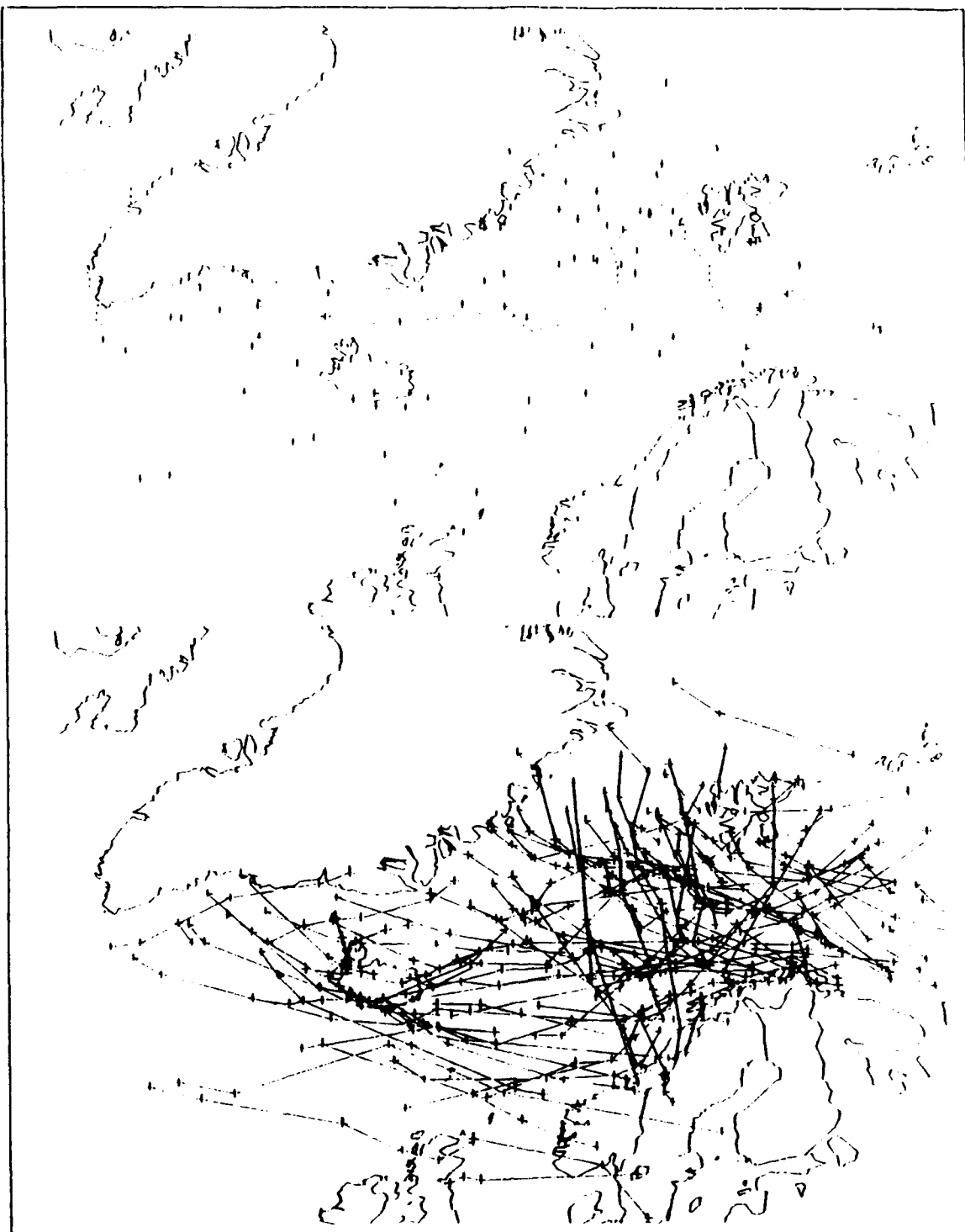


Figure 12e. January polar low detection points with ice edge (upper panel) and storm tracks (lower panel).

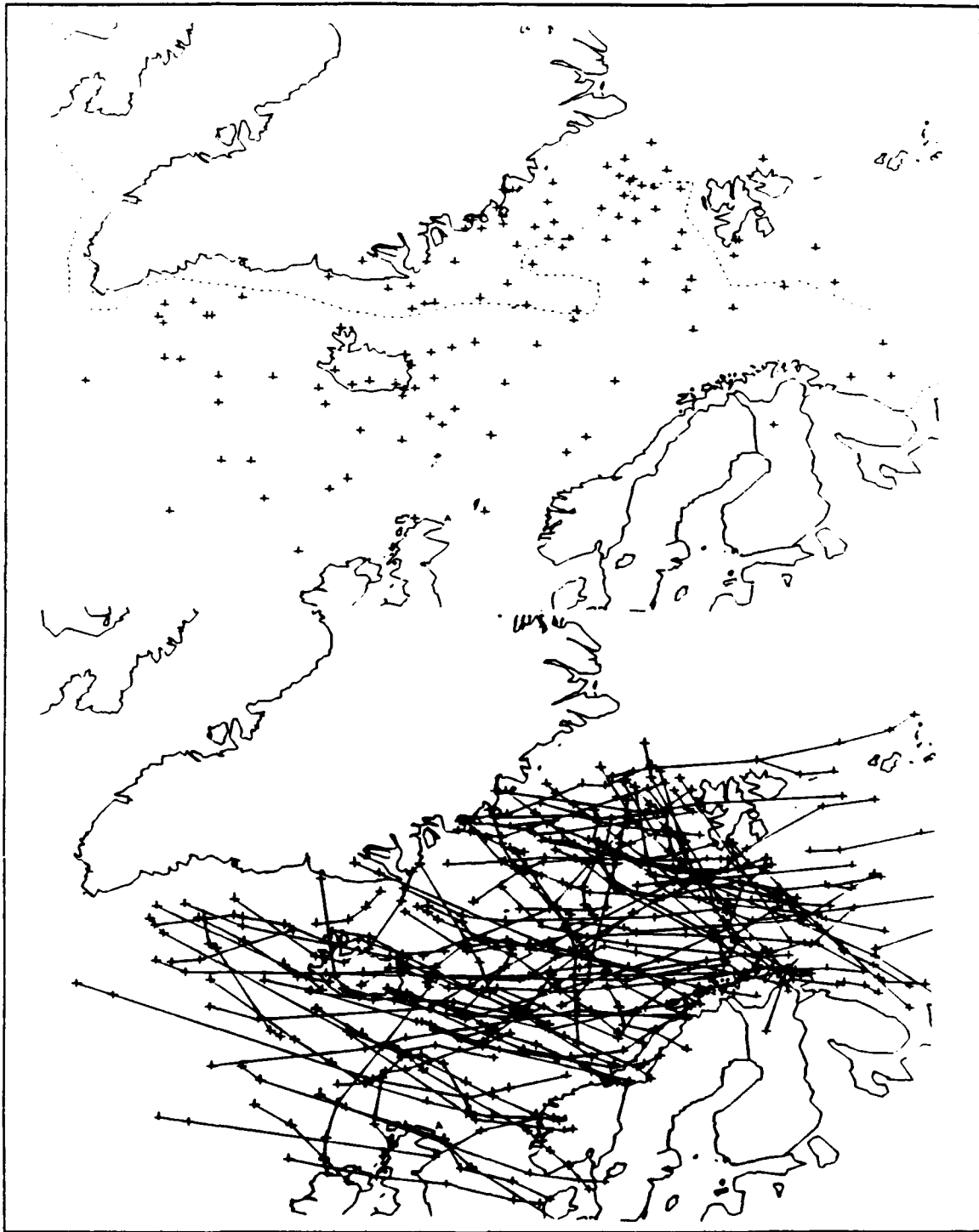


Figure 12f. February polar low detection points with ice edge (upper panel) and storm tracks (lower panel).

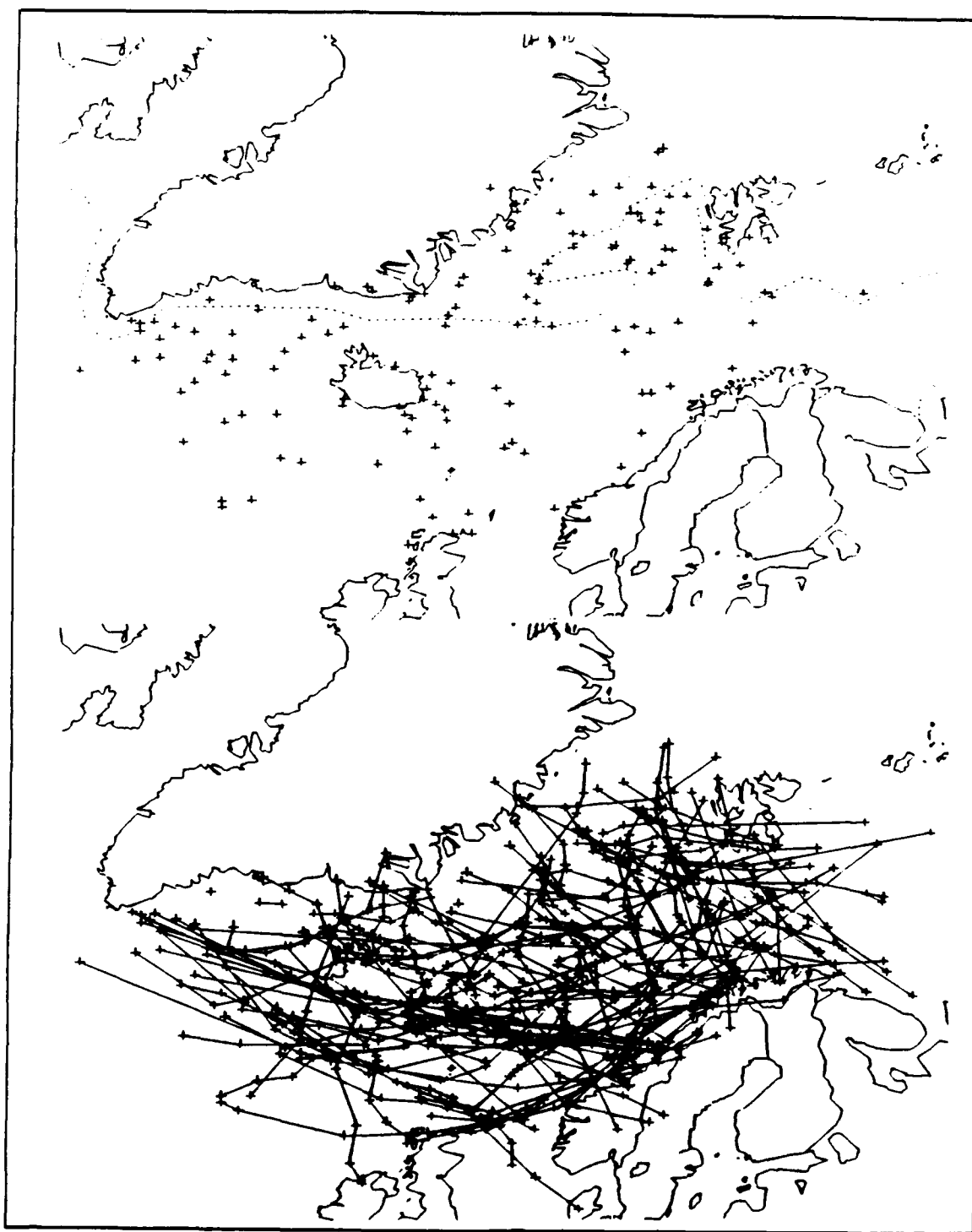


Figure 12g. March polar low detection points with ice edge (upper panel) and storm tracks (lower panel).

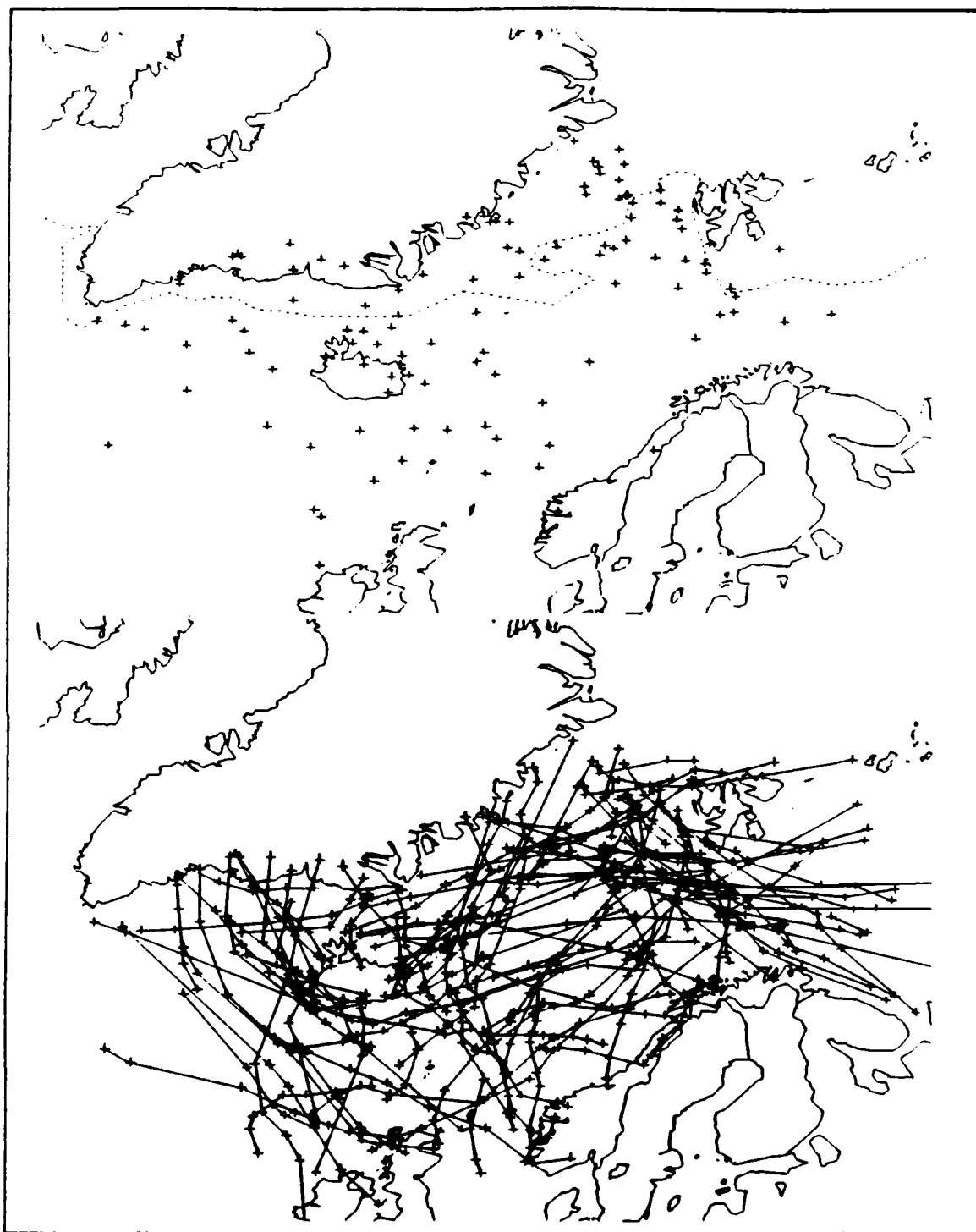


Figure 12h. April polar low detection points with ice edge (upper panel) and storm tracks (lower panel).

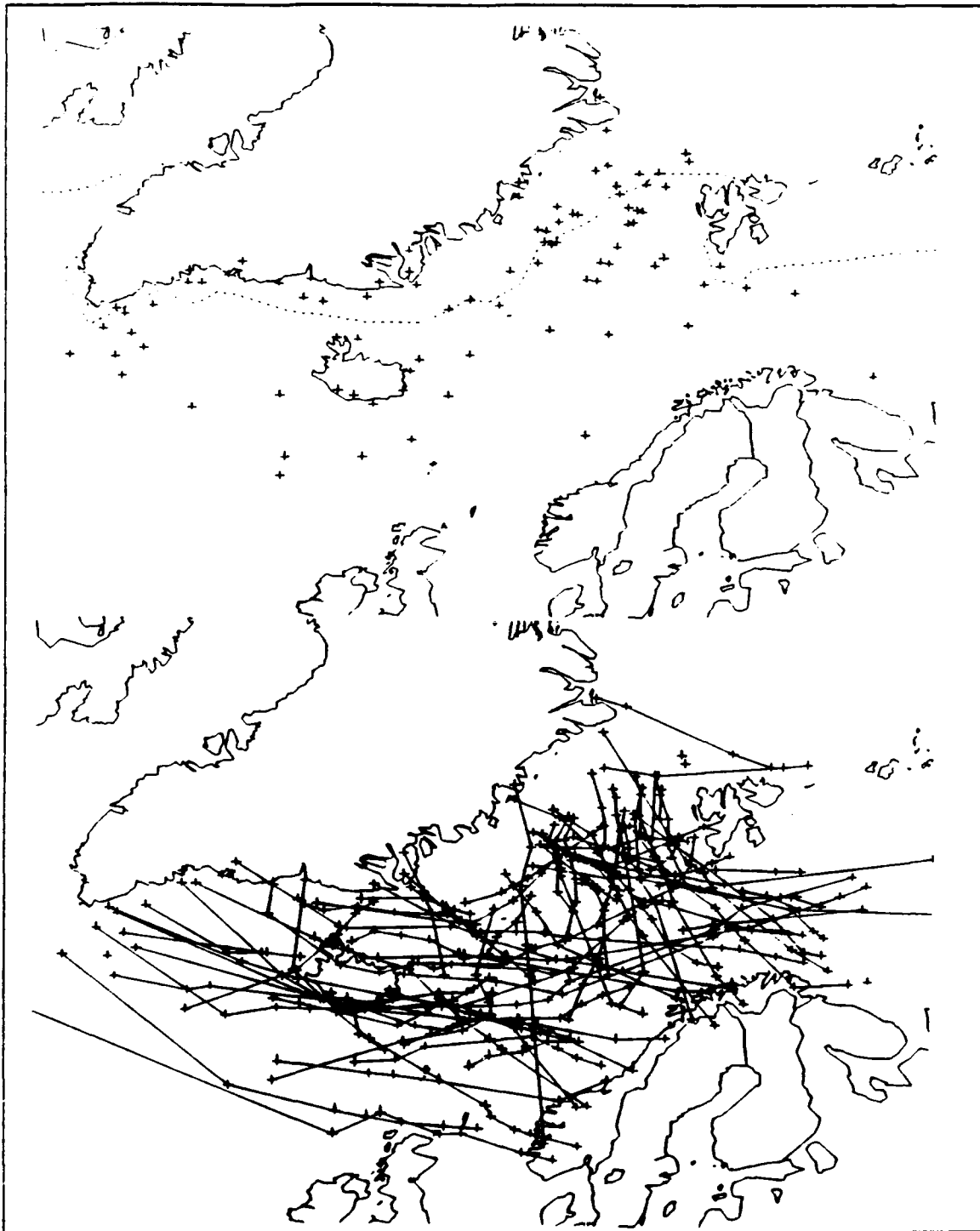


Figure 12i. May polar low detection points with ice edge (upper panel) and storm tracks (lower panel).

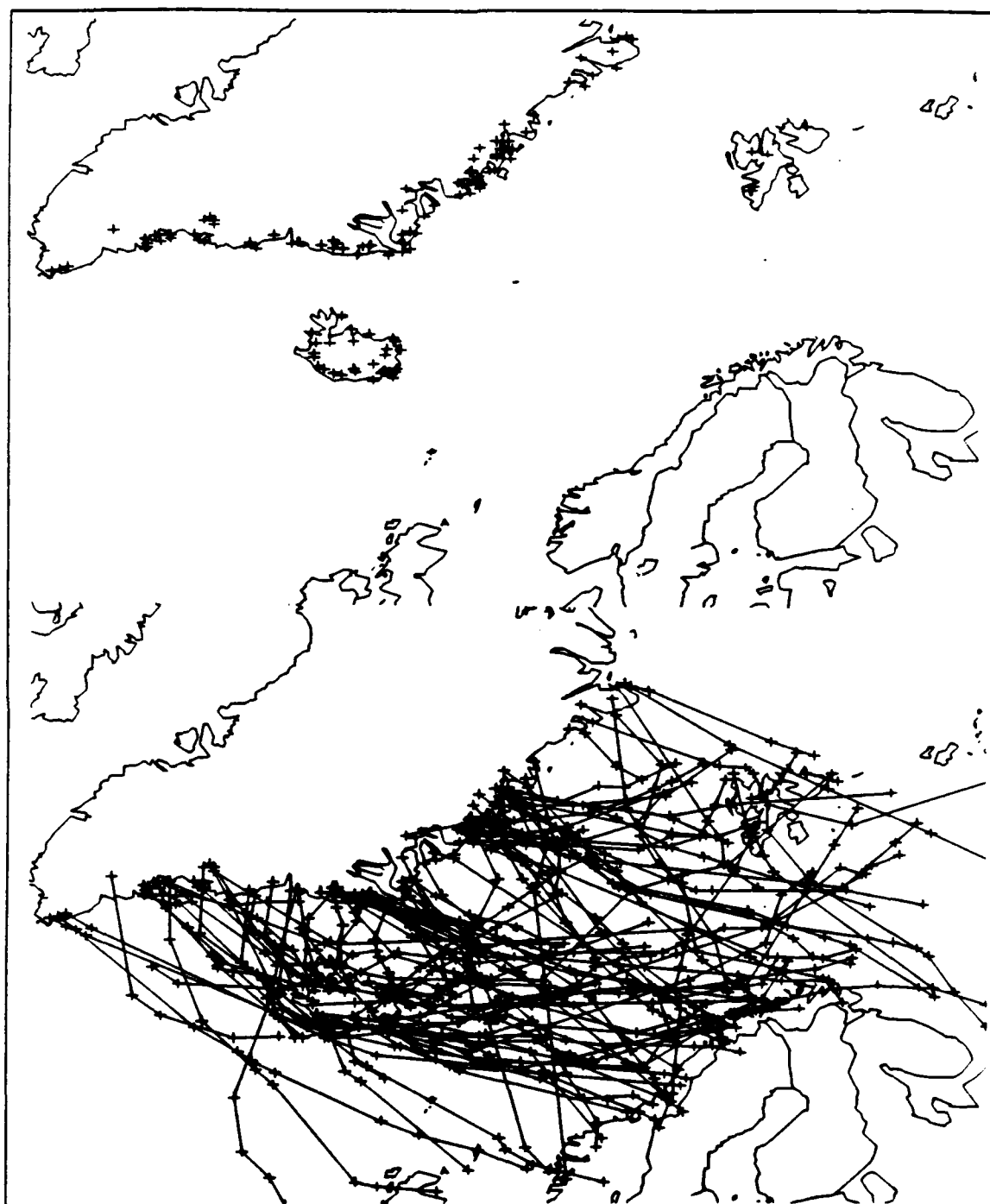


Figure 13. Polar low detection points (upper) with storm tracks (lower) for the entire polar low season.

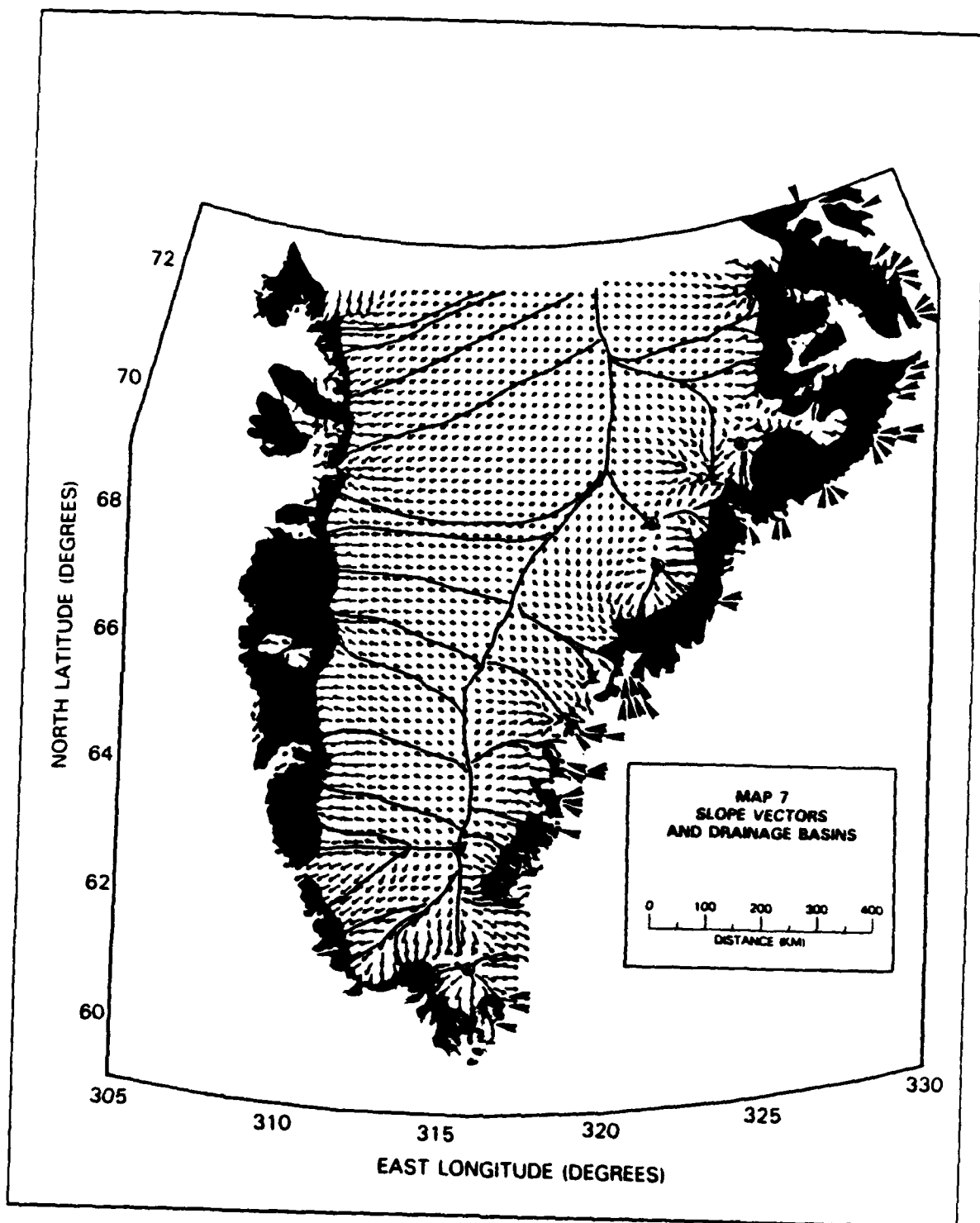


Figure 14a. Polar low formation areas in relation to Southern Greenland topography (Bindschadler 1989).

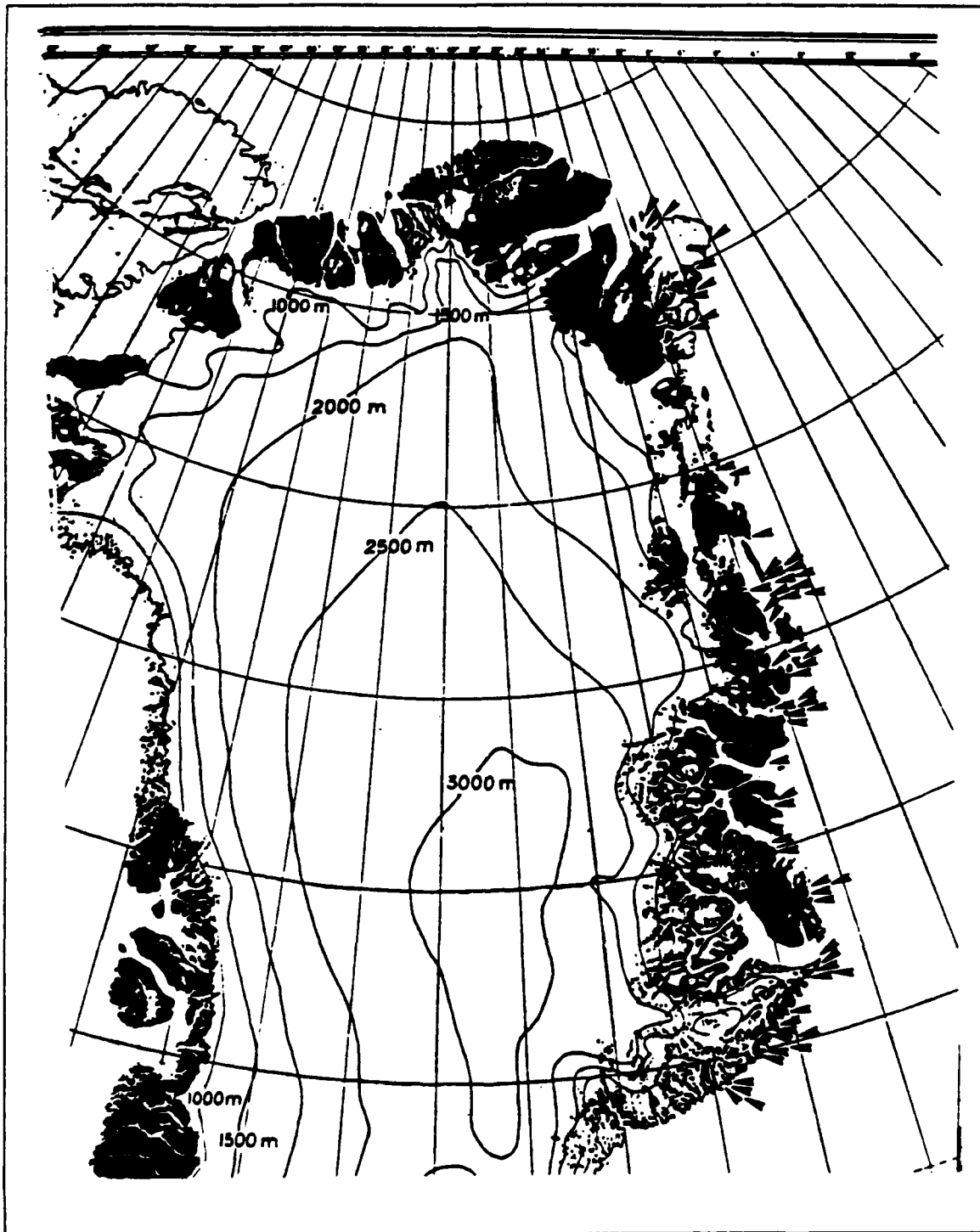


Figure 14b. Polar low formation areas in relation to Northern Greenland topography (Frstrup 1966).

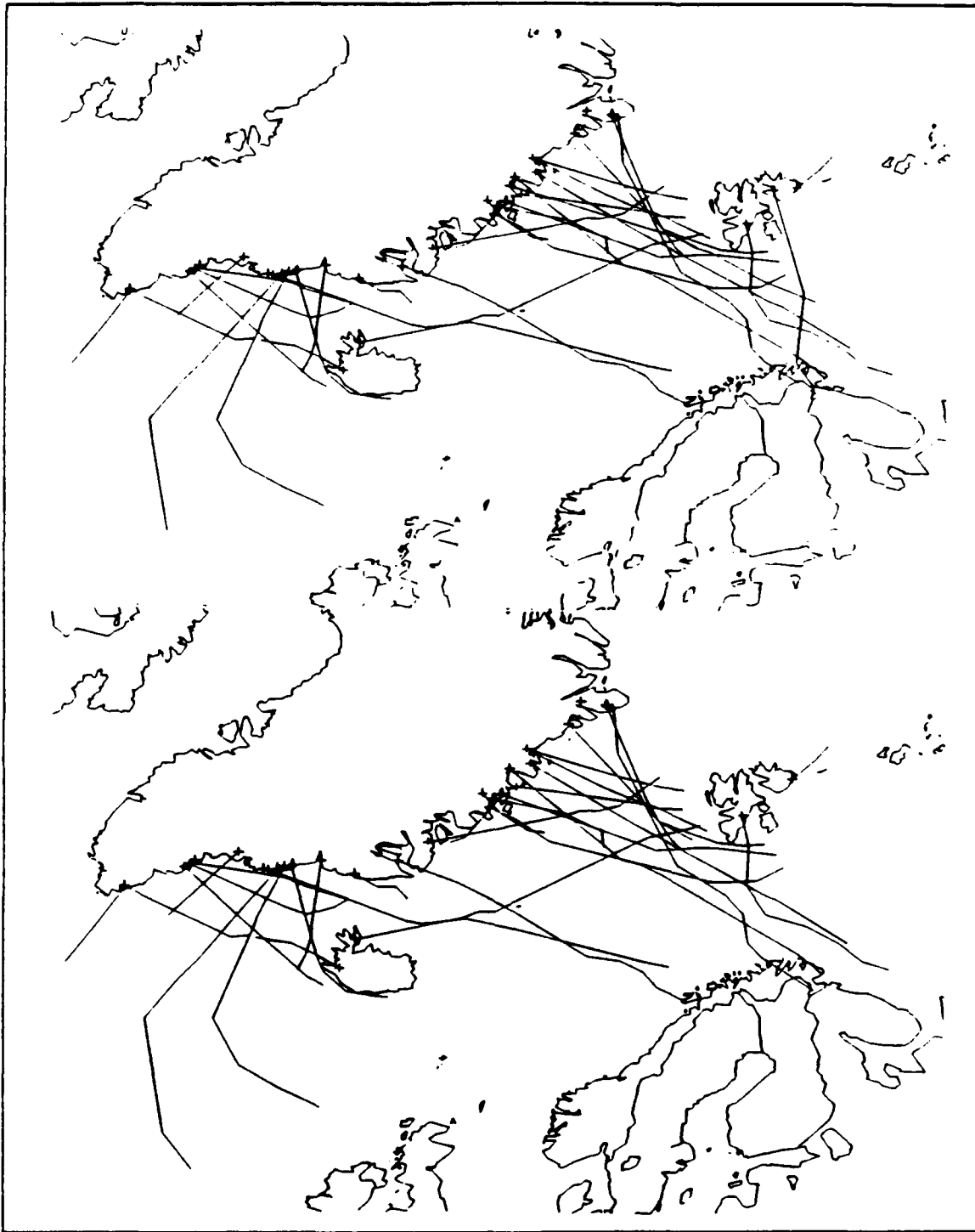


Figure 15a. September backtracked formation areas and storm tracks with no distance limit (upper) and less than 1000 km (lower).

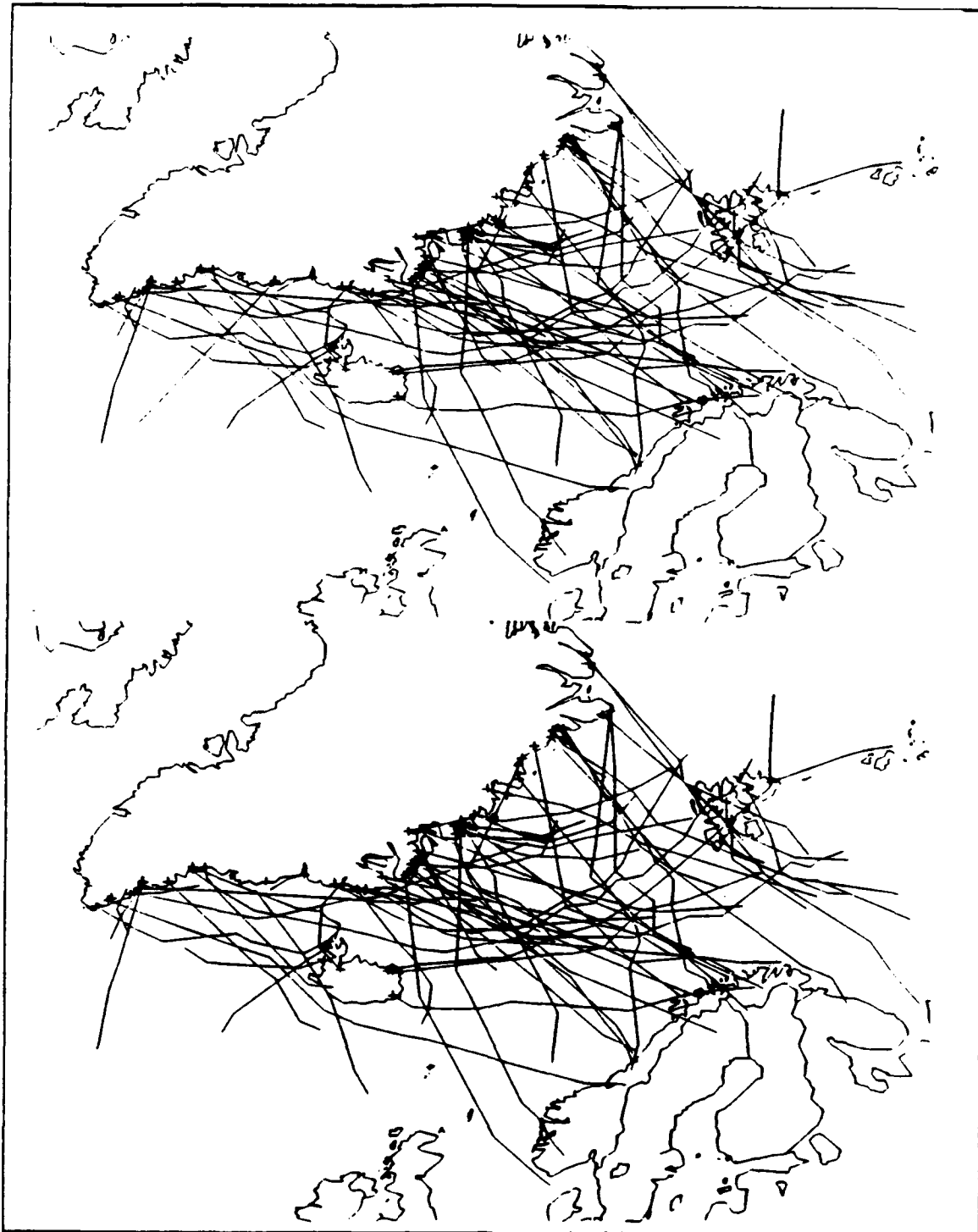


Figure 15b. October backtracked formation areas and storm tracks with no distance limit (upper) and less than 1000 km (lower).

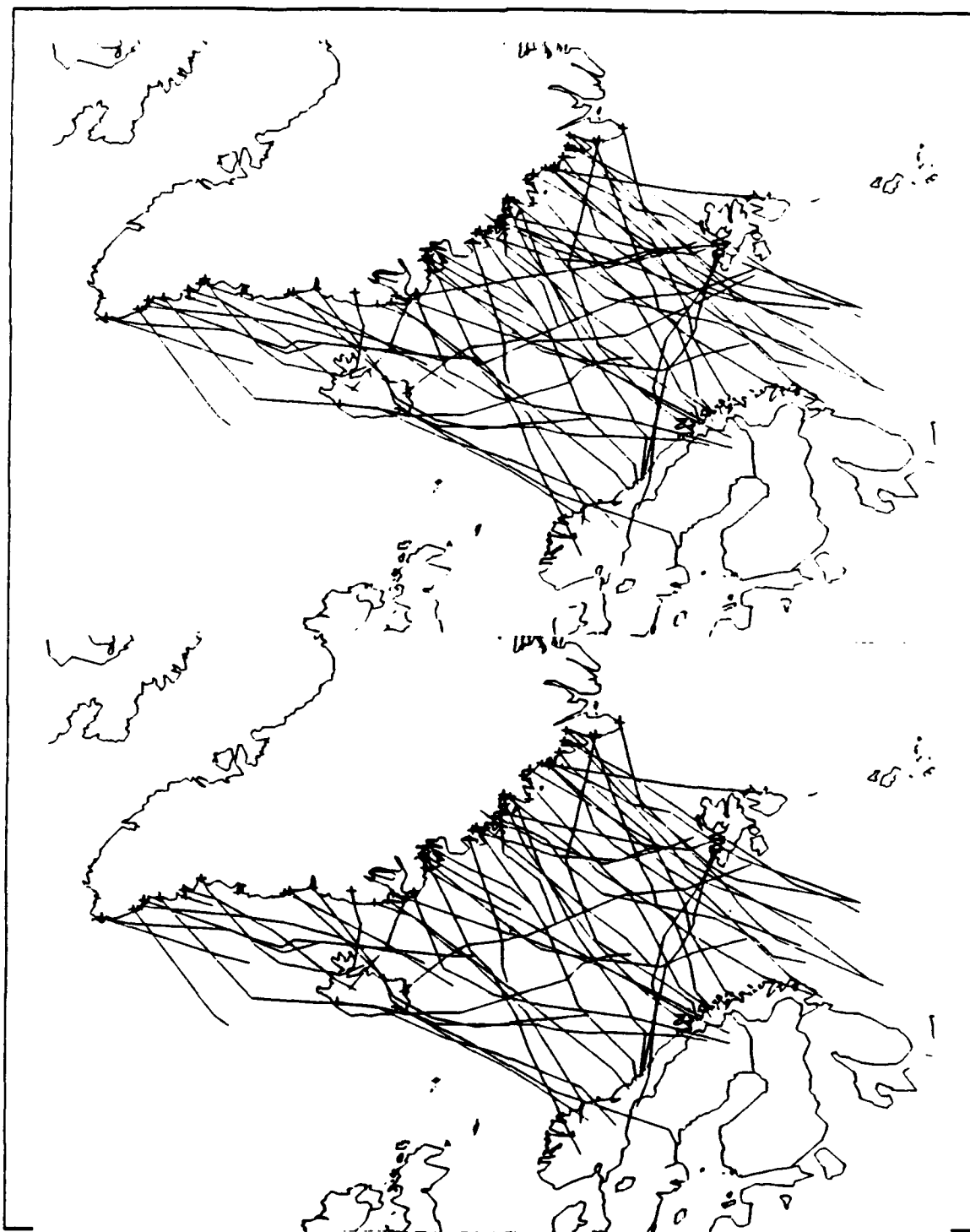


Figure 15c. November backtracked formation areas and storm tracks with no distance limit (upper) and less than 1000 km (lower).

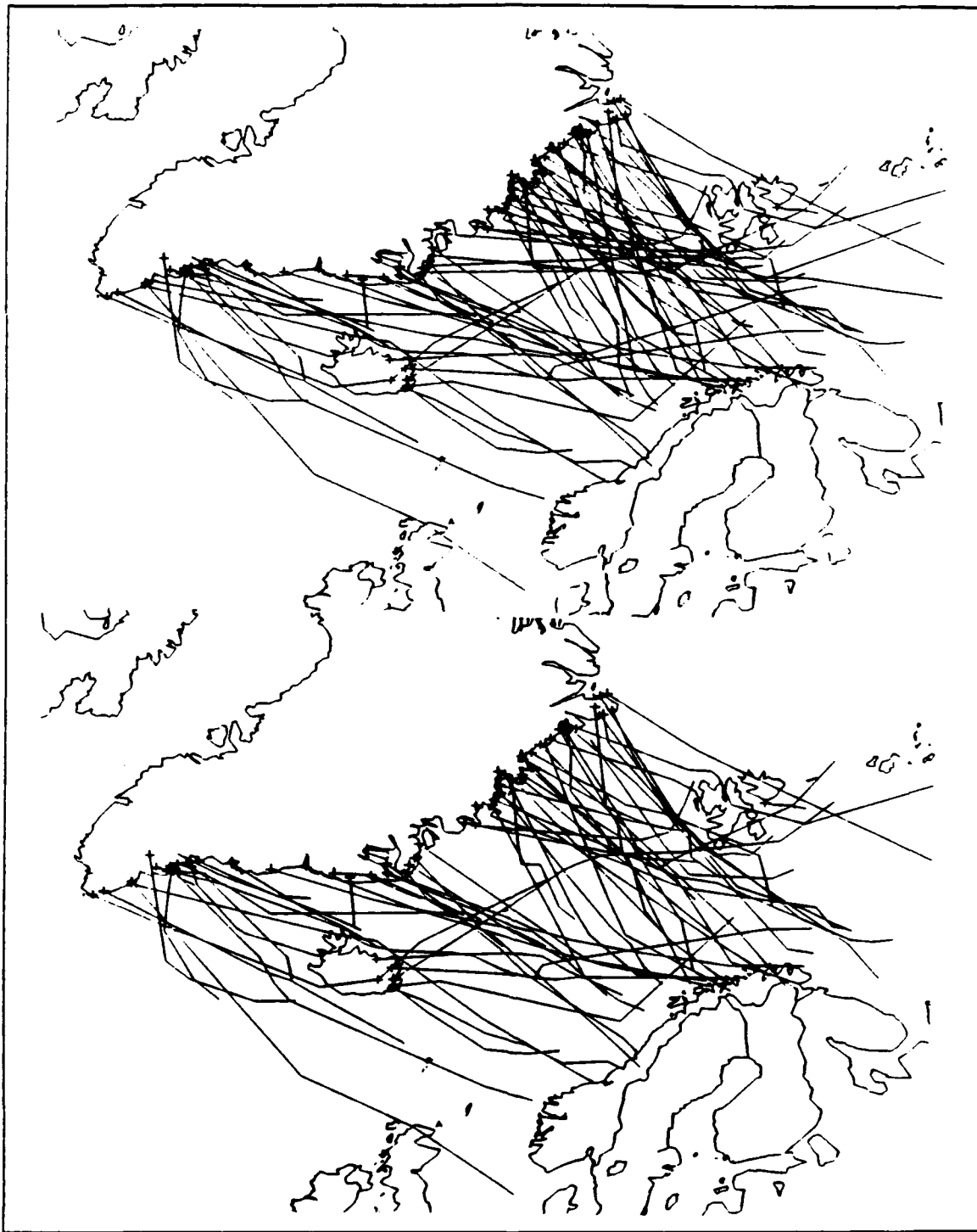


Figure 15d. December backtracked formation areas and storm tracks with no distance limit (upper) and less than 1000 km (lower).

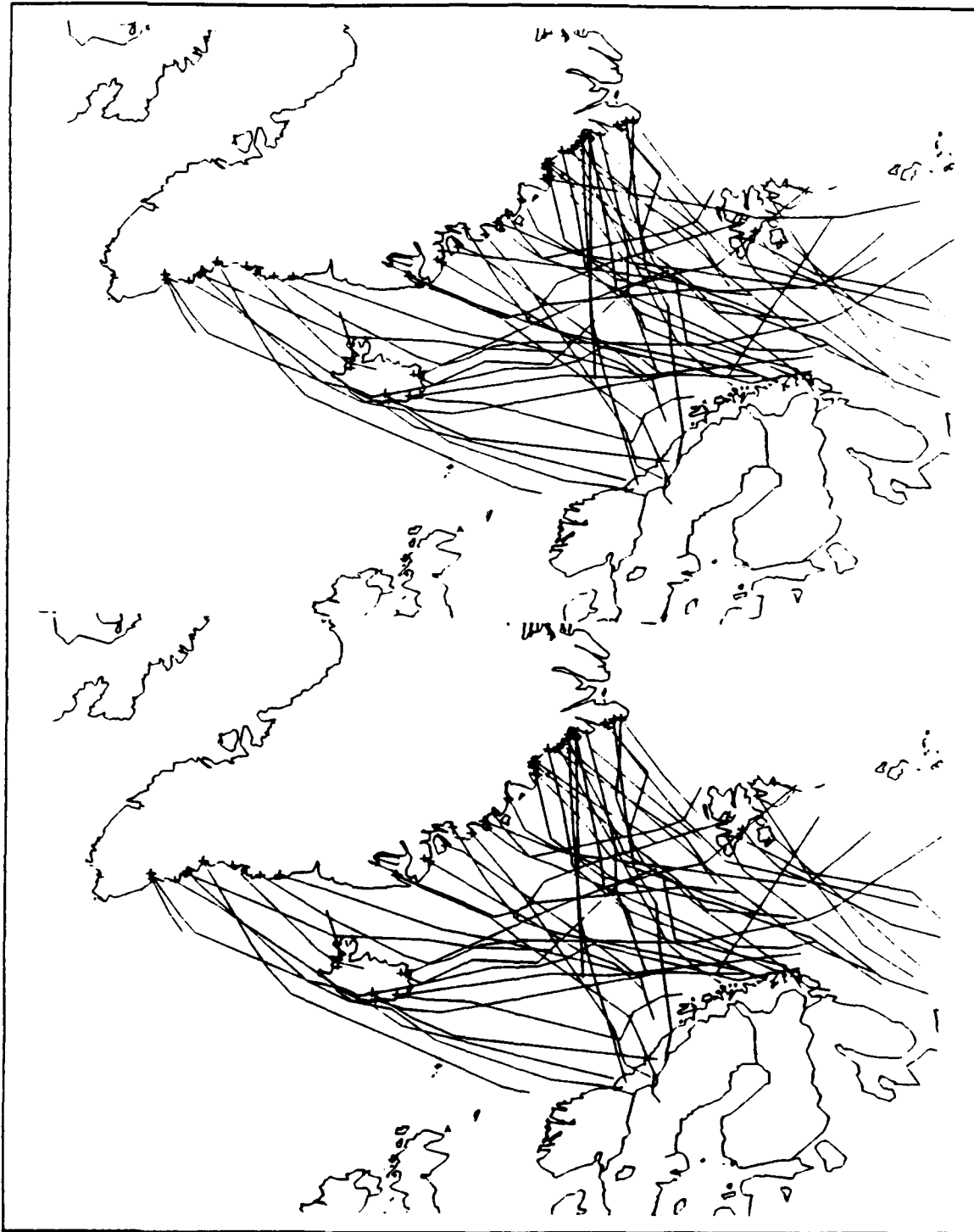


Figure 15e. January backtracked formation areas and storm tracks with no distance limit (upper) and less than 1000 km (lower).

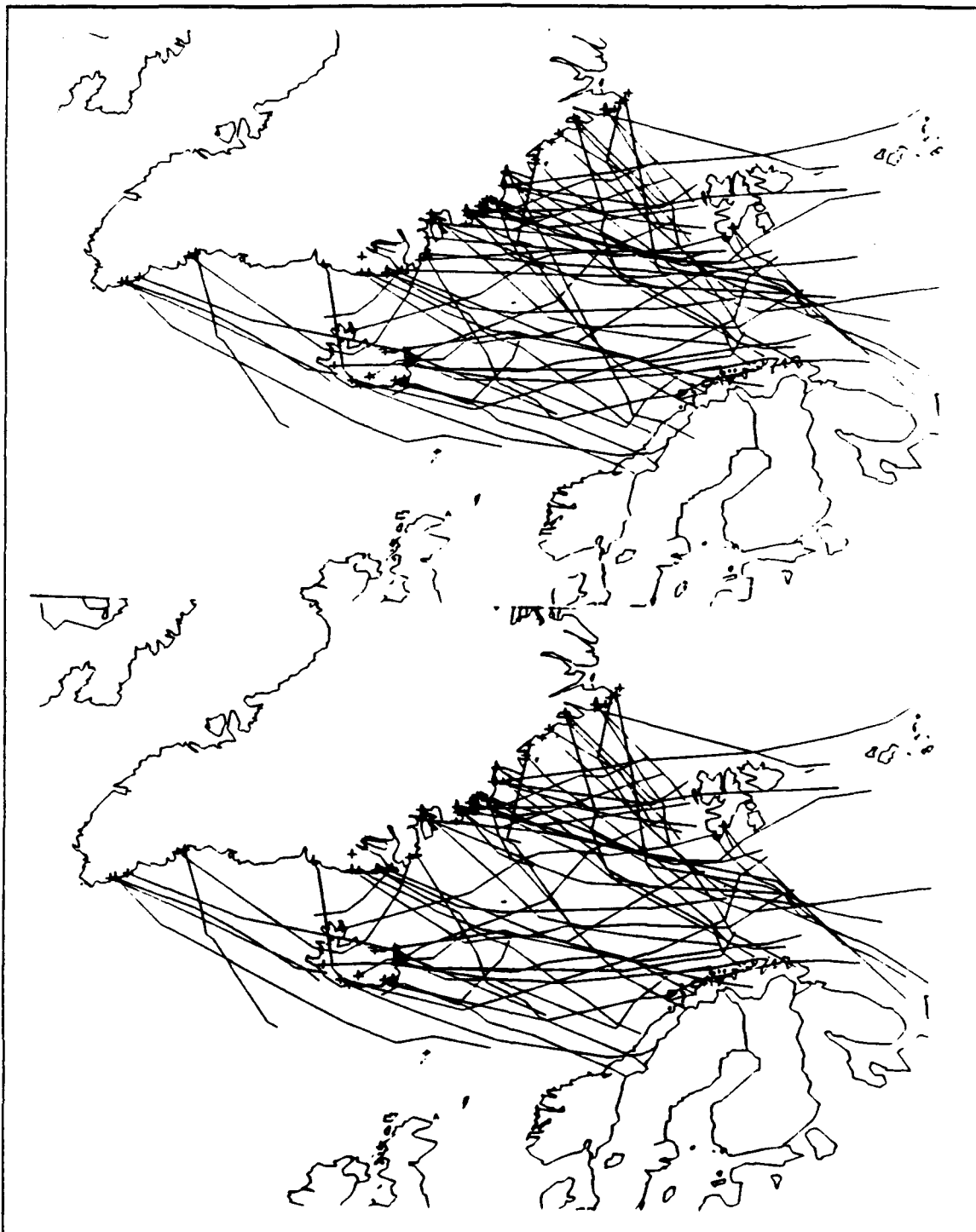


Figure 15f. February backtracked formation areas and storm tracks with no distance limit (upper) and less than 1000 km (lower).

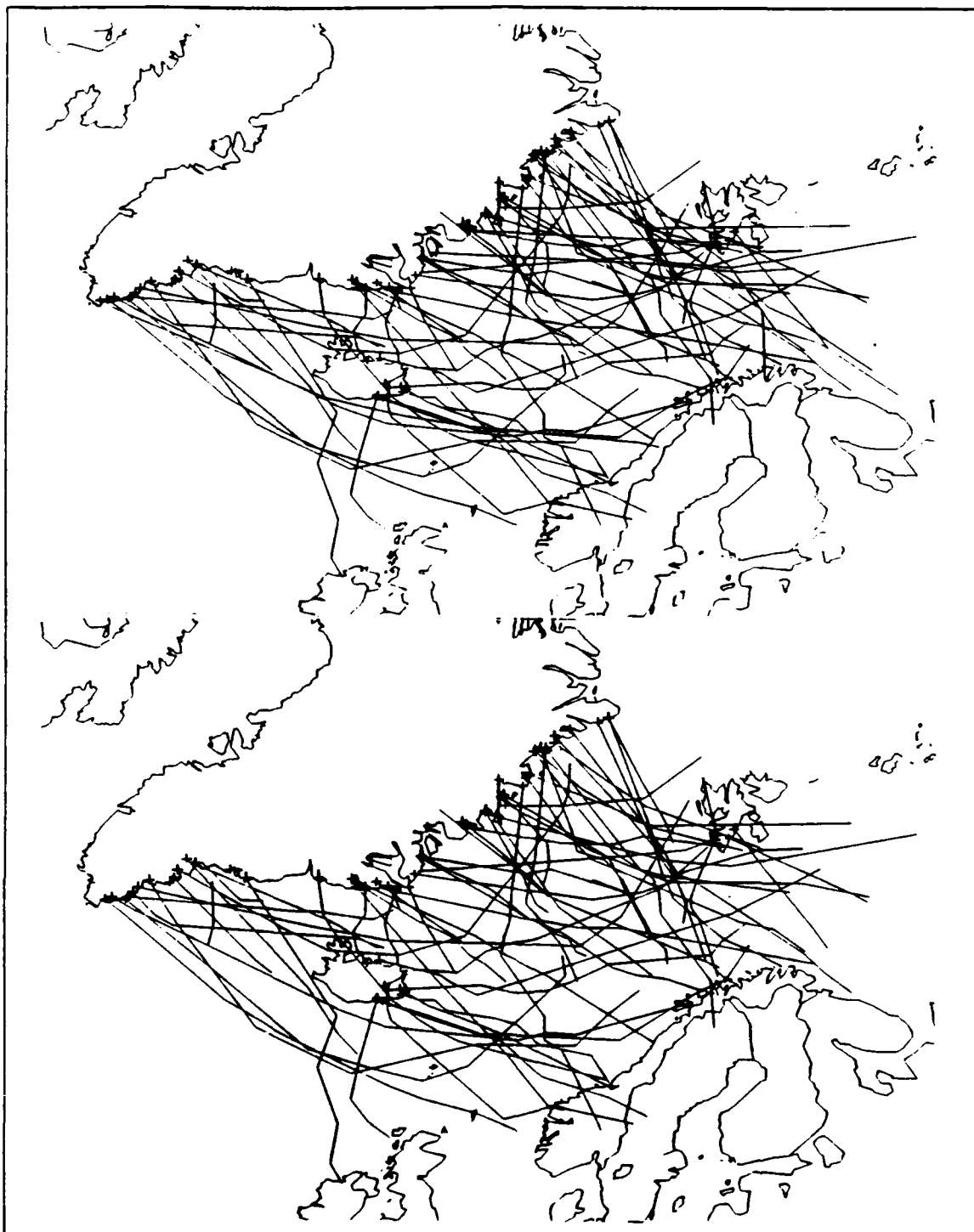


Figure 15g. March backtracked formation areas and storm tracks with no distance limit (upper) and less than 1000 km (lower).

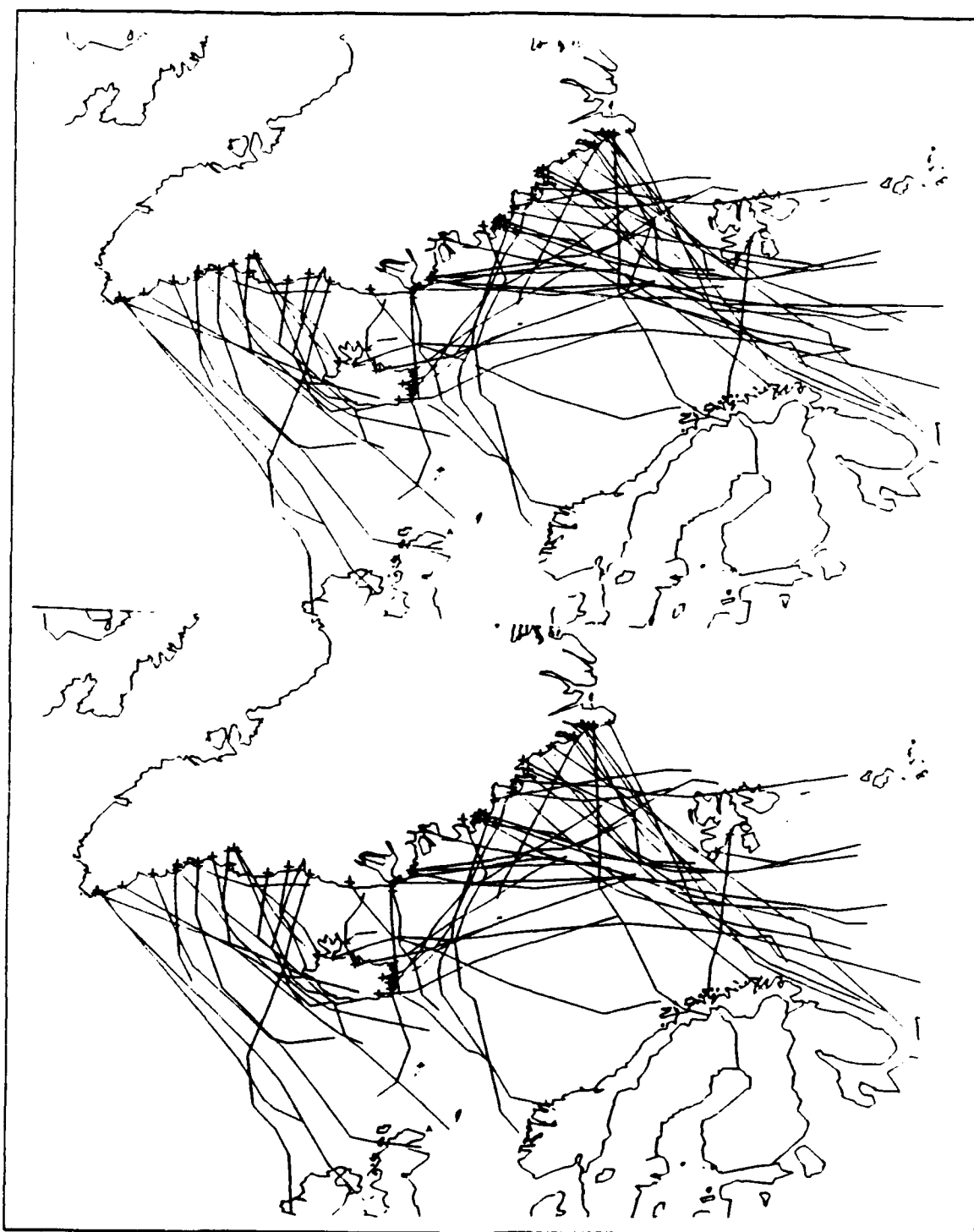


Figure 15h. April backtracked formation areas and storm tracks with no distance limit (upper) and less than 1000 km (lower).

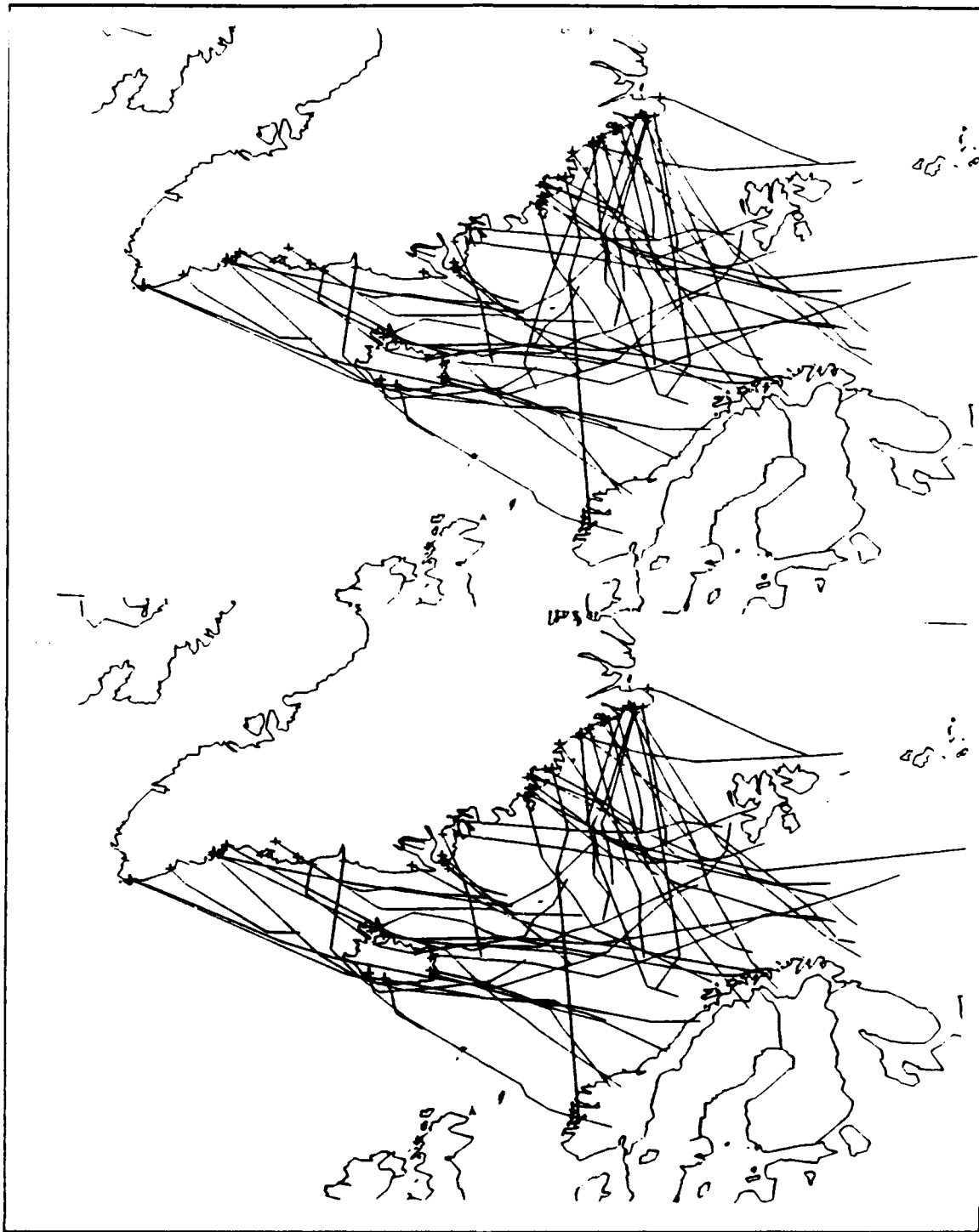


Figure 15i. May backtracked formation areas and storm tracks with no distance limit (upper) and less than 1000 km (lower).

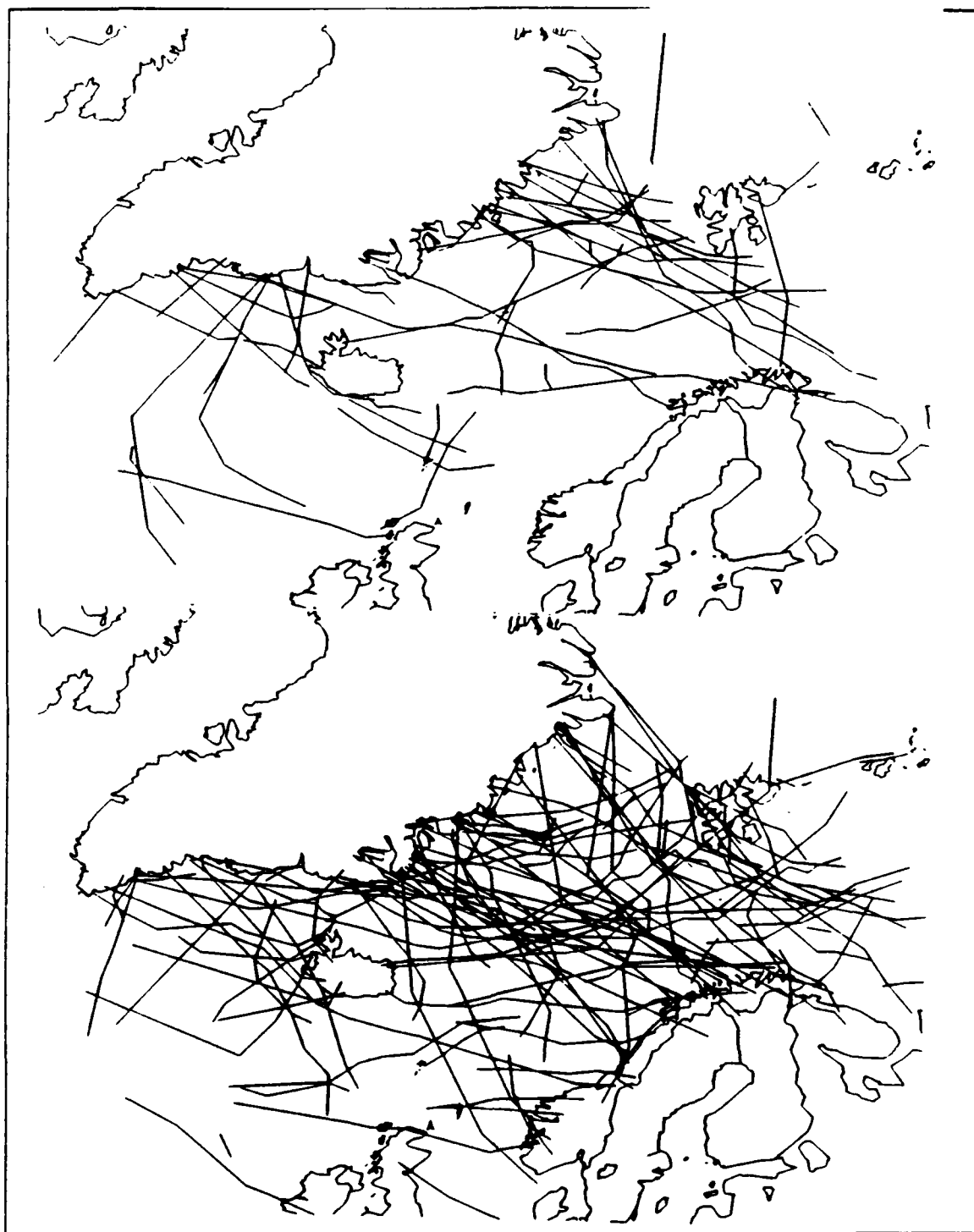


Figure 16a. Combined storm tracks for polar lows detected over land, backtracked or not backtracked for Sep (upper) and Oct (lower).

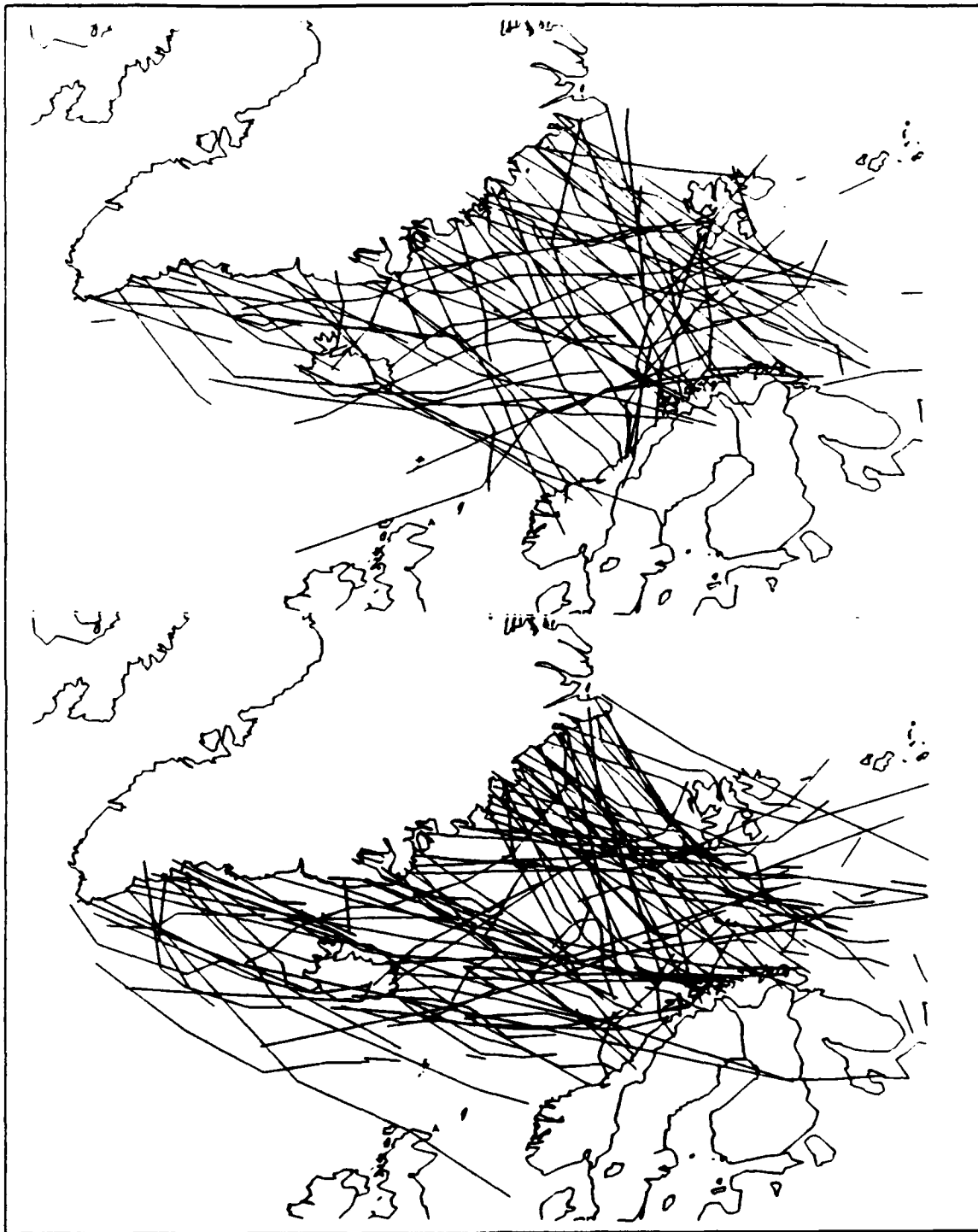


Figure 16b. Combined storm tracks for polar lows detected over land, backtracked or not backtracked for Nov (upper) and Dec (lower).

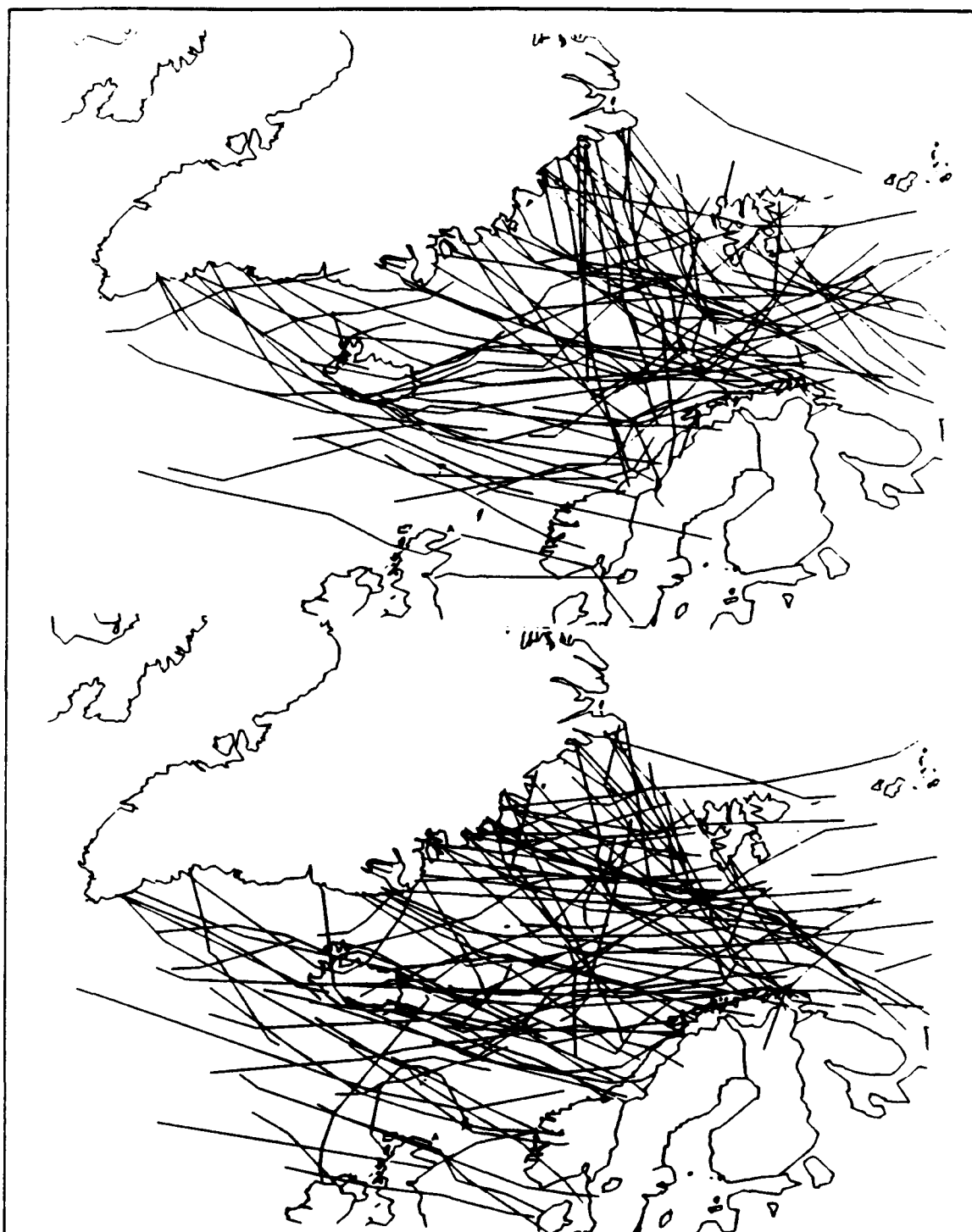


Figure 16c. Combined storm tracks for polar lows detected over land, backtracked or not backtracked for Jan (upper) and Feb (lower).

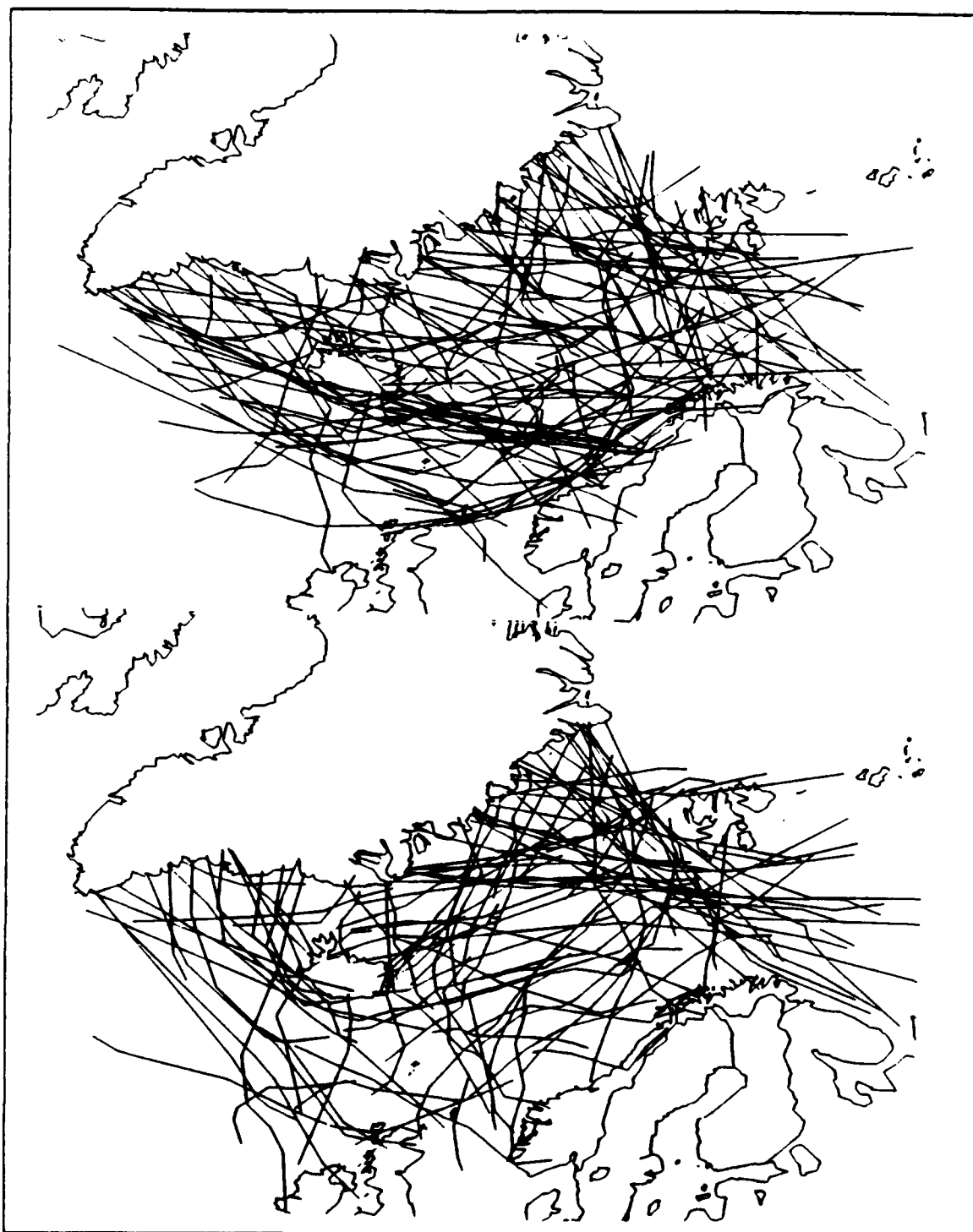


Figure 16d. Combined storm tracks for polar lows detected over land, backtracked or not backtracked for Mar (upper) and Apr (lower).

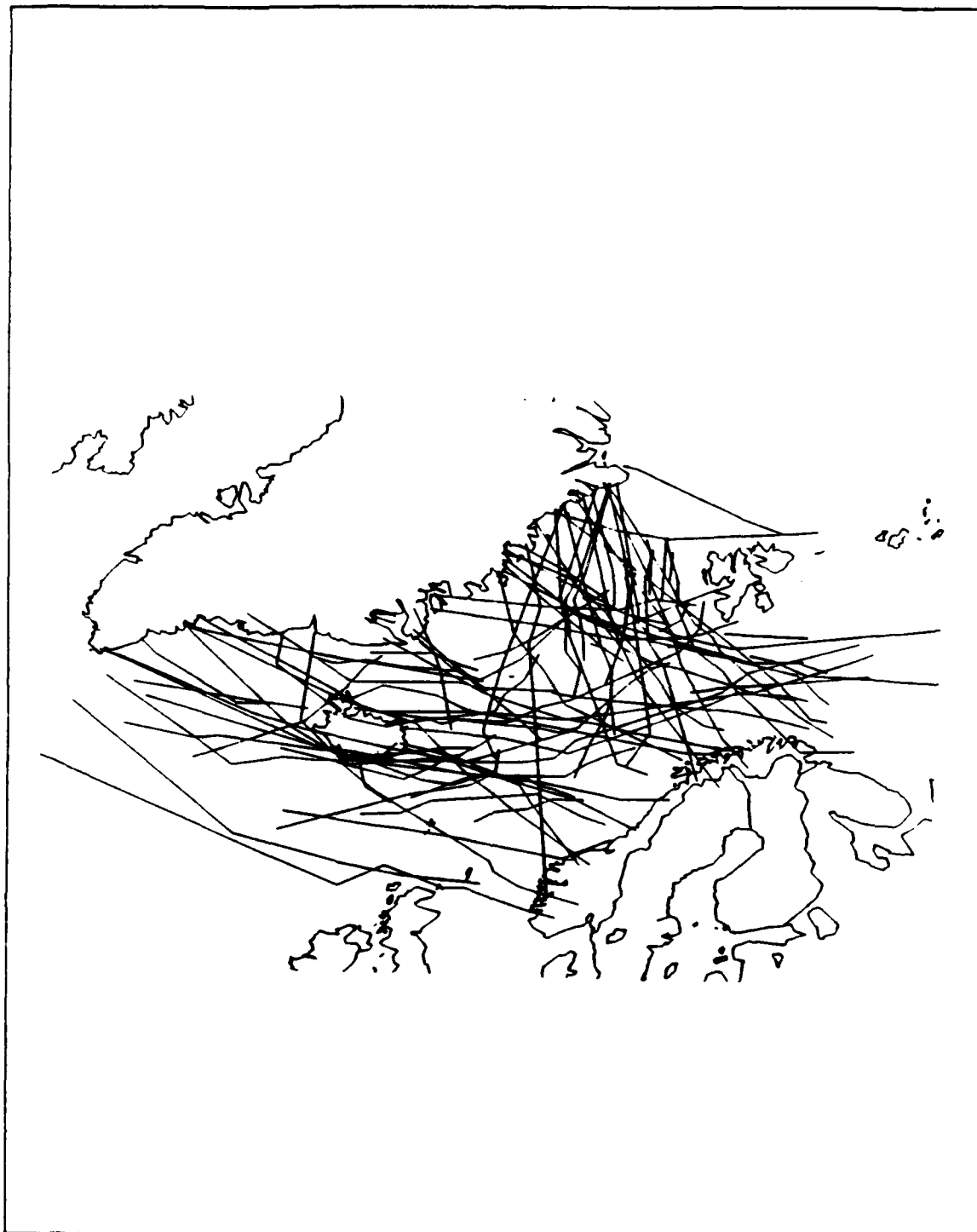


Figure 16e. Combined storm tracks for polar lows detected over land, backtracked or not backtracked for May (upper).

V. SYNOPTIC INDICATORS OF POLAR LOW FORMATION

The major portion of this study examined the overall synoptic situations depicted on the composite 1000 and 500 mb constant pressure level fields for polar lows detected over, or backtracked to:

- Northern Greenland, poleward of 72 degrees North,
- Central Greenland, in the vicinity of Scoresby Sound (68-72 North), and
- Southern Greenland, equatorward of 68 degrees North.

This grouping reflects basic divisions of Greenland's topography. Northern Greenland rises steeply inland from the coasts to the 700 mb level on the inner plateau. The maximum elevation is at 70 North and the steepest inland topography is located between 68 and 72 North. The ice sheet slopes steeply downward to sea level east to Scoresby Sound and west to Sondre Stromfjord and this region should exhibit the strongest katabatic winds. Southern Greenland, below 68 North, is at lower altitudes, only rising to the 850 mb level.

The number of storms detected over, and backtracked to Greenland is depicted in Table 8. The mean synoptic storm charts were compared to the monthly climatologies to determine if there were features common to polar low development for the three areas. Composite charts were also developed for storms that originated over, or were backtracked to Iceland and Svalbard. While these two islands contain extensive glaciers and experience katabatic winds, the height differences are less dramatic than for Greenland. No conclusive results could be drawn for these areas and they are not included in this portion of the study.

The 1000 and 500 mb levels were chosen to represent the low- and upper-level synoptic features of the areas surrounding the polar low development regions. The 1000 mb fields, rather than the surface analyses were used because of the extreme altitude of Greenland. Station pressures are abnormally high when reduced to sea level and when combined with the cold plateau surface temperatures can result in unrealistically strong temperature and pressure gradients. The 1000 mb level better represents the low-level pressure and particularly temperature gradients since observed temperatures are lowered adiabatically to the surface. The standard height of the 1000 mb pressure level is +111 meters while the standard 500 mb height is 5574 meters.

Table 8. STORMS ORIGINATING OVER OR BACKTRACKED TO GREENLAND

Month	Total Lows	North of 72 N		Scoresby Sound (68 - 72 N)		South of 68 N	
		Orig	Back	Orig	Back	Orig	Back
Sep	61	6	10	0	4	0	11
Oct	127	7	18	7	13	0	15
Nov	89	8	17	3	10	2	11
Dec	137	7	29	3	10	5	11
Jan	94	5	19	2	6	2	6
Feb	94	8	25	5	10	1	6
Mar	136	4	21	5	8	3	10
Apr	113	5	22	4	8	10	7
May	90	4	17	4	3	9	4
Total	941	54	180	33	72	32	93

In the following sections, the four major items discussed are:

- The overall monthly climatology,
- The synoptic situations associated with storm detected over each of the three areas of Greenland.
- How the storms backtracked to Greenland differed from those detected there,
- How each situation deviates from climatology.

Heights and temperatures are given in absolute values rather than deviations from climatology as was done in studies by Businger (1985) and Eise et al. (1988). Knowledge of the absolute synoptic pattern associated with storm development is as important as how each pattern deviates from the mean when forecasting likely polar low occurrence. Each geographic feature mentioned in the following discussion can be identified on Fig. 6. In the following section, flow refers to the direction of the geostrophic wind as being on, off or cross shore. The actual winds are probably different, but could not be determined due to lack of observations.

A. SEPTEMBER

1. Summary

The September surface climatology (Fig. 17a) shows the polar front extending southwest from the Central Barents Sea, through the Norwegian Sea and south of Iceland to Cape Farewell. The 500 mb long-wave trough was over the Fram Strait and Iceland. The 31 storms that occurred in September tended to form with higher than normal 1000 mb heights and stronger than normal offshore height gradients. Coastal temperatures were cooler, but over-water temperature gradients were stronger. Northern Greenland storms tended to form with offshore flow, while Southern and Central Greenland storms formed with onshore flow. The southern storms had warm-air advection, while the central and northern storms had cold-air advection. At 500 mb, storms formed under anti-cyclonic turning associated with the short-wave ridge with cold-air advection aloft. Heights were higher than normal but temperatures were near the mean.

2. Mean Structure

At 1000 mb (Fig. 17a), a +40 meter low center located in the Norwegian Sea extended pressure troughs southwest, to the south of Iceland, west into the Denmark Strait and northeast toward Novaya Zemlya. A high over the East Greenland coast ridged east toward Svalbard. At 500 mb, a long-wave trough extended south from the Fram Strait to Iceland with ridging north from south of Cape Farewell to Central Greenland.

3. Greenland North of 72 N.

The six storms detected over Greenland (Fig. 17b) formed with a stronger than normal 1000 mb offshore height gradient between ridging from the south over Scoresby Sound, a low center near Bear Island and a trough west of Svalbard. Overall flow was diagonally offshore with cold-air advection and heights below climatology. At 500 mb, the storms formed ahead of a long-wave ridge with cold-air advection and higher than normal heights. The ten backtracked storms formed under similar conditions, but with the 1000 mb low further east in the Barents Sea. Coastal heights and temperatures were above the mean. There was less anti-cyclonic turning aloft, ahead of the long-wave ridge and behind the long-wave trough.

4. Scoresby Sound.

No storms were detected near Scoresby Sound during September. For the 11 backtracked storms (Fig. 17c), stronger than normal height gradients were established between ridging across Central Greenland and a low in the Norwegian Sea. Flow was

slightly onshore with cold-air advection. Heights were above and temperatures below climatology. At 500 mb, the storms formed under a short-wave ridge propagating through the long-wave trough with cold-air advection and higher than normal heights.

5. Greenland South of 68 N.

No storms were detected over Southern Greenland during September. The four backtracked storms (Fig. 17d), tended to form under a 1000 mb high over the Southern Greenland coast. There were stronger than normal height gradients between the high and a deeper than normal low in the Norwegian Sea. Flow was onshore with warm-air advection. Heights were above, but temperatures below normal. At 500 mb, the storms formed under the long-wave ridge with cold-air advection. Heights were above normal.

B. OCTOBER

1. Summary

The October surface climatology (Fig. 18a) shows the polar front extending southwest from the Barents Sea, over Iceland, then south to west of Scotland and northwest to Cape Farewell. The 500 mb long-wave trough extended southeast from the Denmark Strait to west of France. The 60 storms that occurred in October tended to form with near-normal 1000 mb heights gradients, except for storms detected near Scoresby Sound, which had much stronger gradients. Low-level heights were generally above normal, but temperatures were inconsistent. Flow was offshore in Northern and Central Greenland, but both on and offshore flow was present in the south. There was cold-air advection in all cases, except the Central Greenland detected storms, but some northern storms also experienced warm-air advection. At 500 mb, the storms formed under ridging with cold-air advection. Heights were generally above normal, the exception being the central detected case with the extremely strong height gradient. Temperatures were inconsistent.

2. Mean Structure

At 1000 mb (Fig. 18a), a +60 meter low center located south of Iceland extended pressure troughs southeast to west of Europe; northeast over Iceland into the Barents Sea and northwest to Cape Farewell. A high over Eastern Europe ridged northwest into the Norwegian Sea and a bubble high was located over Scoresby Sound. At 500 mb, a long-wave trough extended southeast from the Denmark Strait to west of Europe while a short-wave ridged north from the Denmark Strait over Central Greenland.

3. Greenland North of 72 N.

The seven storms detected over Northern Greenland (Fig 18b), formed with a near-normal 1000 mb height gradient between ridging from the southwest and a low in the Eastern Barents Sea. Over-all flow was generally offshore, with both warm- and cold-air advection. Heights and temperatures were above the mean. At 500 mb, the storms formed ahead of the short-wave ridge over Central Greenland with cold-air advection. Heights and temperatures were above climatology. The 18 backtracked storms formed under similar conditions, but with stronger offshore 1000 mb height gradients and with only warm-air advection. At 500 mb, the ridging was not as pronounced.

4. Scoresby Sound.

The seven storms detected near Scoresby Sound (Fig. 18c) formed with an extremely strong offshore 1000 mb height gradient between strong ridging over Southern Greenland and a deep low east of Bear Island. Flow was offshore with warm-air advection. Heights and temperatures were below the mean. At 500 mb, the storms formed in non-curving flow and tight height gradients between the short-wave ridge in the Denmark Strait and the long-wave trough over the Fram Strait. Heights and temperatures were below normal and there was cold-air advection aloft. The conditions for the 13 backtracked storms were closer to the mean structure than the detected cases however, with a high over Scoresby Sound and the polar front near Iceland. The 1000 mb height gradient was weaker than the detected cases. Flow was diagonally onshore with cold-air advection. Heights and temperatures were above normal. The 500 mb pattern was similar, but with above, rather than below normal heights and temperatures.

5. Greenland South of 68 N.

There were no storms detected over Southern Greenland in October. The 15 storms backtracked storms (Fig. 18d) formed near a weak 1000 mb low in the Denmark Strait with a weaker than normal height gradient between ridging over Southern Greenland and an elongated trough over Northern Norway. Flow was both on and offshore with both warm- and cold-air advection. Heights and temperatures were below normal. At 500 mb, storms formed under an area of anti-cyclonic turning between the existing long-wave trough and one developing over the Davis Strait. Heights were above, but temperatures below climatology. There was slight cold-air advection aloft.

C. NOVEMBER

1. Summary.

The November surface climatology (Fig. 19a) shows the 1000 mb polar front extending southwest from the Barents Sea, north of Iceland to south of Cape Farewell. The 500 mb long-wave ridge was over Iceland and Eastern Greenland. The 51 November storms formed under varying conditions. The northern and southern storms formed with weak or onshore 1000 mb height gradients, but the central storms had very strong offshore gradients. Low-level flow was on, off or cross-shore. There was cold-air advection in the north and central, but warm-air advection in the south. Heights were generally below the mean, but temperatures were inconsistent. At 500 mb, northern and central storms formed under ridges and cold-air advection while the southern storms formed under troughs and warm-air advection. Height and temperature differences were inconsistent.

2. Mean Structure

At 1000 mb (Fig. 19a), a -40 meter low center near Novaya Zemlya extended pressure troughs north to Franz Josef Land and southwest, north of Iceland, to a 0 meter low center south of Cape Farewell which extended an inverted trough north into the Davis Strait. A high over Western Europe ridged northwest to Iceland and a high near the pole ridged south along the East Greenland coast to Iceland. At 500 mb, a long-wave ridge extended north from west of France, over Iceland and Scoresby Sound to Northern Greenland.

3. Greenland North of 72 N.

The eight cases detected over Northern Greenland (Fig. 19b) formed with weaker than normal 1000 mb offshore height gradients established between the ridging from north and south and a low in the Southern Barents Sea. Flow was generally cross-shore with cold-air advection. Heights and temperatures were above normal. At 500 mb, the storms formed ahead of the long-wave ridge with cold-air advection. Heights and temperatures were above climatology. For the 20 backtracked storms, 1000 mb conditions were similar, except that stronger ridging from the north resulted in diagonally onshore flow. Heights were below the mean. The 500 mb pattern was nearly identical, but with heights and temperatures near climatology.

4. Scoresby Sound.

The three storms detected near Scoresby Sound (Fig. 19c), formed with an extremely strong 1000 mb height gradient between ridging from Northern Greenland and a deep low south of Bear Island. Flow was diagonally onshore with cold-air advection.

Heights were near the mean, but temperatures were significantly below normal. At 500 mb, storms formed ahead of a short-wave ridge with divergent flow and cold-air advection. Heights and temperatures were below normal. The ten storms backtracked to Scoresby Sound formed under similar 1000 mb conditions, but with cross-shore flow and temperatures slightly warmer than climatology. At 500 mb, storms formed ahead of the long-wave ridge, and both heights and temperatures were above the mean.

5. Greenland South of 68 N.

The two storms detected over Southern Greenland (Fig. 19d) formed with a weak onshore 1000 mb height gradient between ridging from the United Kingdom and a low in the Davis Strait. Flow was onshore with warm-air advection. Heights were below and temperatures above the mean. At 500 mb, the storms were formed under a short-wave trough that propagated over the long-wave ridge that shifted eastward to over the Norwegian Sea. There was warm-air advection aloft. Heights and temperatures were both below normal. The 11 backtracked storms formed under different 1000 mb conditions with a stronger offshore gradient between ridging from Southern Greenland and a trough over Iceland and the Denmark Strait. Flow was generally cross-shore with neutral temperature advection. At 500 mb, the storms formed under the long-wave trough with neutral temperature advection.

D. DECEMBER

1. Summary.

The December surface climatology (Fig. 20a) shows the polar front extending southwest from the Barents Sea across Northern Iceland onto the Denmark Strait and over Southern Greenland. The 500 mb long-wave ridge was located over the Norwegian Sea. The 65 storms that occurred in December tended to form with 1000 mb height gradients slightly above climatology. Overall flow was onshore for central storms, but with off and cross-shore for northern and southern storms. Temperatures were generally below normal, but heights were inconsistent. At 500 mb, northern and southern storms formed under troughs while Scoresby Sound storms were formed under ridges. There was cold-air advection aloft except one case with no advection. Heights and temperatures were generally below climatology.

2. Mean Structure

At 1000 mb (Fig. 20a), a -20 meter low center in the Denmark Strait extended pressure troughs northeast, across Iceland into the Barents Sea and north into the Davis Strait. A high west of France ridged north toward Iceland and ridging from Northern

Greenland extended south along the East Greenland coast to Iceland. At 500 mb, a long-wave ridge extended north from west of France over the Norwegian Sea, while a trough extended southeast from Baffin Bay to Southern Greenland. A short-wave ridge was centered west of Scoresby Sound.

3. Greenland North of 72 N.

The seven storms detected over Northern Greenland (Fig. 20b) were formed in a weak 1000 mb offshore height gradient between ridging from Northern Greenland and south from Scoresby Sound and a trough east of Franz Josef Land. Flow was offshore with warm-air advection. Heights were below the mean. At 500 mb, the storms formed under a short-wave trough that propagated across the long-wave ridge. Temperatures were above climatology, but there was cold-air advection aloft. The 29 backtracked storms formed under similar 1000 mb conditions with a stronger offshore height gradient between ridging from Northern Greenland and a trough near Bear Island. Flow was generally cross-shore with cold-air advection. Heights were above, but temperatures below the mean. At 500 mb, the storms formed under slightly cyclonic turning ahead of a short-wave ridge with cold-air advection.

4. Vicinity of Scoresby Sound.

The three storms detected near Scoresby Sound (Fig. 20c) were formed in a cross-coast 1000 mb height gradient between a high north of Scoresby Sound and a trough over Iceland. Flow was onshore with neutral advection. Heights were also below normal. At 500 mb, storms were formed under a short-wave ridge with divergent flow and cold-air advection. Heights were below the mean. The 10 backtracked storms formed under similar conditions. At 1000 mb, the cross-shore gradient was established between a high north of Scoresby Sound and lows in the Denmark Strait and west of the Lofoten Islands. There was onshore flow and cold-air advection. Heights were higher and temperatures colder than normal. Conditions at 500 mb were similar except the storms formed under convergent, rather than divergent, flow ahead of the short-wave ridge.

5. Greenland South of 68 N.

The five storms detected over Southern Greenland (Fig. 20d) were formed in a stronger than normal 1000 mb height gradient between ridging from Northern Canada and a low in the Denmark Strait. Flow was offshore with cold-air advection. Temperatures were below climatology. At 500 mb, the storms formed under the long-wave trough that moved east over Eastern Greenland. Heights and temperatures were below the mean and there was cold-air advection aloft. The 11 backtracked storms formed

with similar 1000 mb conditions, but with cross-shore flow and both warm- and cold-air advection. Heights and temperatures were below climatology. At 500 mb, the storms were formed under a short-wave trough propagating across the long-wave ridge with neutral temperature advection.

E. JANUARY

1. Summary.

The January surface climatology pattern (Fig. 21a) shows the polar front extending southwest from the Barents Sea across Northern Iceland, through the Denmark Strait to Cape Farewell. At 500 mb, a long-wave trough was located over Southern Greenland and a short-wave ridge over Scoresby Sound. The 40 storms that occurred in January tended to form with stronger than normal 1000 mb offshore height gradients and with generally cold-air advection, except for the southern detected case. Heights were generally higher than the mean for northern and central storms, but lower for southern cases. Temperatures tended to be below the mean. At 500 mb, northern storms formed under both troughs and ridges while central storms were associated with ridges and the southern storms with troughs. There was cold-air advection aloft in all but one situation. Temperatures tended to be below the mean. Heights were above normal in the north and center but lower in the south.

2. Mean Structure

At 1000 mb (Fig. 21a), a -100 meter low center in the Denmark Strait extended pressure troughs west to Southern Greenland, northeast into the Barents Sea and north northeast to west of Svalbard. A high ridged northwest from Europe into the Norwegian Sea. A ridge extended south from Northern Greenland along the East Greenland coast to Iceland. At 500 mb, a 4920 meter low over Northern Canada extended a trough south over Southern Greenland into the Denmark Strait while a ridge extended north from France to the Fram Strait. A short-wave ridge extended northwest from Jan Mayen Island to Central Greenland.

3. Greenland north of 72 N.

The five storms detected over Northern Greenland (Fig. 21b) were formed with a stronger than normal 1000 mb offshore height gradient between ridging from Northern Greenland and a trough in the Fram Strait. Flow was diagonally onshore with cold-air advection. Heights were below the mean. At 500 mb, the three southern storms formed under a short-wave ridge, while the three northern storms formed under a trough. There was cold-air advection aloft for all cases. Heights and temperatures were near

climatology. The 19 backtracked storms formed under similar conditions, but with a stronger offshore height gradient between ridging from Northern Norway and a low in the Northern Norwegian Sea. Heights were above normal. At 500 mb, the southern storms formed under a ridge, while the northern storms formed under a trough. Heights were above the mean.

4. Scoresby Sound.

The two storms detected near Scoresby Sound (Fig. 21c) were formed in a very strong 1000 mb offshore height gradient between ridging along the East Greenland coast and a low in the Northern Norwegian Sea. Flow was diagonally onshore with cold-air advection. Heights and temperatures were significantly above climatology. At 500 mb, the storms formed under a slight short-wave ridge with cold-air advection. Heights were higher than the mean. Conditions were similar for the six backtracked storms, except that 1000 and 500 mb temperatures were colder and there was warm-air advection at 500 mb.

5. Greenland South of 68 N.

The two storms detected over Southern Greenland (Fig. 21d) were formed in a very strong diagonally offshore 1000 mb height gradient between ridging from Southern Greenland and a deep low in the Denmark Strait. Flow was diagonally offshore with slight warm-air advection. Heights and temperatures were significantly below climatology. At 500 mb, the storms formed under a sharp long-wave trough with cold-air advection. Heights and temperatures were below the mean. The six backtracked storms formed under nearly identical conditions, except for onshore flow and warm-air advection for the northern storms and offshore flow and cold-air advection for the southern.

F. FEBRUARY

1. Summary.

The February surface climatology (Fig. 22a) shows the polar front extending southwest from the Barents Sea, across Iceland and the Denmark Strait to Southern Greenland. The 500 mb long-wave trough was located across Southern Greenland and the long-wave ridge over Scandinavia. The 55 February storms tended to form in regions of enhanced 1000 mb offshore height and over-water temperature gradients. These were produced by the anti-cyclonic turning and offshore ridging in Northern storms and the influence of deep Denmark Strait lows in the Southern storms. At 500 mb, northern storms formed under ridges while southern storms formed under cold troughs.

2. Mean Structure

At 1000 mb (Fig. 22a), a -120 meter low center northeast of Iceland extended pressure troughs southwest over Iceland to Cape Farewell; northeast into the Barents Sea and north northeast to west of Svalbard. Ridging extended south from Northern Greenland along the East Greenland coast to Iceland. At 500 mb, a 4920 meter low over Northeast Canada extended a long-wave trough southeast across Southern Greenland into the Denmark Strait. A long-wave ridge extended north from Central Europe to Northern Norway. A short-wave ridge extended northwest from Jan Mayen Island to Northwest Greenland.

3. Greenland North of 72 N.

The eight storms detected over Northern Greenland (Fig. 25b) tended to form in very strong offshore 1000 mb height gradients between ridging from Northern Greenland and a low in the Northern Norwegian Sea. Flow was diagonally onshore with cold-air advection. Heights were below and temperatures above climatology. At 500 mb, storms formed under anti-cyclonic, divergent flow with neutral temperature advection. Temperatures were above normal. The 25 backtracked storms formed under similar conditions with a strong offshore gradient, but with the Norwegian Sea low further to the south. However, heights were above and temperatures below the mean. At 500 mb, storms formed under a sharper short-wave ridge with cold-air advection. Heights were above and temperatures below climatology.

4. Vicinity of Scoresby Sound.

The five storms detected near Scoresby Sound (Fig 22c) formed just ahead of a 1000 mb low over Southern Greenland and in a very strong offshore height gradient between Greenland and a very deep low west of Central Norway. Flow was diagonally onshore with cold-air advection. Heights were higher and temperatures lower than climatology. At 500 mb, the storms formed under slightly anti-cyclonic flow behind a cut-off low over the Norwegian Sea and ridging over Central Greenland. There was neutral temperature advection aloft. The 10 backtracked storms formed under similar 1000 mb conditions, except the Norwegian Sea low was not as deep and temperatures were near the mean. At 500 mb, the storms formed under a short-wave ridge with neutral advection. Heights were above the mean, but temperatures were near normal.

5. Greenland South of 68 N.

The single storm detected over Southern Greenland (Fig. 22c) formed just ahead of a 1000 mb low over Southern Greenland and in a very strong off-shore height gradient between Greenland and a very deep low in the North Sea. Flow was diagonally onshore

with cold-air advection. Heights and temperatures were above climatology. At 500 mb, the storm formed southwest of a bubble high in divergent flow with cold-air advection. Heights were above the mean. The six backtracked storms formed in a very strong 1000 mb height gradient between ridging from the Davis Strait and a deep low in the Denmark Strait. Flow was cross-shore with warm-air advection. Heights and temperatures were lower than the mean. At 500 mb, the storms formed under a sharp long-wave trough with cold-air advection. Heights and temperatures were below climatology.

G. MARCH

1. Summary.

The March surface climatology (Fig. 23a) shows the polar front extending southwest from the Barents Sea, south of Iceland to Southern Greenland. The 500 mb long-wave trough lay over Southern Greenland and a short-wave ridge over Scoresby Sound. The 51 March storms formed with no apparent pattern. There were very strong 1000 mb height gradients, but the Scoresby Sound cases tended to have cross-shore rather than offshore gradients. Flow was onshore for north and central cases, but cross-shore for southern storms. There was cold-air advection in all cases except the southern backtracked storms which had both warm- and cold-air advection. Heights and temperatures were both above and below climatology. At 500 mb, storms tended to form with heights below and temperatures above the mean. Storms formed under ridges and troughs and both divergent and convergent flow. Temperature advection was warm, cold and neutral.

2. Mean Structure

At 1000 mb (Fig. 23a), a -100 meter low center in the Denmark Strait extended pressure troughs west to Cape Farewell, northeast into the Barents Sea, north northeast to west of Svalbard and north through the Denmark Strait to Central Greenland. Ridging from Northern Greenland extended south along the East Greenland coast toward Iceland. At 500 mb, A 4980 meter low over Northeast Canada extended a trough southeast over Southern Greenland into the Denmark Strait. A short-wave ridged northwest from Jan Mayen Island over Scoresby Sound to Central Greenland and a trough extended southeast from Northeast Greenland toward the Lofoten Islands.

3. Greenland North of 72 N.

The four storms detected over Northern Greenland (Fig. 23b) formed in a very strong 1000 mb offshore height gradient between ridging from Northern Greenland and a low west of Central Norway. Flow was diagonally onshore with cold-air advection.

Heights were below and temperatures above climatology. At 500 mb, the storms formed under anti-cyclonic turning and divergent flow with neutral temperature advection. Heights and temperatures were near the mean. The 21 backtracked storms formed in strong offshore height gradients, but the gradient was more zonal due to a trough in the Norwegian Sea. Temperatures were near the mean. At 500 mb, the pattern was slightly different with anti-cyclonic, converging flow and slight cold-air advection. Heights were below climatology.

4. Scoresby Sound.

The five storms detected near Scoresby Sound (Fig. 23c) formed in a strong bi-directional offshore 1000 mb height gradient between ridging from Northern Greenland and lows in the Northern Norwegian Sea and the Southern Denmark Strait. Flow was diagonally onshore with cold-air advection. Heights were above and temperatures below climatology. At 500 mb, the storms formed under a short-wave ridge with divergent flow and warm-air advection. Heights and temperatures were near the mean. The eight backtracked storms formed in a strong cross-shore height gradient between ridging from Northern Greenland and a deep low in the Denmark Strait. The storms formed in anti-cyclonic turning between inverted troughs in the Fram Strait and over Southern Greenland. Flow was onshore with generally cold-air advection. Heights were below normal, but temperatures were near the mean. At 500 mb, the storms formed under divergent flow between a short-wave ridge over Central Greenland and a trough over the Norwegian Sea. There was warm-air advection aloft. Temperatures were above the mean.

5. Greenland South of 68 N.

The three storms detected over Southern Greenland (Fig. 23d) were formed in a weaker than normal 1000 mb offshore height gradient between ridging from Baffin Bay and a low in the Denmark Strait. Flow was cross-shore with cold-air advection. Heights and temperatures were near normal. At 500 mb, the storms formed under a long-wave trough in divergent flow west of a cut-off low. There was cold-air advection aloft. Heights and temperatures were above normal. The 10 backtracked storms formed under similar 1000 mb conditions, but with both warm- and cold-air advection in the cross-shore flow. Heights were above and temperatures below climatology. At 500 mb, the storms formed under a long-wave trough with divergent flow. Heights and temperatures were below the mean.

H. APRIL

1. Summary.

April surface climatology (Fig. 24a) shows the polar front extending southwest from the Barents Sea across Northern Iceland and the Denmark Strait to south of Cape Farewell. The 500 mb long-wave trough was located over Southern Greenland and the Denmark Strait while a short-wave ridge was over Scoresby Sound. The 52 April storms formed with weaker offshore 1000 mb height gradients in the north and south, but strong gradients near Scoresby Sound. Flow was generally onshore with cold-air advection, except for the southern backtracked case which had cross-shore flow and neutral advection. Height and temperature differences had no pattern. At 500 mb, there was also no apparent pattern with storms forming under lows, troughs and ridges and in convergent and divergent flow. Warm-air was the preferred temperature advection.

2. Mean Structure

At 1000 mb (Fig. 24a), a +60 meter low center in the Denmark Strait extended pressure troughs west to Cape Farewell, northeast into the Barents Sea and north northeast to west of Svalbard. Ridging extended south from Northern Greenland along the East Greenland Coast toward Iceland. At 500 mb, a long-wave trough extended southeast from Baffin Bay across Southern Greenland to Western Europe. A long-wave ridge extended north from Russia into the Barents Sea and over Svalbard and short-wave ridges extended northeast from Scoresby Sound to Northwest Greenland.

3. Greenland North of 72 N.

The five storms detected over Northern Greenland (Fig. 24b) formed with a near normal 1000 mb offshore height gradient between ridging from Northern Greenland and a trough in the Fram Strait. Flow was diagonally onshore with cold-air advection. Heights were below and temperatures above climatology. At 500 mb, the storms formed just west of a cut-off low in the Fram Strait with warm-air advection. Heights were above and temperatures near the mean. The 22 backtracked storms formed under similar 1000 mb conditions, but with much weaker offshore height gradients. Heights and temperature trends were reversed, with heights above and temperatures below the mean. At 500 mb, the storms formed under straight-line, but converging flow and cold-air advection. Heights were below the mean.

4. Scoresby Sound.

The four storms detected near Scoresby Sound (Fig. 24c) formed with a bi-directional offshore 1000 mb height gradient between a high over Northeast Greenland, a low in the Norwegian Sea and a trough in the Denmark Strait. Flow was diagonally

onshore with cold-air advection. Heights were above and temperatures near the mean. At 500 mb, the storms formed under a short-wave ridge that propagated through a long-wave trough with cold-air advection. Heights and temperatures were above the mean. The eight backtracked storms formed in a diagonally offshore 1000 mb height gradient between ridging from Northern Greenland and a low over Southwest Iceland. Flow was onshore with cold-air advection. Heights and temperatures were both below climatology. At 500 mb, the storms also formed under a short-wave ridge, but with warm-air advection. Heights and temperatures were both below the mean.

5. Greenland South of 68 N.

The 10 storms detected over Southern Greenland (Fig. 24d) formed in a weak 1000 mb offshore height gradient between ridging from Central Greenland and a weak trough in the Denmark Strait. Flow was onshore with cold-air advection. Heights were above the mean. At 500 mb, the storms formed under a long-wave ridge with warm-air advection. Heights and temperatures were above the mean. The seven backtracked storms formed in stronger offshore height gradient between ridging from Central Greenland and a low in the Denmark Strait with cross-shore flow and neutral advection. Heights were below climatology. At 500 mb, the storms formed under a long-wave trough with divergent flow and warm-air advection. Heights were much higher than normal with temperatures just below the mean.

I. MAY

1. Summary.

The May surface climatology (Fig. 25a) shows the polar front extending southwest from the Barents Sea across Northern Iceland to Southern Greenland. The 500 mb long-wave was located over Southern Greenland. The 41 May storms were generally formed with weaker than normal 1000 mb offshore height gradients with onshore flow and cold-air advection. Heights and temperatures were both below climatology. At 500 mb, storms formed under a variety of upper-air patterns, but generally with cold-air advection aloft. Heights and temperatures were also both generally below the mean.

2. Mean Structure.

At 1000 mb (Fig. 25a), a +80 meter low centered in the Denmark Strait extended pressure troughs west to Cape Farewell and northeast into the Barents Sea. A trough also extended north from Bear Island to Svalbard. Ridging extended south from Northern Greenland along the East Greenland coast to Iceland. At 500 mb, a 5220

meter low over Northern Canada extended troughs east, through the Fram Strait, into the Barents Sea and southeast, across Central Greenland to Iceland.

3. Greenland North of 72 N.

The four storms detected over Northern Greenland (Fig. 25b) were formed in a diagonally offshore 1000 mb height gradient between ridging over Northern Greenland and lows over Central Norway and the Denmark Strait. Flow was diagonally onshore with cold-air advection. Heights and temperatures were below climatology. At 500 mb, two southern storms were formed under a short-wave ridge while the two northern storms formed in divergent flow. All four were associated with cold-air advection. Heights and temperatures were below normal. The 17 backtracked storms formed with a nearly identical 1000 mb pattern, but with a stronger offshore height gradient with a low near Bear Island. At 500 mb, storms formed under a short-wave trough, but like the detected case, there was cold-air advection and both heights and temperatures were below climatology.

4. Scoresby Sound.

The four storms detected near Scoresby Sound (Fig. 25c) formed in a weak bi-directional 1000 mb offshore height gradient between ridging from Northern Greenland and lows south of Bear Island and in the Denmark Strait. Flow was cross-shore with cold-air advection. Heights were below climatology. At 500 mb, the storms formed under a slight short-wave ridge with divergent flow and cold-air advection. Heights and temperatures were below the mean. The three backtracked storms formed with a much stronger, but along-shore 1000 mb height gradient with onshore flow and cold-air advection. Heights and temperatures were below climatology. At 500 mb, the storms formed north of a cut-off low in convergent flow and warm-air advection. Heights were below the mean, but temperatures were near normal.

5. Greenland South of 68 N.

The nine storms detected over Southern Greenland (Fig. 25d) formed near a bubble high in the Denmark Strait with very little 1000 mb height gradient. Flow was generally onshore with warm-air advection. Heights were above and temperatures below the mean. At 500 mb, the storms formed under a weak short-wave ridge with cold-air advection. Heights and temperatures were both above climatology. The four backtracked storms formed in a weak 1000 mb height gradient between ridging from the Davis Strait and a low in the Denmark Strait. Flow was onshore for the three northern storms and offshore for the southern storm. There was cold-air advection in both cases.

Heights and temperatures were below the mean. At 500 mb, the storms formed under a long-wave trough with neutral temperature advection.

J. INTERPRETATIONS OF RESULTS

As depicted in Table 8, over half the polar lows either detected over or backtracked to Greenland were associated with Northern Greenland, probably due to the sheer size of the landmass. The fewest storms were detected over Southern Greenland, possibly due to the less frequent satellite coverage of the area. However, a larger percentage of storms were backtracked there from better observed areas, indicating that the number of backtracked storms may be a more accurate representation of the formation frequency. The fewest storms can be attributed to Scoresby Sound, but this area may be the most active polar low genesis region because the storms are concentrated to a 4 degree latitude range.

Polar lows detected over and backtracked to the three regions of Greenland form with no clear-cut common synoptic-scale pattern, but some general trends appear when the storms for each case are compared for the entire season. Tables 9 through 14 compare the listed parameters for the three regions for each month.

The following low-level parameters were examined:

- Direction of flow (on-shore/off-shore),
- Temperature advection,
- Strength and direction of height gradient (on-shore/off-shore),
- Temperature and height differences from climatology,

and the following upper-level parameters were examined:

- Direction of curvature (cyclonic/anti-cyclonic),
- Indications of upper-level horizontal divergence or convergence,
- Temperature advection,
- Temperature and height deviations from climatology.

Overall, polar lows form with stronger than normal offshore 1000 mb height gradients, except in Southern Greenland during November where detected storms formed with onshore gradients. The low-level height and temperature gradients tended to be stronger than climatology and perpendicular to the coast line, although cross-shore gradients were seen in some Scoresby Sound cases. Tables 9 - 17 compare the above listed parameters for the three geographic areas for each month. Development in

regions of enhanced offshore height gradients agrees with Kanestrom et al. (1988), who examined pressure gradients in various locations in the Nordic Seas.

Polar lows formed under both troughs and ridges, with on-shore and off-shore flow, under divergent and convergent flow, with cold- and warm-air advection at both upper- and lower-levels and with positive and negative Central Greenland temperature deviations. The overall synoptic patterns differed between months, locations and between detected and backtracked storms.

1. Northern Greenland

Polar lows detected over Northern Greenland (Table 9) tended to form with

Table 9. STORMS DETECTED OVER NORTHERN GREENLAND

Month	1000 mb				500 mb			
	ΔH	ΔT	Flow	Advection	ΔH	ΔT	Flow	Advection
Sep	-20	--	Off-shore (Cross)	CAA (WAA)	--	--	Ridge (Neutral)	CAA
Oct	60-80	+5	Off-shore (Cross)	WAA CAA (CAA)	+120	+3-4	Ridge	CAA
Nov	+20	+2-3	Cross-shore (On)	CAA	+60	+3-5	Ridge	CAA
Dec	-20	--	Off-shore (Cross)	WAA (CAA)	--	+2-3	Trough (Ridge)	CAA
Jan	-40	--	Onshore	CAA	--	--	Trough Ridge (Ridge)	CAA
Feb	-20	+2-4	Onshore	CAA	--	+2-3	Ridge Div (Ridge)	Neutral (CAA)
Mar	-20	+3	Onshore	CAA	--	--	Div (Trough)	Neutral (CAA)
Apr	-40	+2	Onshore	CAA	+60	--	Under Low (Trough)	WAA (CAA)
May	-20	-3-5	Onshore (Cross)	CAA	-60-90	-5-6	Ridge Div (Div)	CAA

a low-level trough near Bear Island or Svalbard, or a low in the Barents Sea. Ridging or divergent flow was present at 500 mb, but troughing was also seen in December and January and storms formed under a cut-off low in April. Low-level flow was offshore in September through December and onshore in January through May. Both upper- and lower-level temperatures were warmer over the coast. Heights were lower than the mean at 1000 mb, but higher than normal aloft. There was cold-air advection at both levels. The 1000 mb height gradients between the Greenland coast and the minimum offshore low or trough were generally stronger than climatology (Table 10). The conditions for storms backtracked to Northern Greenland were similar to those for storms detected there with ridging over Northern Greenland and a low or trough offshore. The offshore height gradients shown in Table 10 were slightly stronger than the detected case, but both were stronger than climatology.

Table 10. NORTHERN GREENLAND HEIGHT GRADIENTS

Month	Detected	Back-tracked	Climatology
Sep	+ 50	+ 40	+ 25
Oct	+ 30	+ 40	+ 30
Nov	+ 20	+ 50	+ 60
Dec	+ 20	+ 50	+ 40
Jan	+ 80	+ 80	+ 50
Feb	+ 160	+ 160	+ 120
Mar	+ 140	+ 160	+ 100
Apr	+ 50	+ 20	+ 50
May	+ 80	+ 60	+ 40
Avg	+ 70	+ 75	+ 45

Table 11 shows the ridging aloft is less prevalent than the detected cases, again with troughing in December, January and May and neutral flow in September and April. There was cold-air advection at both levels. Low-level flow is generally onshore which advects moisture onto the pack-ice from the Fram Strait. Major differences are that 1000 and 500 mb temperatures over the coast are colder rather than higher than climatology and 1000 mb heights are higher, rather than lower than the mean. The 500 mb heights are higher than normal in September through February and lower than

normal in March through May, where there is troughing aloft. Low-level heights are higher than climatology, while 500 mb heights are higher through February, then lower for the rest of the season.

Table 11. STORMS BACKTRACKED TO NORTHERN GREENLAND

Month	1000 mb				500 mb			
	ΔH	ΔT	Flow	Advection	ΔH	ΔT	Flow	Advection
Sep	+20	+1-2	Off-shore (Cross)	CAA (WAA)	+60	--	Neu- tral	CAA
Oct	+20	--	Off-shore (Cross)	WAA (CAA)	+60	--	Ridge	CAA
Nov	-20	--	Onshore	CAA	--	--	Ridge	CAA
Dec	20-30	-3-5	Cross-shore	CAA	--	--	Trough (Ridge)	CAA
Jan	+20	--	Onshore	CAA	+30	--	Trough Div (Ridge)	CAA
Feb	+20	-2	Onshore	CAA	30-60	-2-3	Ridge	CAA
Mar	-20-40	--	Onshore	CAA	-30-40	--	Conv (Trough)	CAA
Apr	+60	-2-3	Onshore	CAA	-40-60	--	Neu- tral Conv (Trough)	CAA
May	-20-30	-2-3	Onshore	CAA	-90	-2-4	Trough (Div)	CAA

The ridging aloft supports the presence of low level convergence and ascending air, a necessary condition for polar low formation. This tends to produce lower heights at the surface, seen in the detected, but not the backtracked cases. However, 500 mb heights are generally higher than climatology, suggesting that subsidence and katabatic flows have previously occurred and that polar low cyclogenesis mechanisms have taken over to deepen the initial disturbance. The cold-air advection at both levels tends to reduce the upward motion.

Polar low formation is not dependent on the low-level flow. As noted by Bromwich (1989 and 1991), on-shore winds advect moisture and warmer temperatures

onto the pack ice and establish the main baroclinic zone closer to the coast. Off-shore winds advect colder air over the warmer open water, moving the main baroclinic zone offshore.

2. Scoresby Sound

Storms detected over Scoresby Sound tend to form with a low in the Denmark Strait and or Norwegian Sea and ridging from Northern or Central Greenland which establishes strong offshore height and over water temperature gradients. The off-shore 1000 mb height gradients were much stronger than climatology (Table 12). Storms formed under ridging or divergent flow aloft (Table 13), except for September, which had no turning. Low-level flow was generally onshore, with cold-air advection. There was generally also cold-air advection aloft. Temperatures at both levels were colder than climatology and there was cold-air advection aloft. Heights at 1000 mb were above the mean, but generally below normal at 1000 mb.

Table 12. SCORESBY SOUND HEIGHT GRADIENTS

Month	Detected	Back-tracked	Climatology
Sep	--	+ 85	+ 50
Oct	+ 120	+ 30	+ 20
Nov	+ 240	+ 100	+ 50
Dec	+ 60	+ 90	+ 50
Jan	+ 210	+ 120	+ 70
Feb	+ 340	+ 140	+ 120
Mar	+ 120	+ 160	+ 140
Apr	+ 80	+ 100	+ 70
May	+ 80	+ 160	+ 30
Avg	+ 155	+ 110	+ 65

Polar lows backtracked to Scoresby Sound formed under similar conditions to detected storms with a low or trough over open water and off-shore ridging. Storms formed under 500 mb ridging or divergent flow except in May where storms formed north of a cut-off low (Table 14). There was low-level cold-air advection for all months, but at 500 mb, there was cold-air advection for September through December and warm-air or neutral advection for the rest of the season. Flow was onshore in all months

Table 13. STORMS DETECTED OVER SCORESBY SOUND

Month	1000 mb				500 mb			
	ΔH	ΔT	Flow	Advection	ΔH	ΔT	Flow	Advection
Sep	--	--	--	--	--	--	--	--
Oct	-20-40	-2-3	Off-shore (Cross)	WAA (CAA)	-90	-3	Neu-tral	CAA
Nov	--	-7	Onshore (Cross)	CAA	-120	-5	Ridge Div (Ridge)	CAA
Dec	-20	--	Onshore	Neutral (CAA)	-30	--	Ridge Div (Ridge)	CAA
Jan	+ 100	+ 5	Onshore	CAA	+ 90	--	Ridge	CAA (WAA)
Feb	+ 60	-5	Onshore	CAA	--	-5	Ridge (Col)	Neutral
Mar	+ 20	-3	Onshore	CAA	--	--	Ridge Div (Ridge)	WAA
Apr	+ 30	--	Onshore	CAA	+ 60	+ 2	Ridge (Conv)	CAA (Neu-tral)
May	-30	--	Cross-shore (On)	CAA	-40	-2-3	Ridge	CAA

except for November. The 1000 and 500 mb heights and temperatures were above normal during the early season, but were below climatology in the later season. The 1000 mb offshore height gradients were much stronger than both climatology and the northern storm cases, but less than for the storms backtracked to Scoresby Sound.

3. Southern Greenland

Polar lows detected south of 68° North are generally associated with a deep synoptic low in the Denmark Strait ridging over Southern Greenland or the Davis Strait with a sharp, cold 500 mb trough aloft (Table 15).

However, there is ridging aloft in April and May. Storms generally form behind the low with offshore cold-air advection over warmer water, but some form with on-shore warm-air advection north of the low. Heights at 1000 and 500 mb are below the mean

Table 14. STORMS BACKTRACKED TO SCORESBY SOUND

Month	1000 mb				500 mb			
	ΔH	ΔT	Flow	Advection	ΔH	ΔT	Flow	Advection
Sep	+ 20	-2-3	Onshore	CAA	+ 30	-3-5	Ridge	CAA
Oct	+ 20	+ 5	Onshore	CAA	+ 60	+ 2	Ridge	CAA
Nov	-20	+ 1-2	Cross-shore	CAA	+ 20	+ 2	Ridge	CAA
Dec	+ 40	-5	Onshore	CAA	-20	-2-3	Ridge Conv (Ridge)	CAA
Jan	20-40	-2	Onshore	CAA	+ 20	-2	Ridge Div	WAA
Feb	+ 20	--	Onshore	CAA	+ 60	--	Ridge (Col)	Neutral
Mar	-40	--	Onshore	CAA	-30	+ 2	Div (Ridge)	WAA
Apr	-80	-2-3	Onshore	CAA	-60	-2	Ridge Div (Conv)	WAA (Neutral)
May	-60	-2	On-shore	CAA	-90	--	North of Low (Div)	WAA (CAA)

for November through January, but above climatology for the rest of the season. Early season 500 mb temperatures are below normal, but above the mean later in the season. There is both warm- and cold-air advection at 1000 and 500 mb. Offshore 1000 mb height gradients are weaker than northern and central cases (Table 16), but are stronger during polar low cases than climatology.

Polar lows backtracked to Southern Greenland form with nearly identical conditions to storms that are detected there, generally forming under 500 mb troughs with deep synoptic lows in the Denmark Strait. However, ridging is present in September and October (Table 17). Heights and temperatures at 1000 and 500 mb are generally lower than There is no pattern to the temperature advection at either 1000 or 500 mb. Flow at 1000 mb was on, of and cross-shore. The offshore height gradients were less than the detected case, but more than climatology.

Table 15. STORMS DETECTED OVER SOUTHERN GREENLAND

Month	1000 mb				500 mb			
	ΔH	ΔT	Flow	Advection	ΔH	ΔT	Flow	Advection
Sep	--	--	--	--	--	--	--	--
Oct	--	--	--	--	--	--	--	--
Nov	-20-40	+2	Onshore	WAA	-60	-4	Trough (Ridge)	WAA
Dec	--	-3-4	Off- shore (On)	CAA (WAA)	-60	-3	Trough	CAA (Neu- tral)
Jan	-60-80	-5-10	Off- shore (On Off)	WAA (WAA CAA)	-120	-5	Trough	CAA
Feb	+100	+3-5	Onshore (On Off)	CAA (CAA WAA)	+150	--	Div (Trough)	CAA (Neu- tral)
Mar	--	--	Cross- shore (On Off)	CAA (WAA CAA)	+60	+3	Trough Div (Trough)	CAA
Apr	20-30	--	Onshore	CAA (WAA)	60-80	+3	Ridge (Trough Div)	WAA (Neu- tral)
May	+20	-2-3	Onshore	WAA (CAA)	+60	+3	Ridge Div (Div)	CAA (WAA)

4. Summary

Indirect evidence suggests that katabatic influences play a role in polar low formation over Northern and Central Greenland. In nearly all cases, off-shore height gradients were stronger than climatology. The strongest height gradients were seen in the Scoresby Sound cases, with weaker gradients for Northern Greenland. In contrast, very weak gradients were observed in Southern Greenland. Katabatic influences seem to play the largest role in Scoresby Sound area of Central Greenland, with a lesser influence over Northern Greenland. Katabatic winds may contribute to polar low formation, but to a lesser extent than other triggering and formation mechanisms.

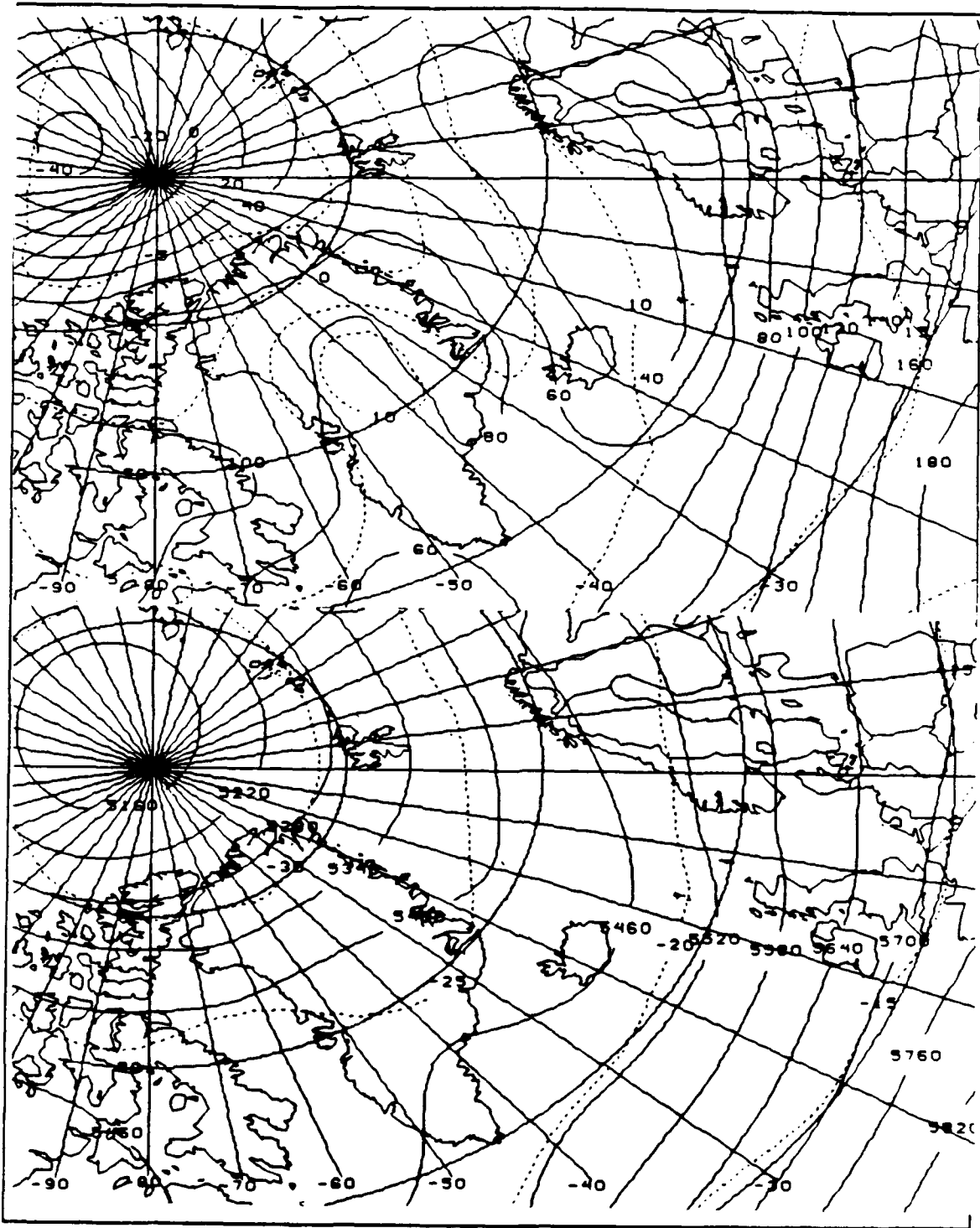


Figure 17a. September climatological NOGAPS fields for 1000 mb (upper) and 500 mb (lower).

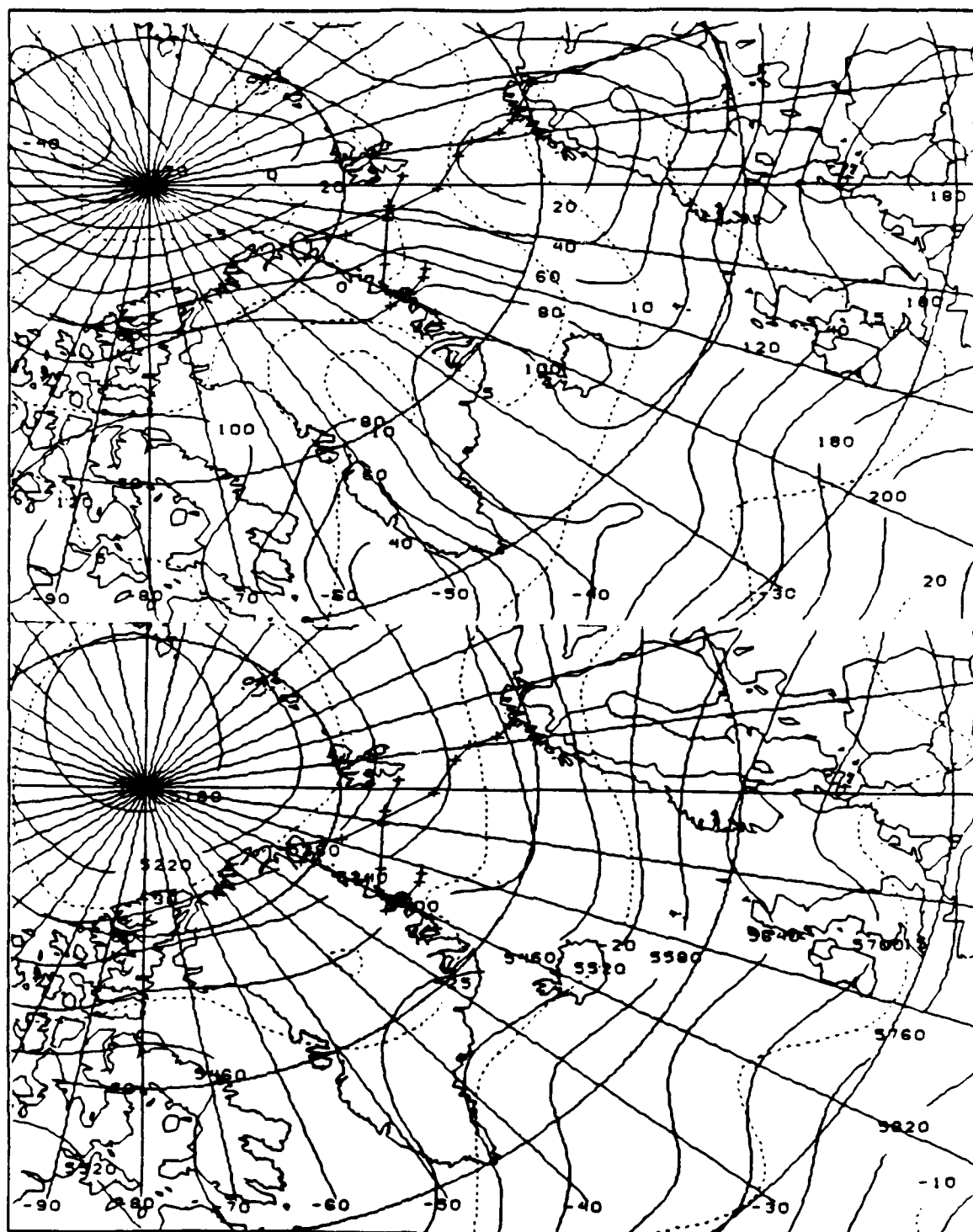


Figure 17b. September mean 1000 mb (upper) and 500 mb (lower) NOGAPS fields for polar lows detected over Northern Greenland.

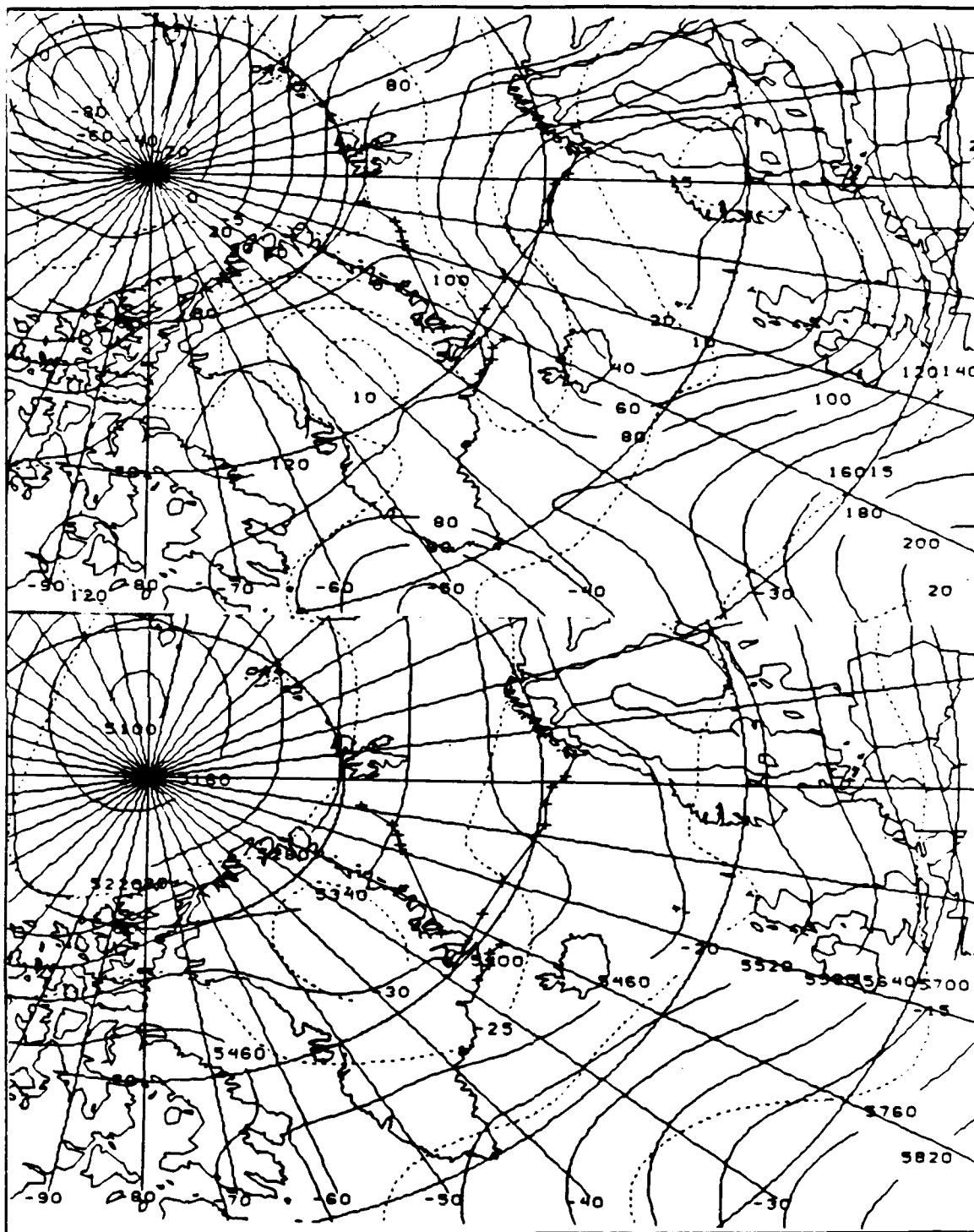


Figure 17c. September mean 1000 mb (upper) and 500 mb (lower) NOGAPS fields for polar backtracked to the Scoresby Sound region.

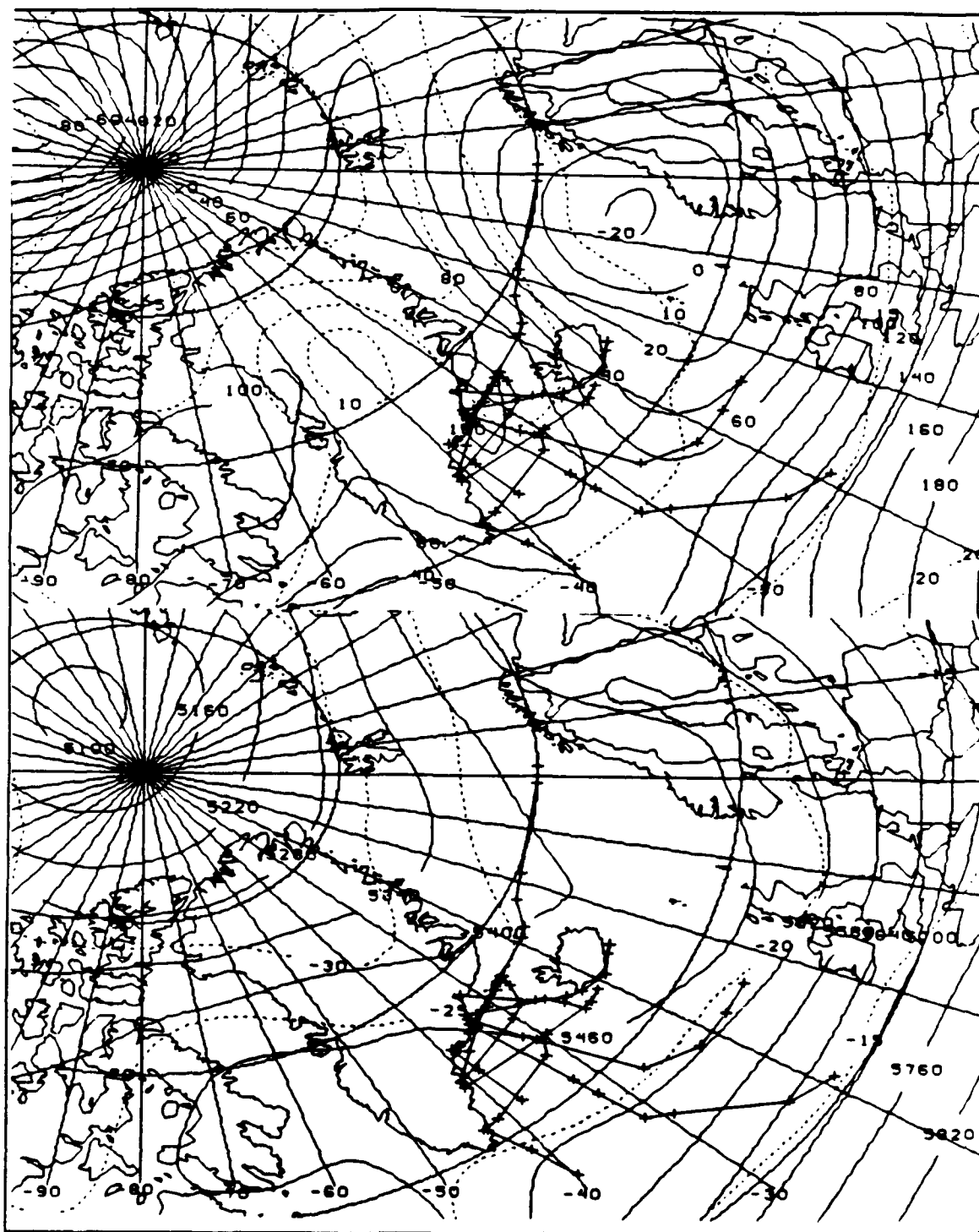


Figure 17d. September mean 1000 mb (upper) and 500 mb (lower) NOGAPS fields for polar lows backtracked to Southern Greenland.

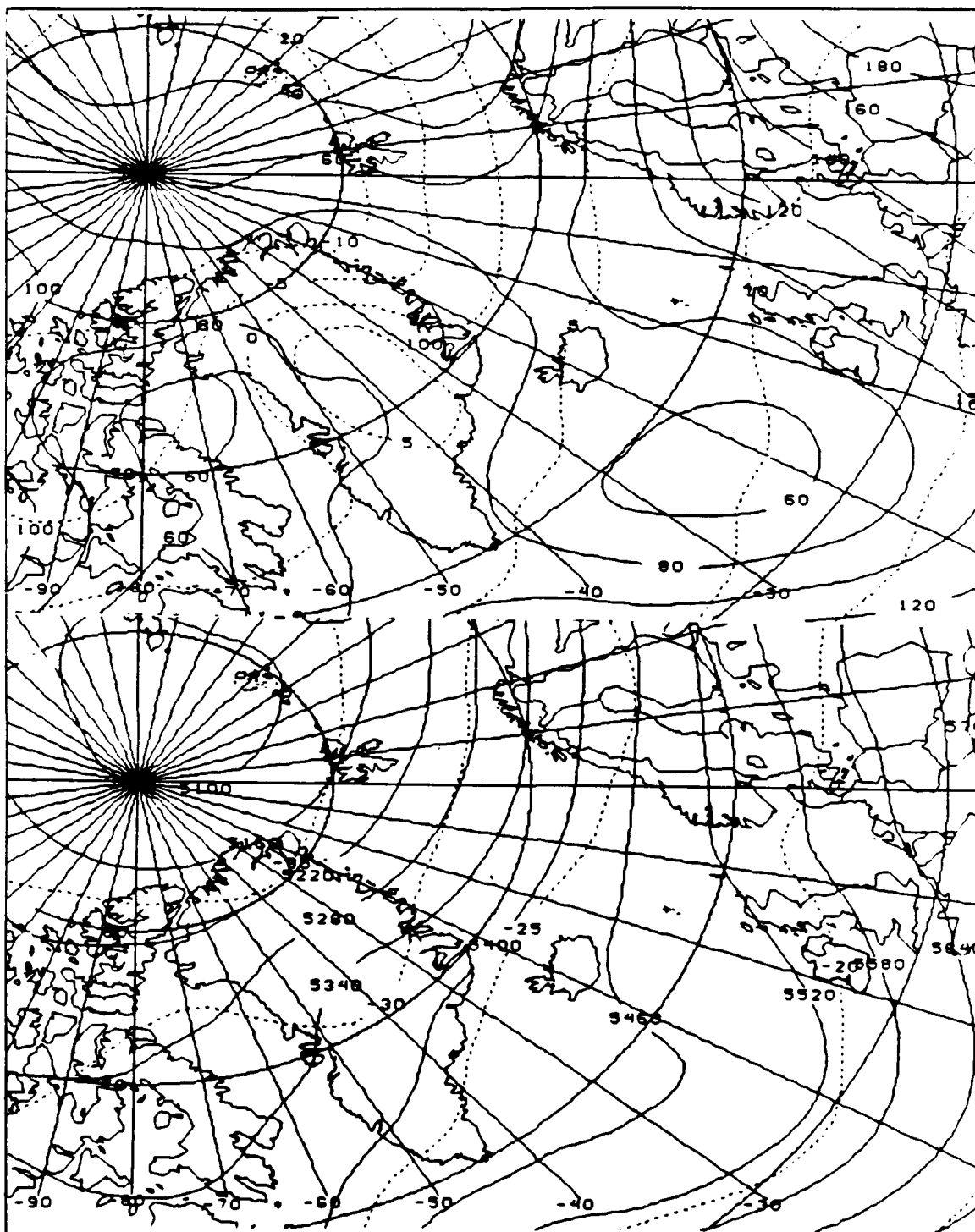


Figure 18a. October climatological NOGAPS fields for 1000 mb (upper) and 500 mb (lower).

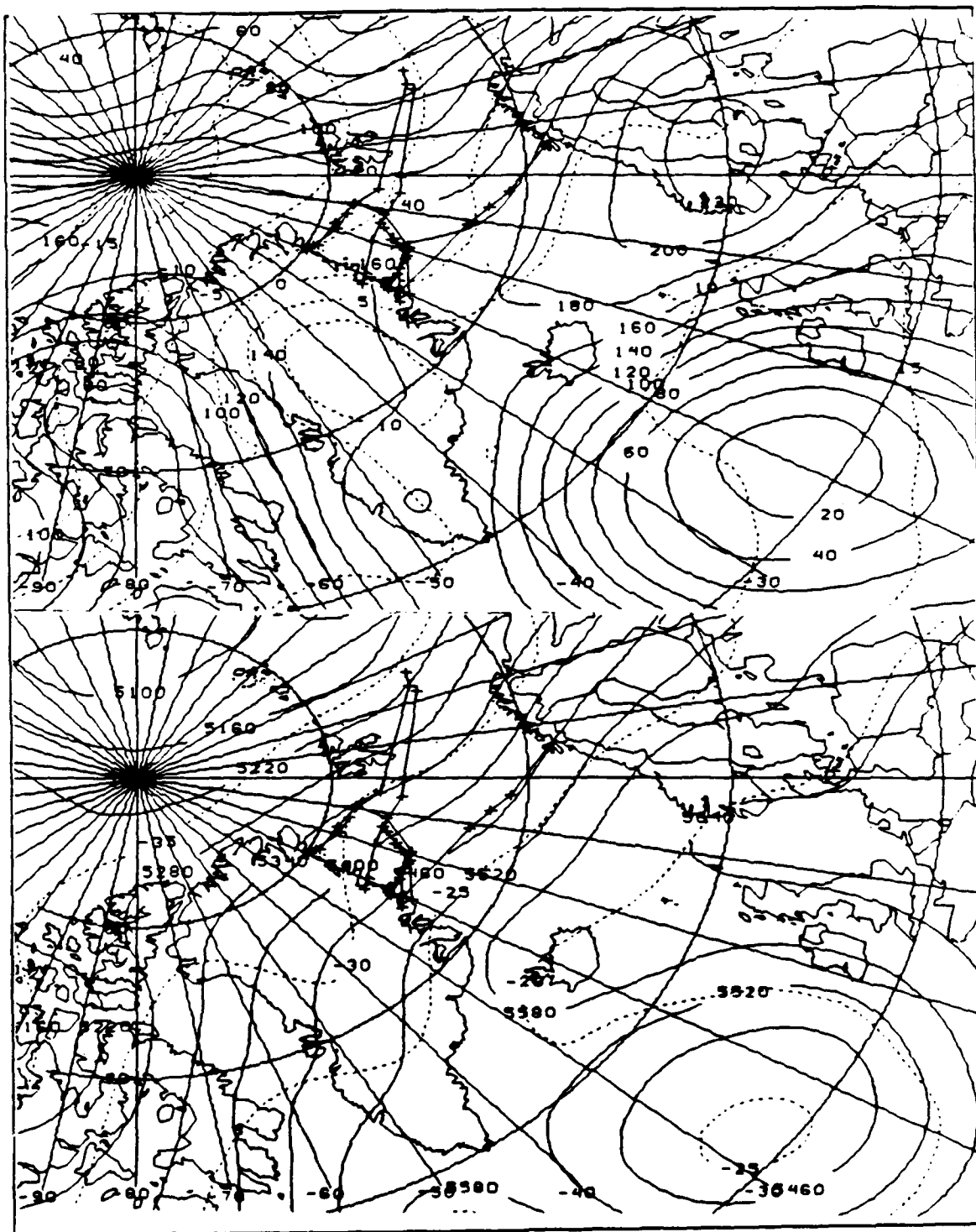


Figure 18b. October mean 1000 mb (upper) and 500 mb (lower) NOGAPS fields for polar lows detected over Northern Greenland.

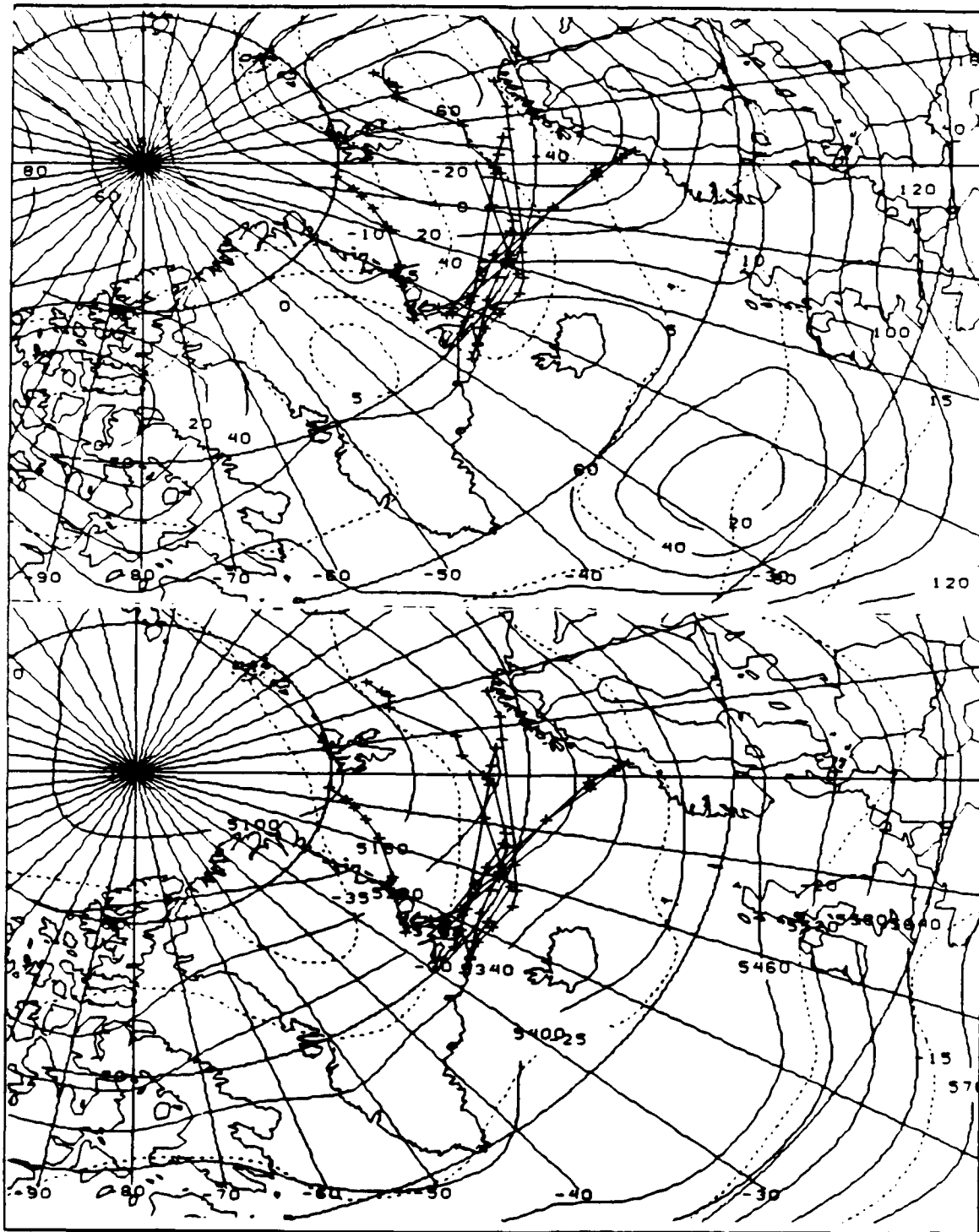


Figure 18c. October mean 1000 mb (upper) and 500 mb (lower) NOGAPS fields for polar lows detected over the Scoresby Sound region.

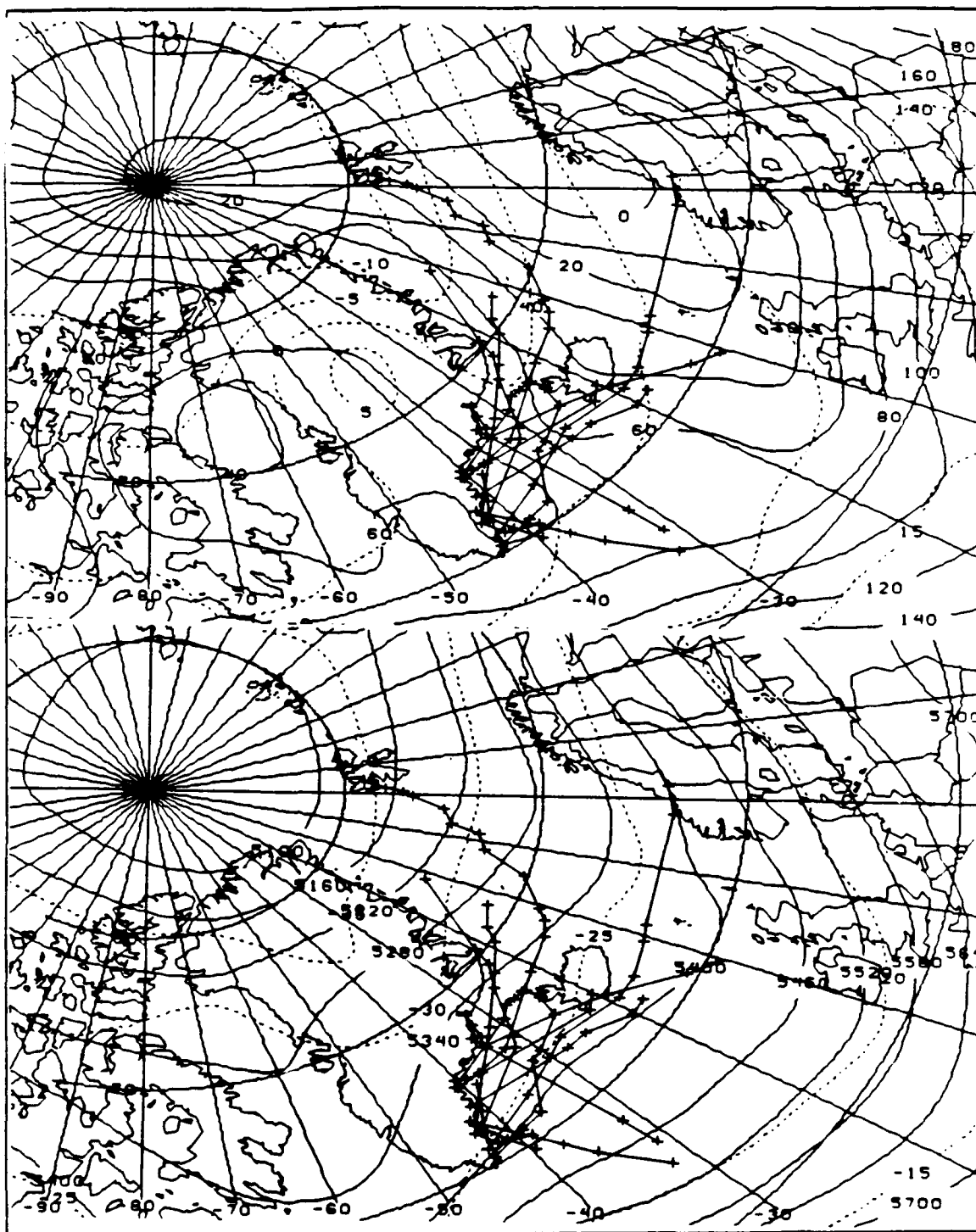


Figure 18d. October mean 1000 mb (upper) and 500 mb (lower) NOGAPS fields for polar lows backtracked to Southern Greenland.

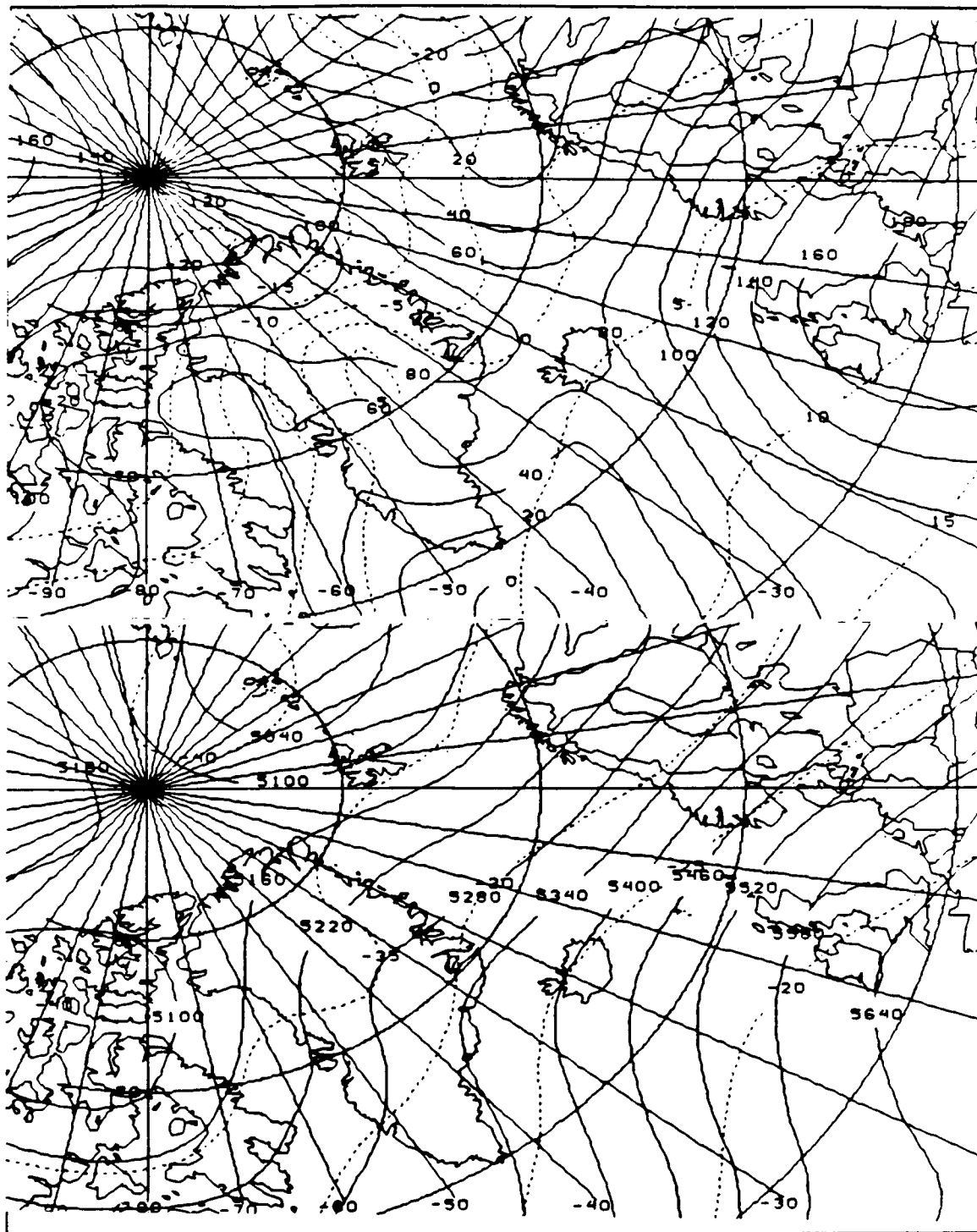


Figure 19a. November climatological NOGAPS fields for 1000 mb (upper) and 500 mb (lower).

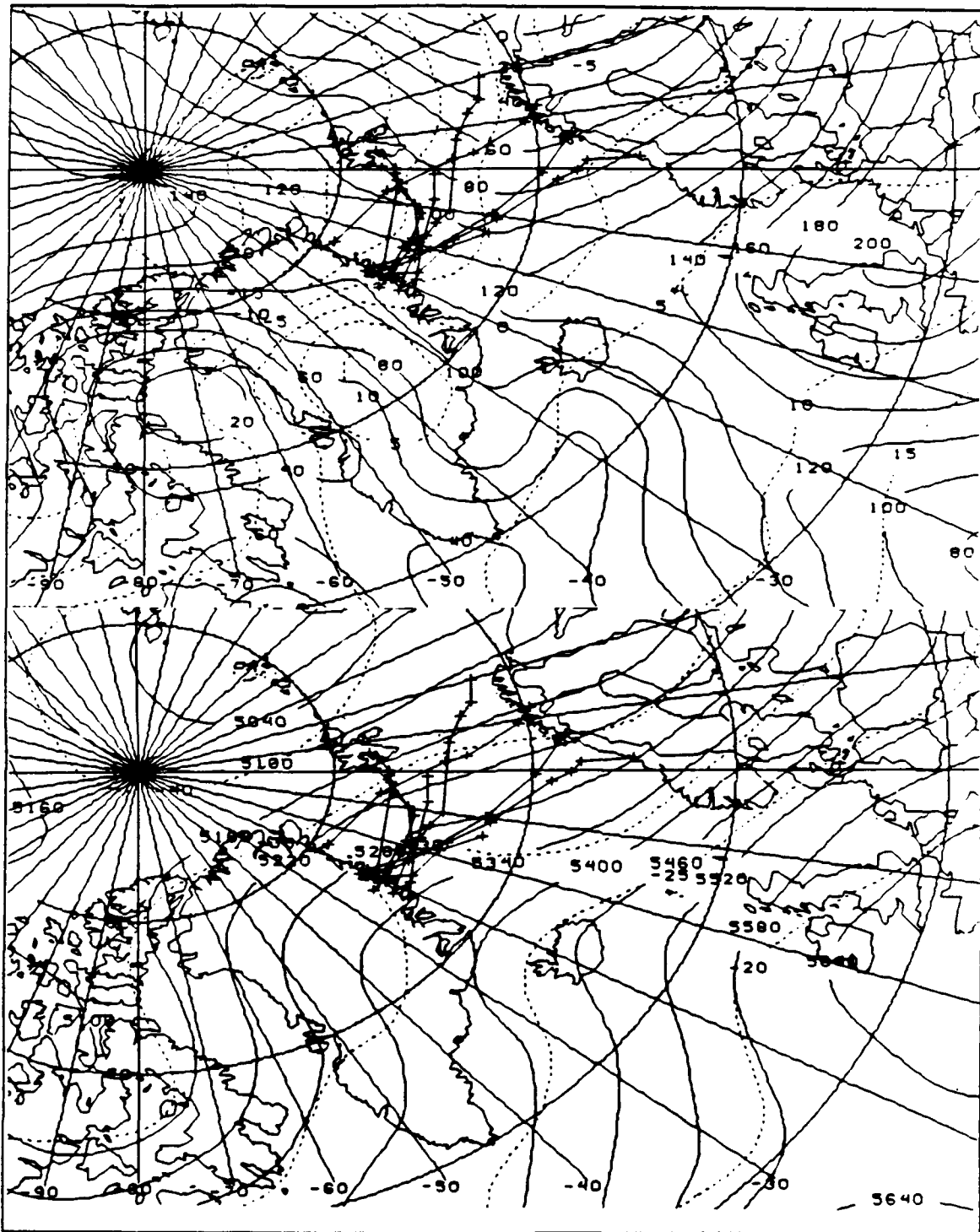


Figure 19b. November mean 1000 mb (upper) and 500 mb (lower) NOGAPS fields for polar lows detected over Northern Greenland.

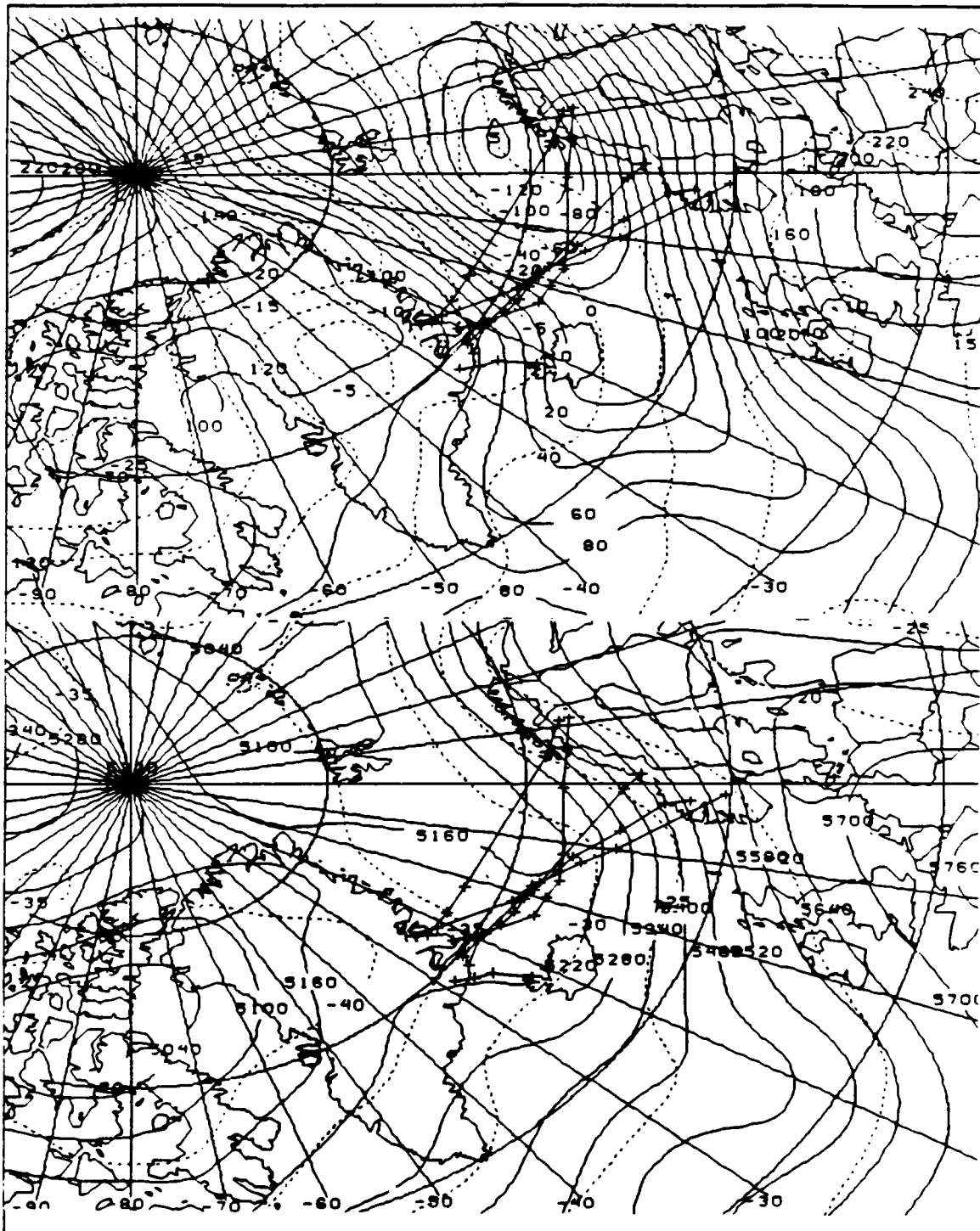


Figure 19c. November mean 1000 mb (upper) and 500 mb (lower) NOGAPS fields for polar lows detected over the Scoresby Sound region.

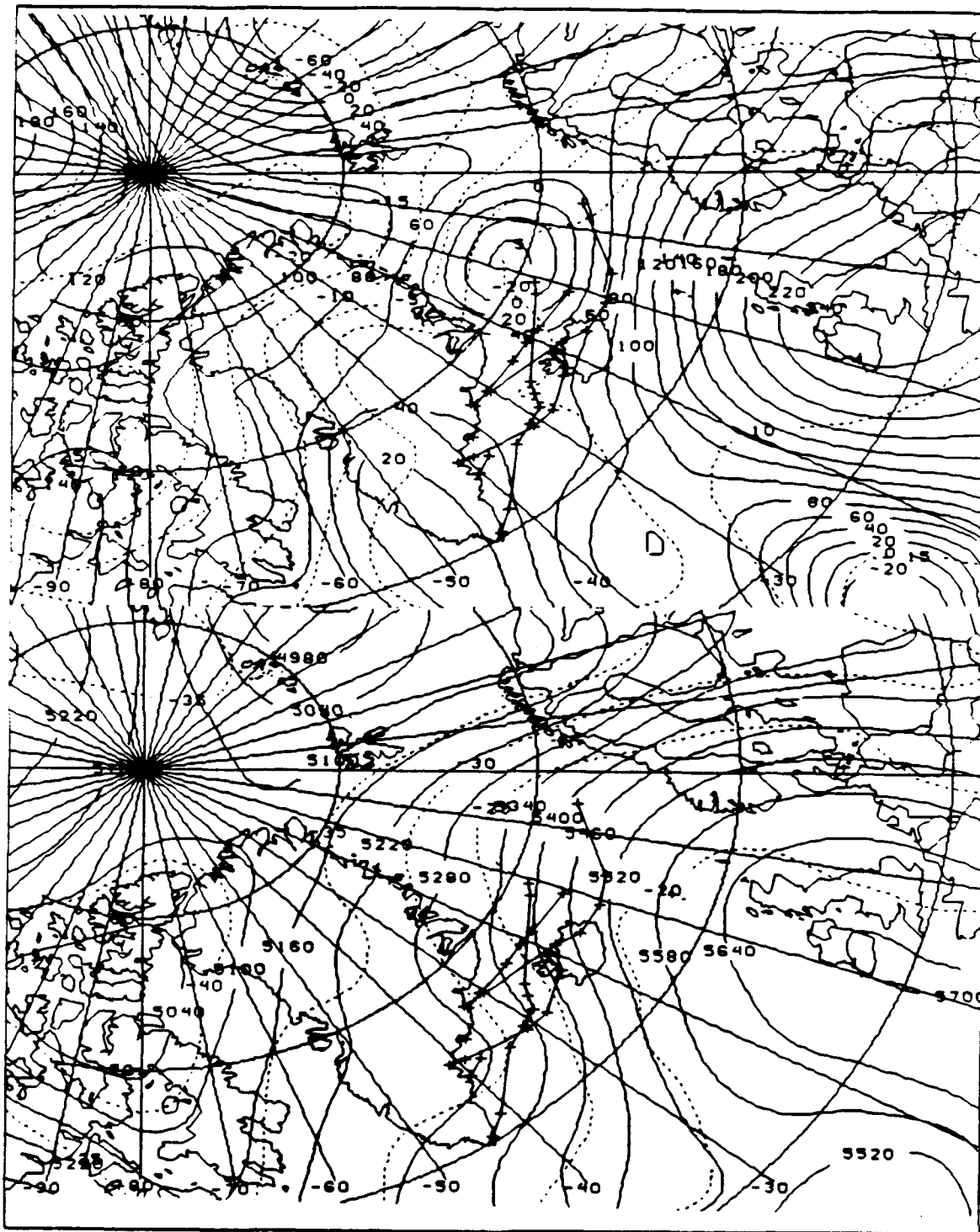


Figure 19d. November mean 1000 mb (upper) and 500 mb (lower) NOGAPS fields for polar lows detected over Southern Greenland.

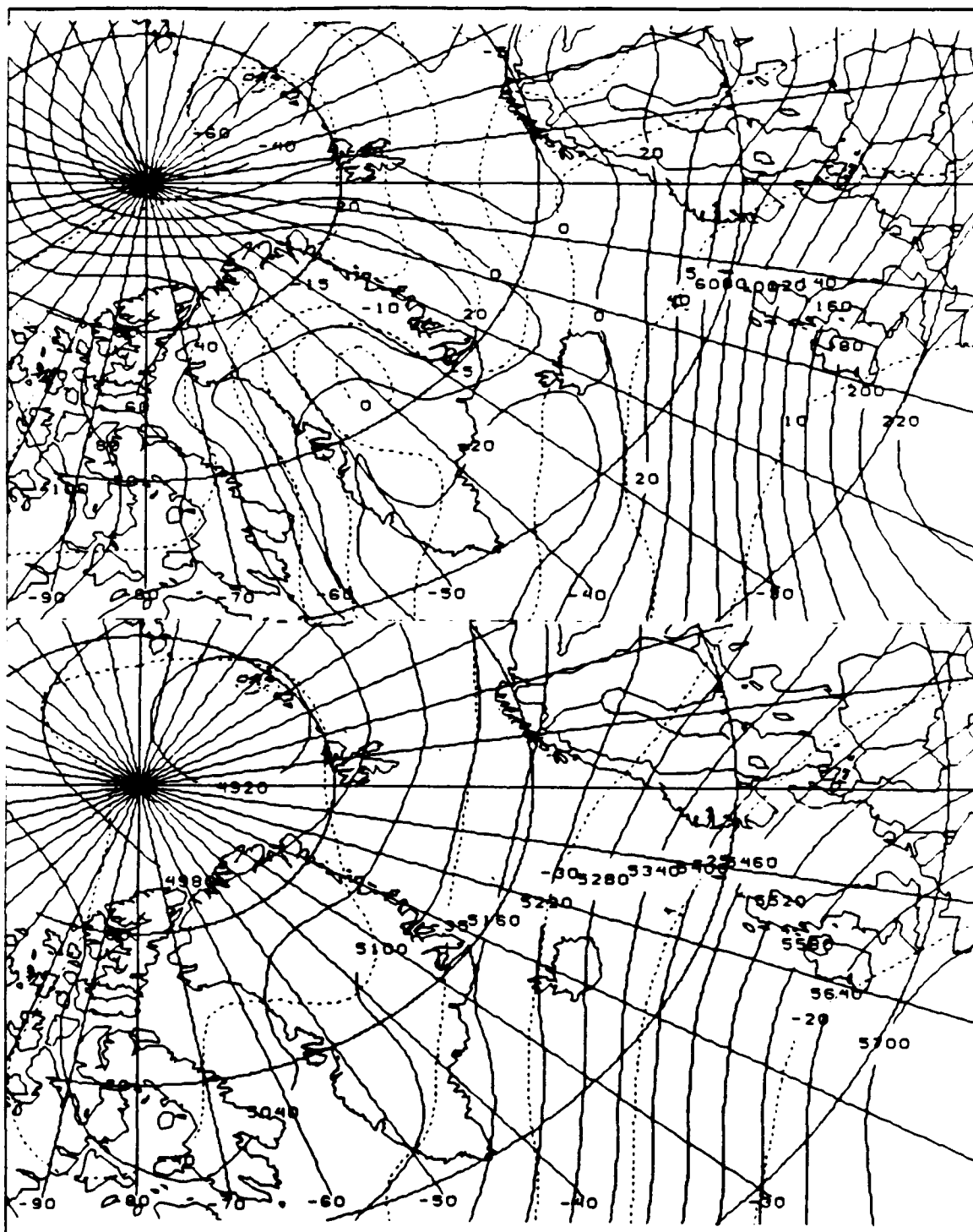


Figure 20a. December climatological NOGAPS fields for 1000 mb (upper) and 500 mb (lower).

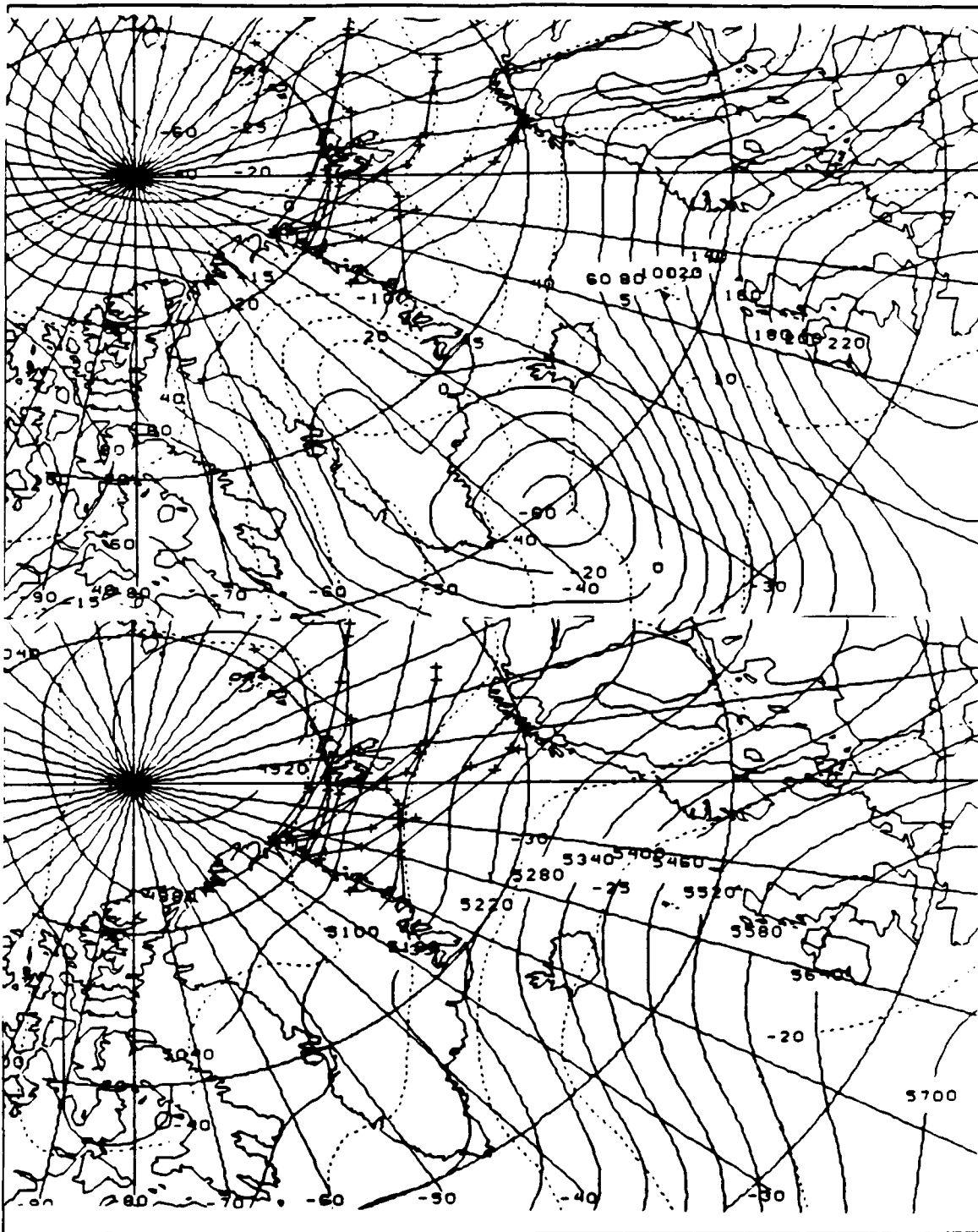


Figure 20b. December mean 1000 mb (upper) and 500 mb (lower) NOGAPS fields for polar lows detected over Northern Greenland.

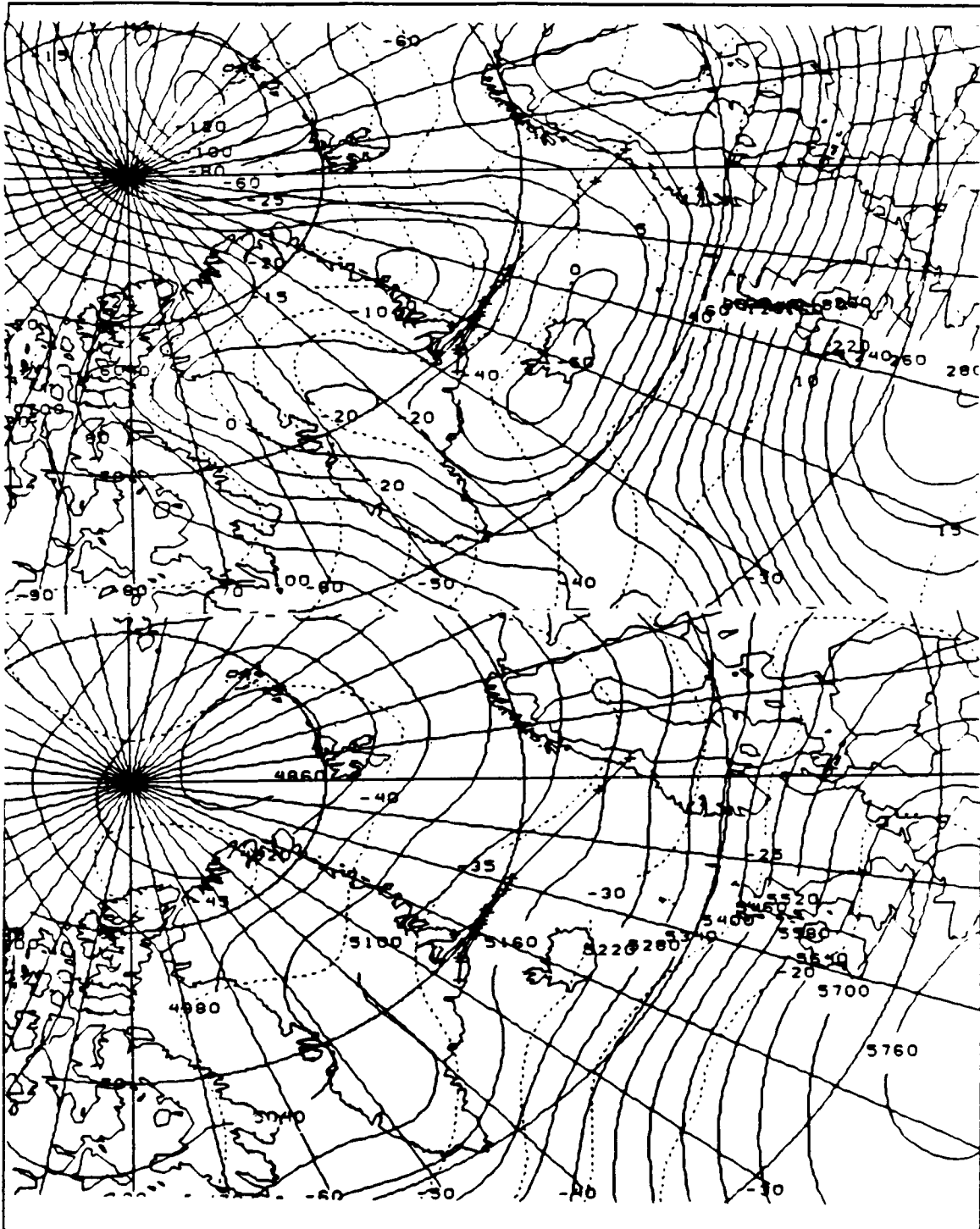


Figure 20c. December mean 1000 mb (upper) and 500 mb (lower) NOGAPS fields for polar lows detected over the Scoresby Sound region.

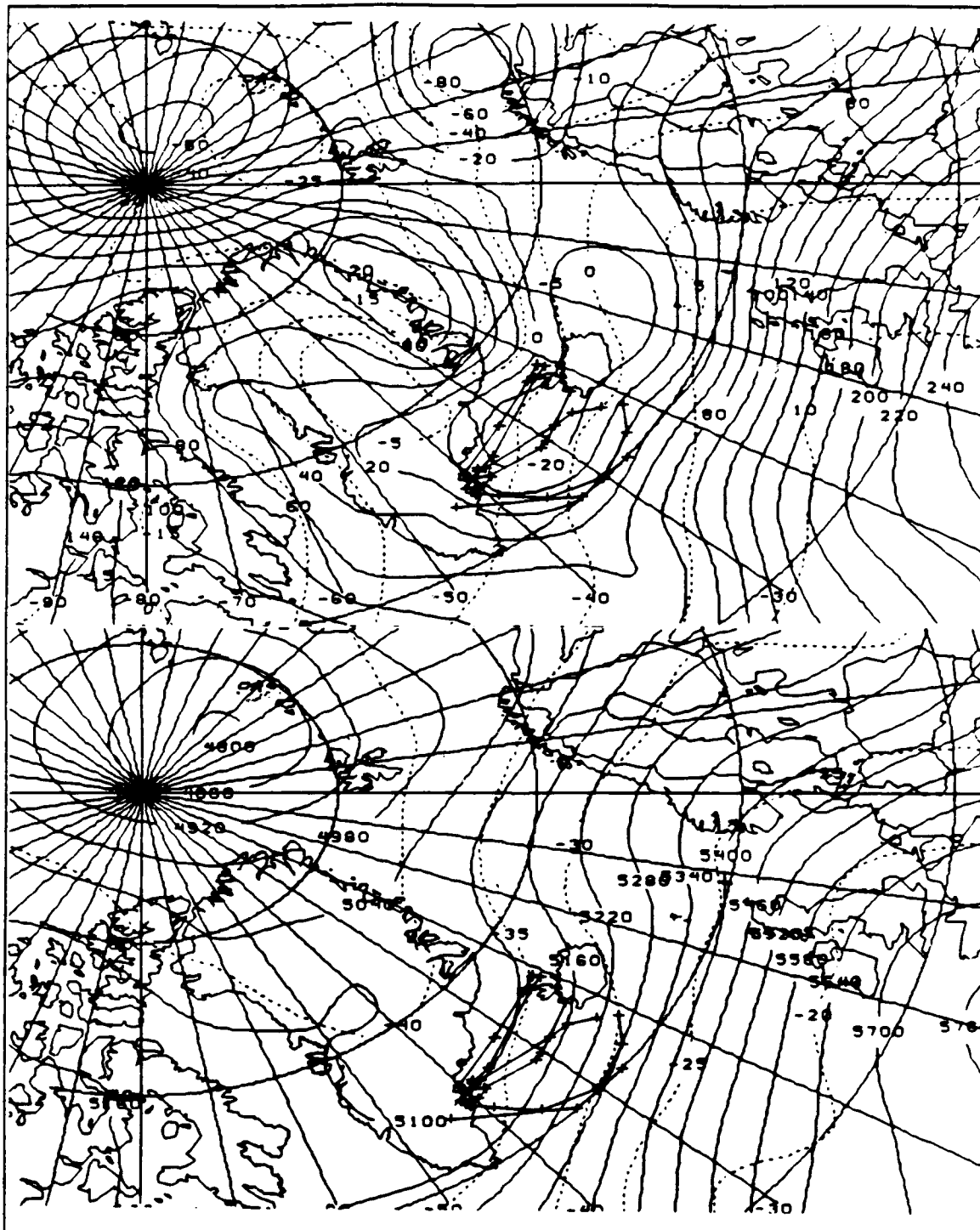


Figure 20d. December mean 1000 mb (upper) and 500 mb (lower) NOGAPS fields for polar lows detected over Southern Greenland.

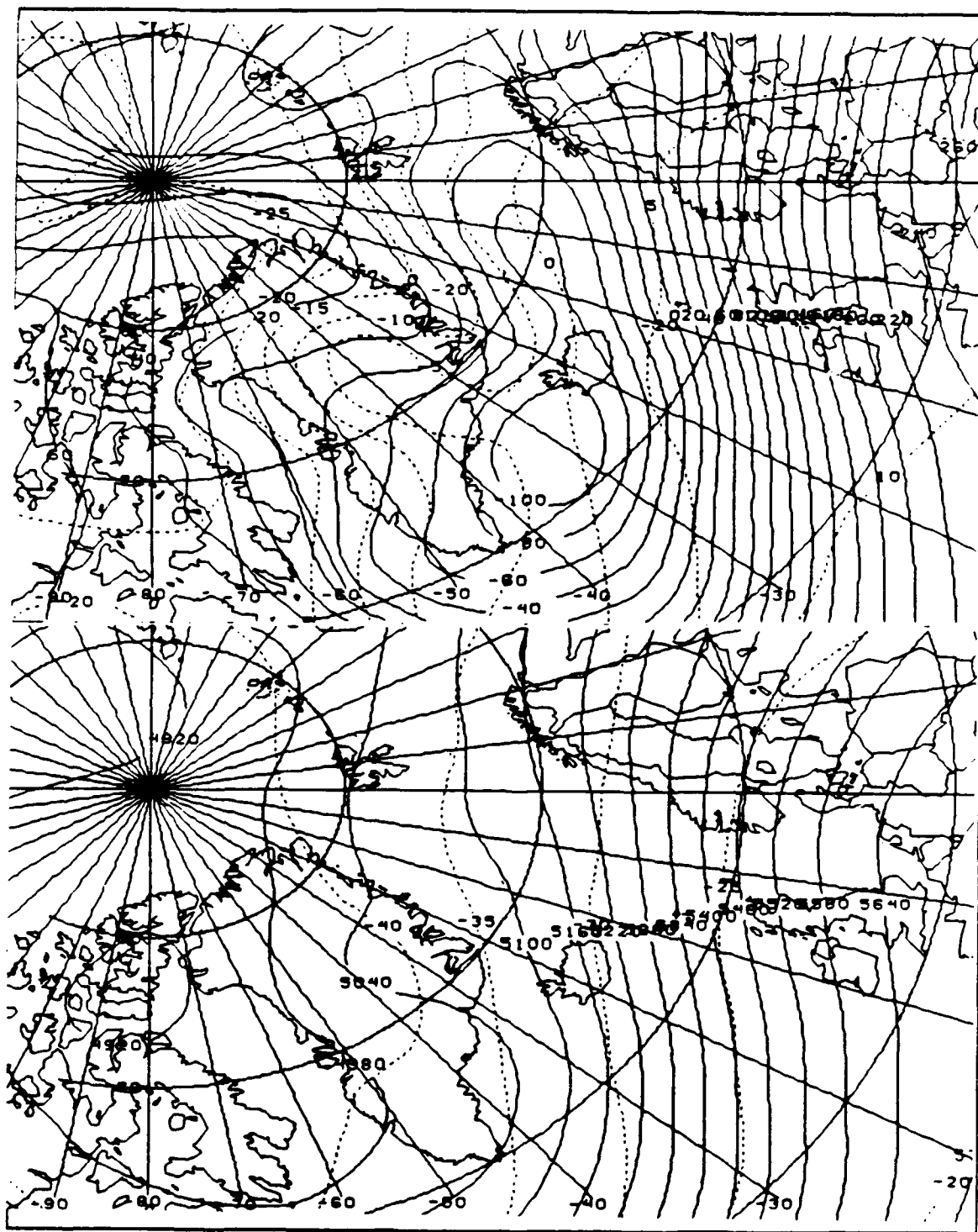


Figure 21a. January climatological NOGAPS fields for 1000 mb (upper) and 500 mb (lower).

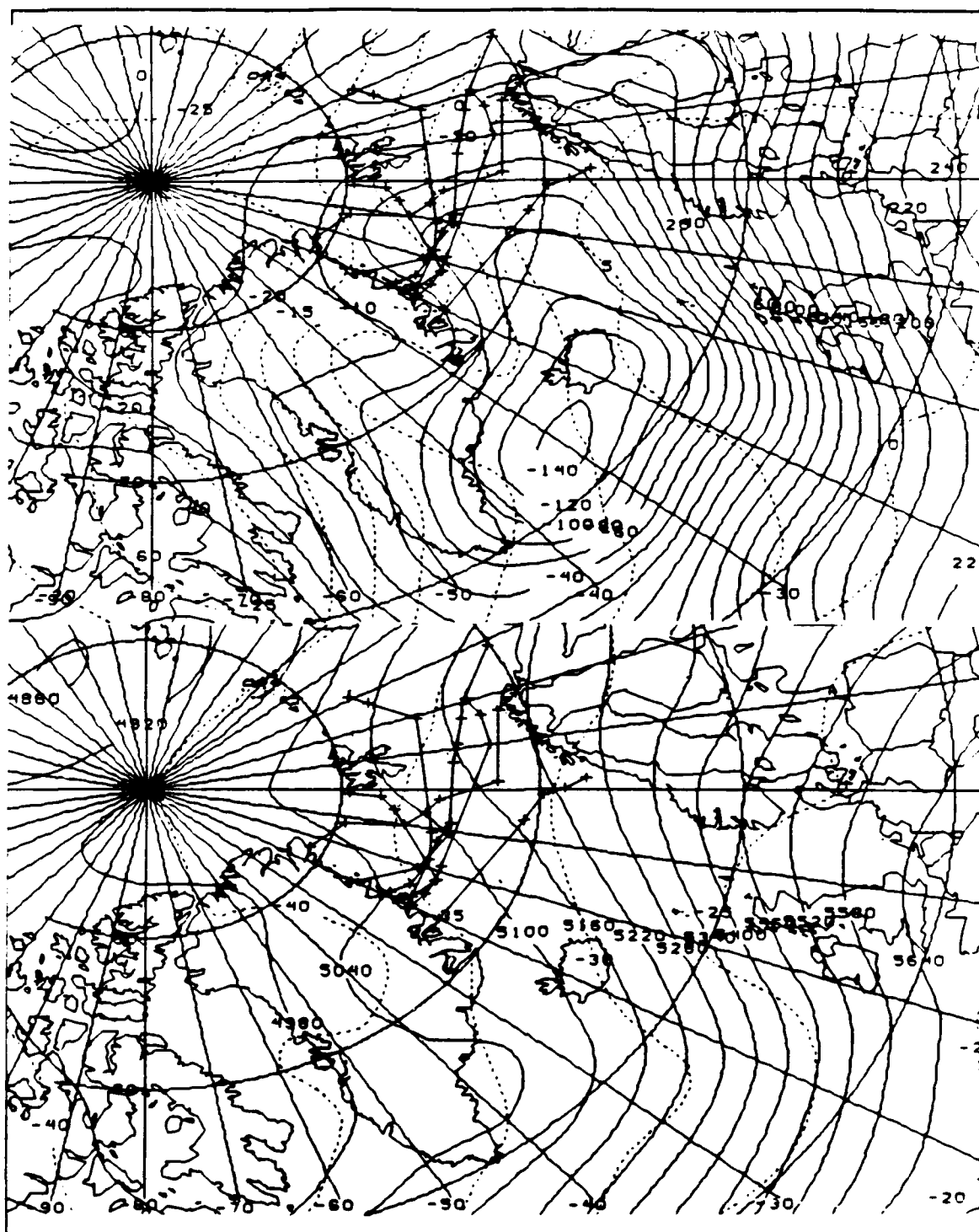
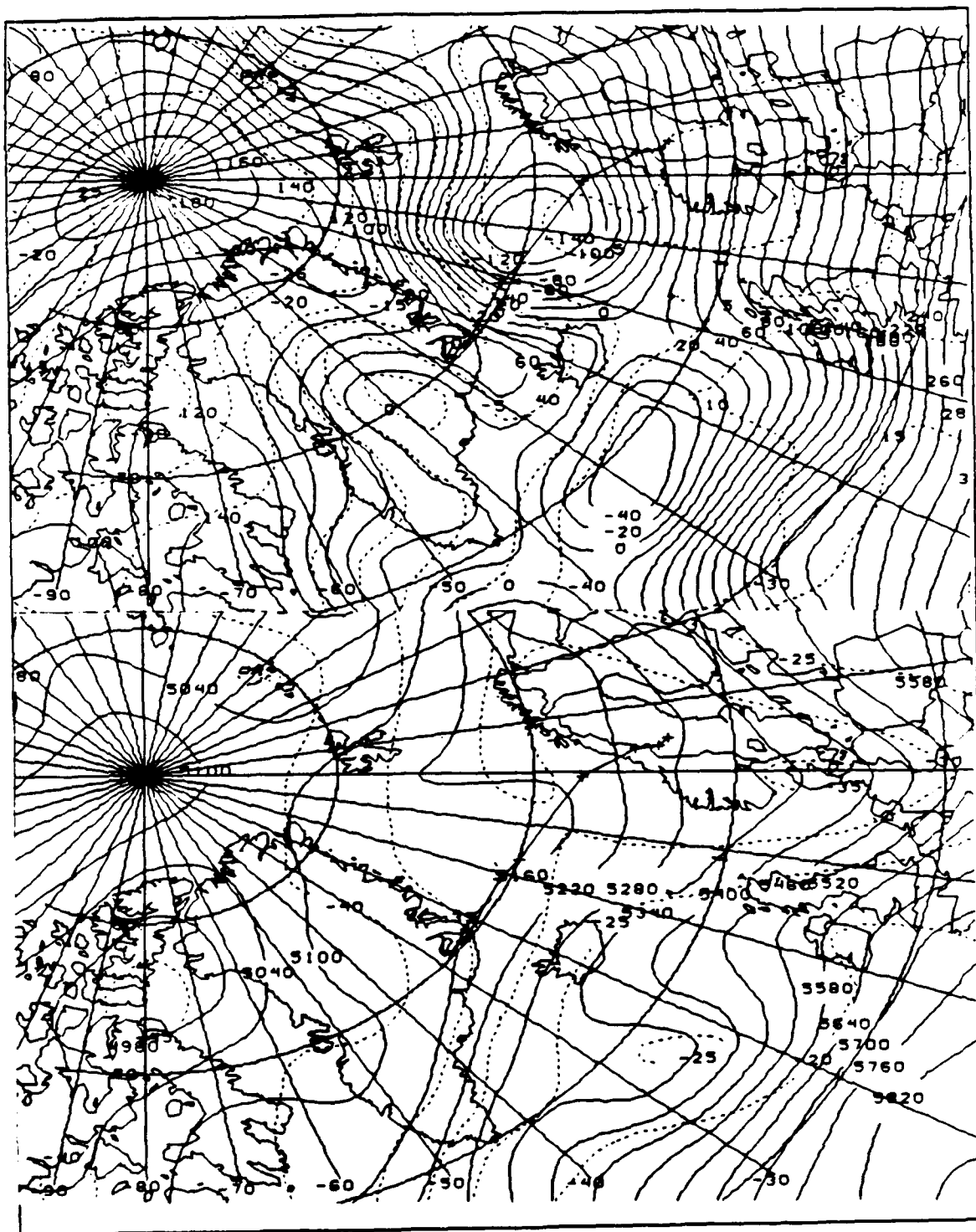


Figure 21b. January mean 1000 mb (upper) and 500 mb (lower) NOGAPS fields for polar lows detected over Northern Greenland.



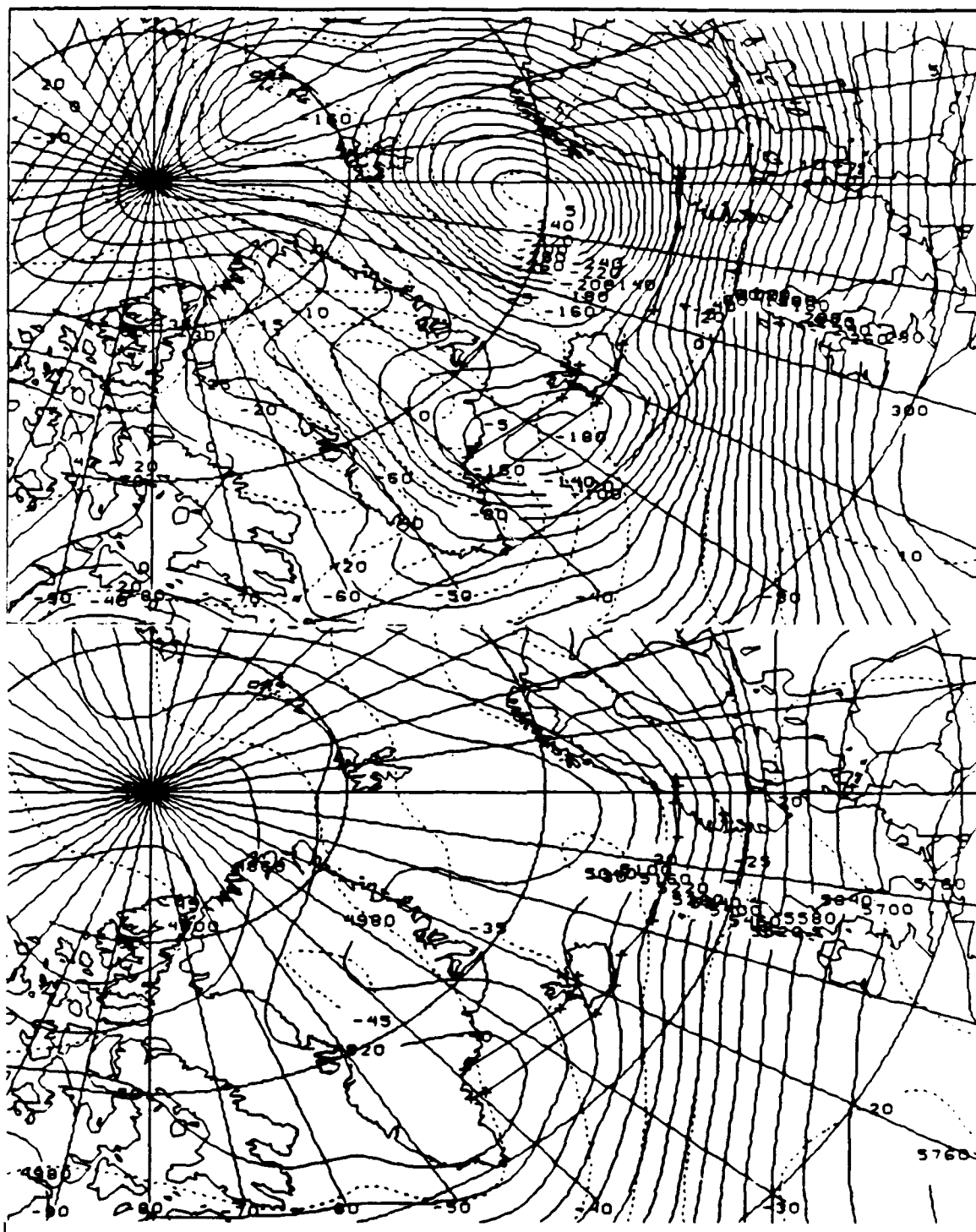


Figure 21d. January mean 1000 mb (upper) and 500 mb (lower) NOGAPS fields for polar lows detected over Southern Greenland.

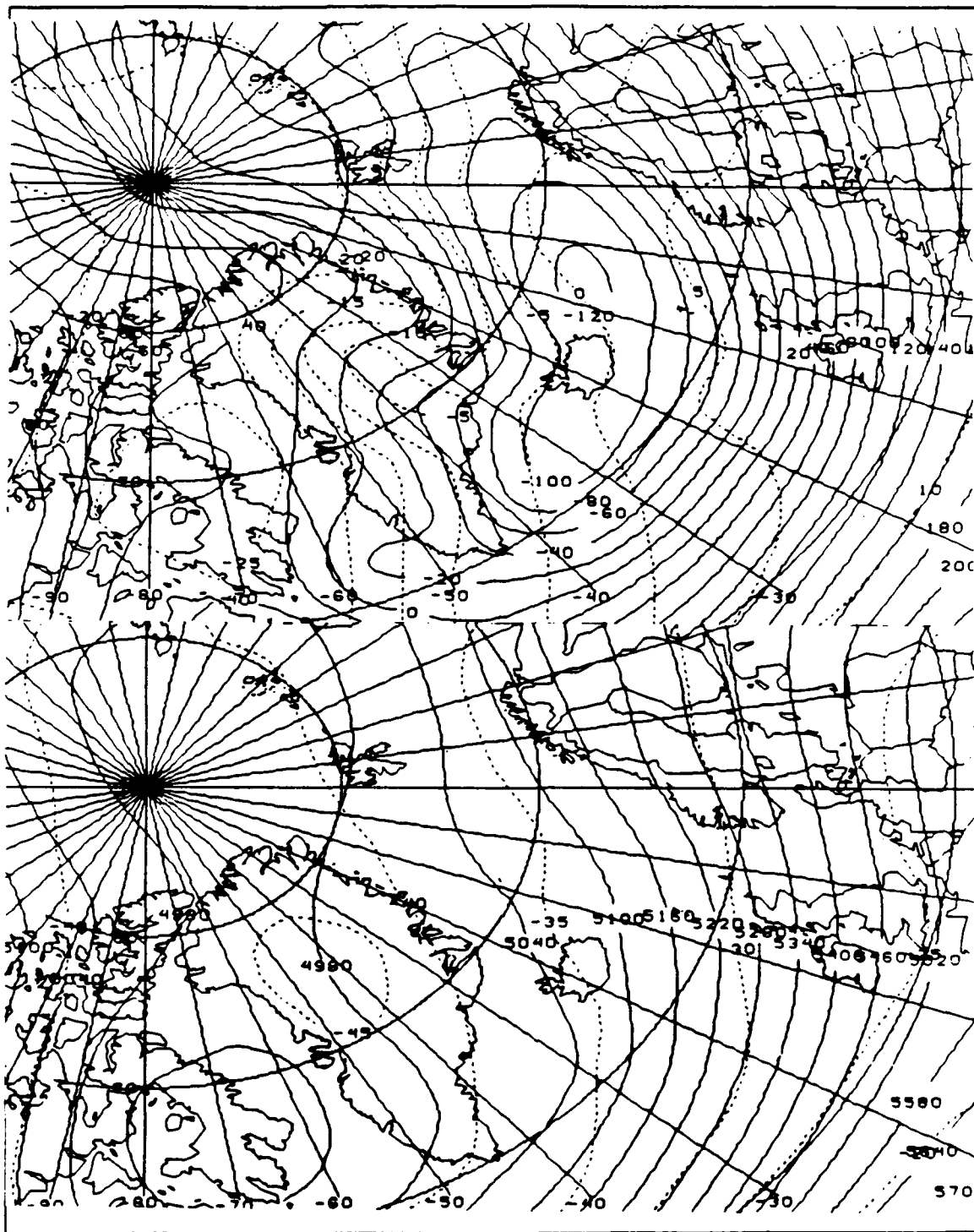


Figure 22a. February climatological NOGAPS fields for 1000 mb (upper) and 500 mb (lower).

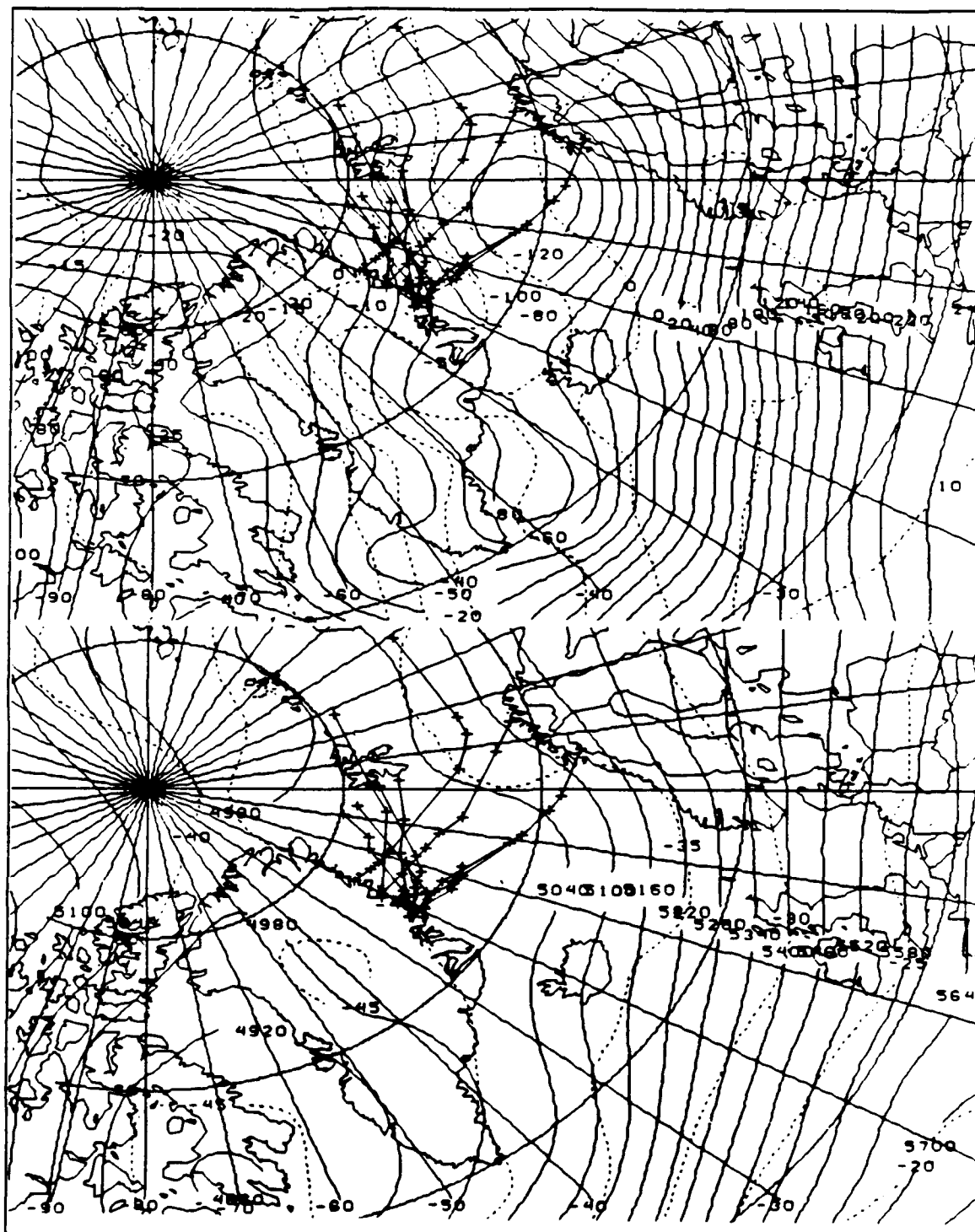


Figure 22b. February mean 1000 mb (upper) and 500 mb (lower) NOGAPS fields for polar lows detected over Northern Greenland.

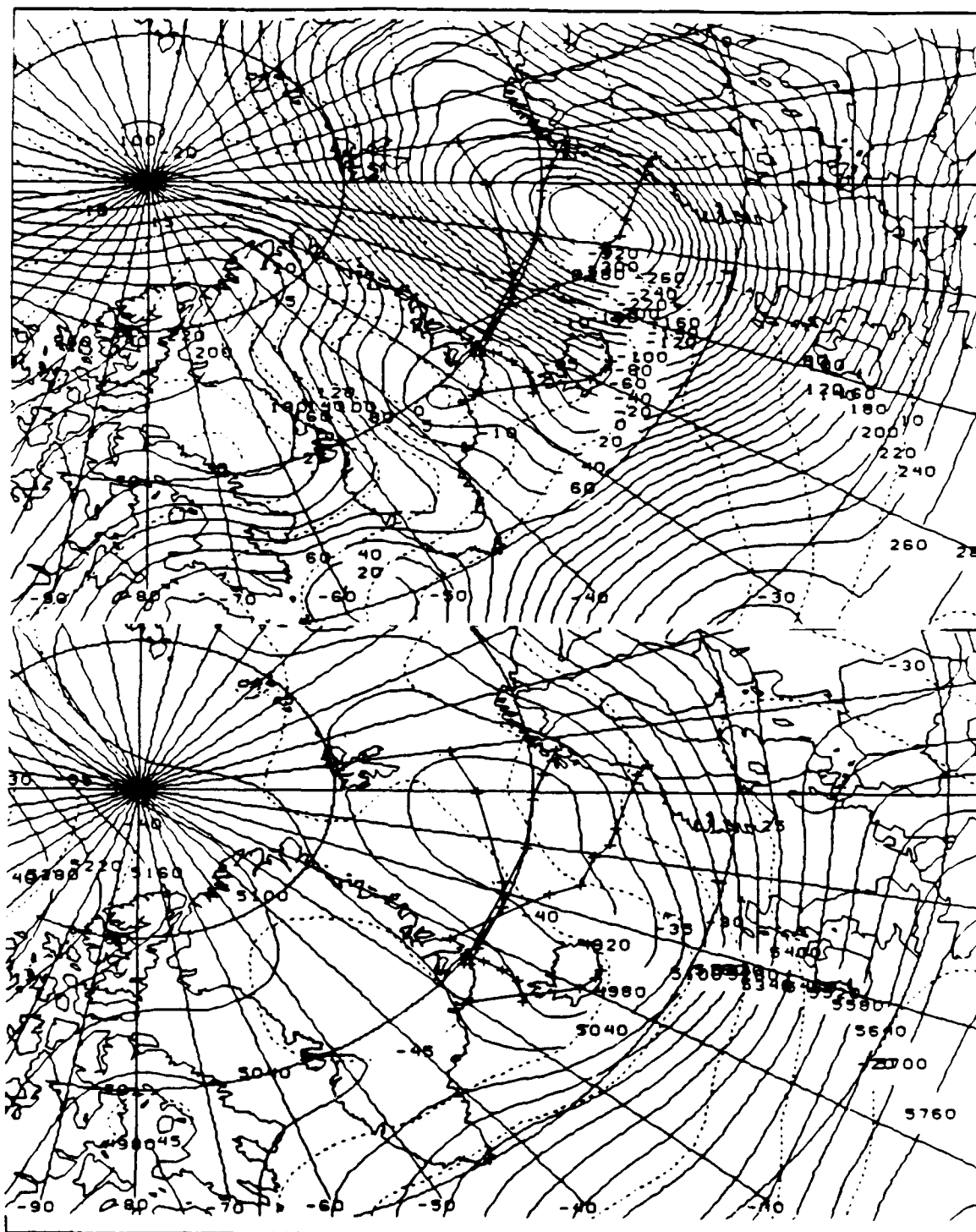


Figure 22c. February mean 1000 mb (upper) and 500 mb (lower) NOGAPS fields for polar lows detected over the Scoresby Sound region.

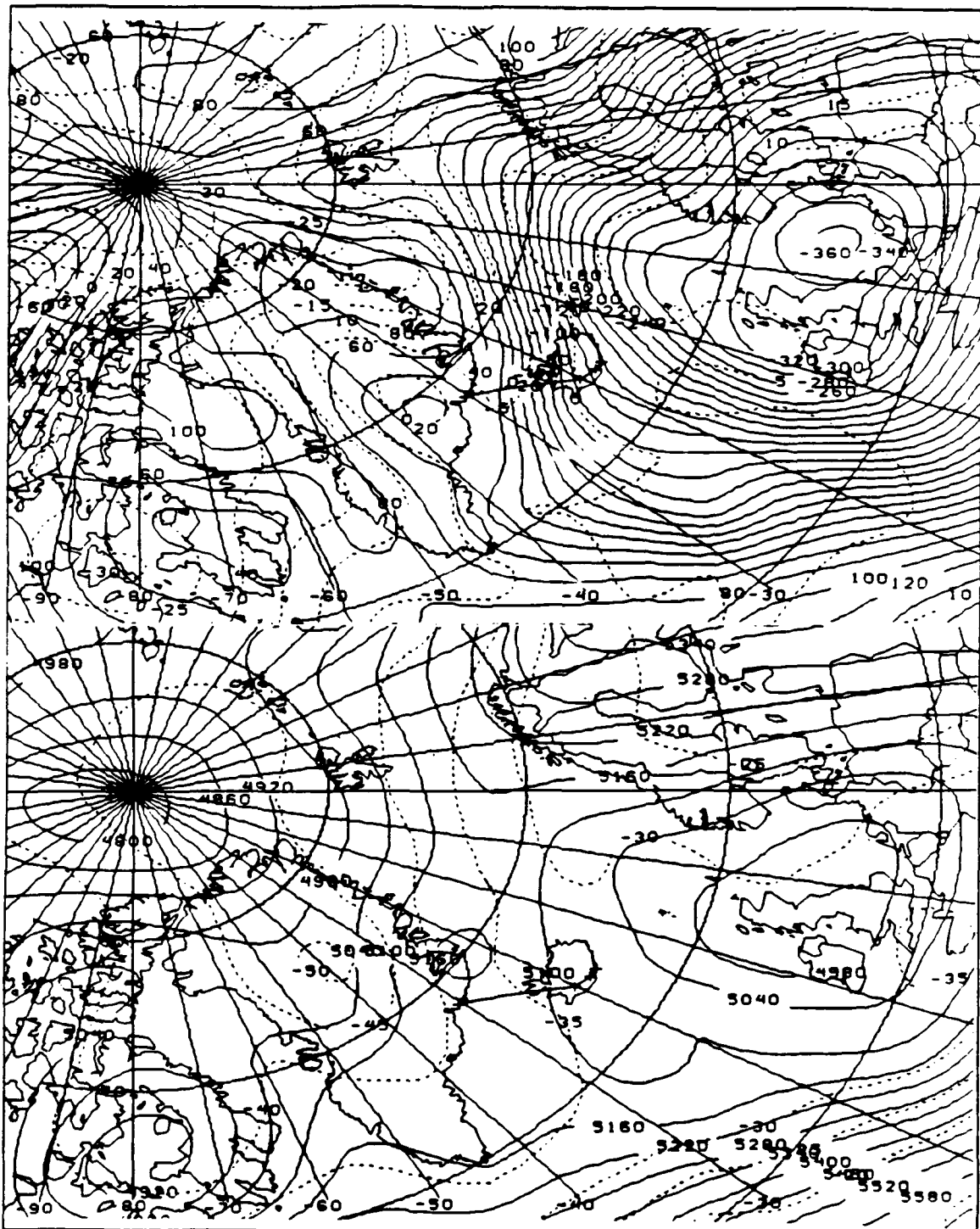


Figure 22d. February mean 1000 mb (upper) and 500 mb (lower) NOGAPS fields for polar lows detected over Southern Greenland.

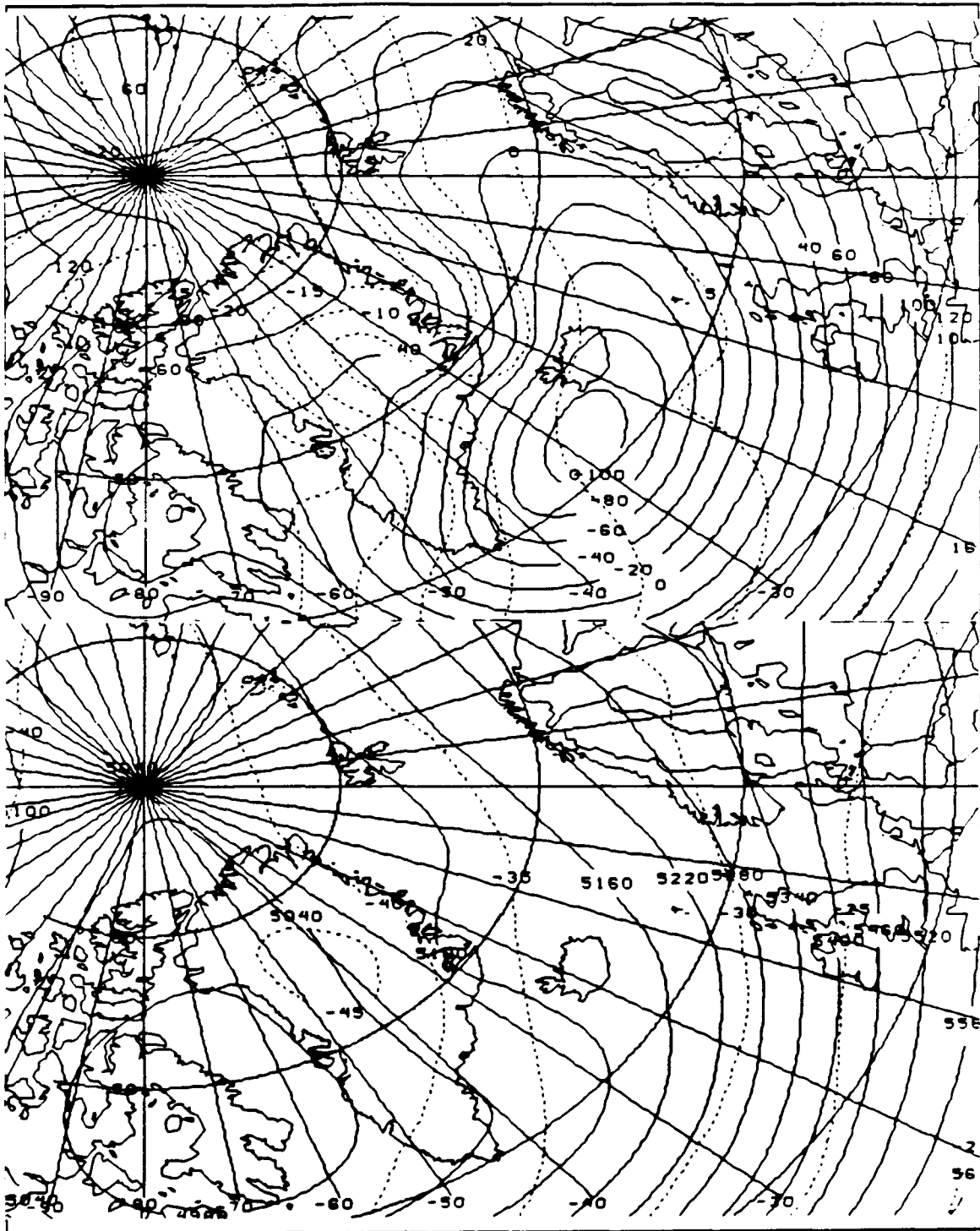


Figure 23a. March climatological NOGAPS fields for 1000 mb (upper) and 500 mb (lower).

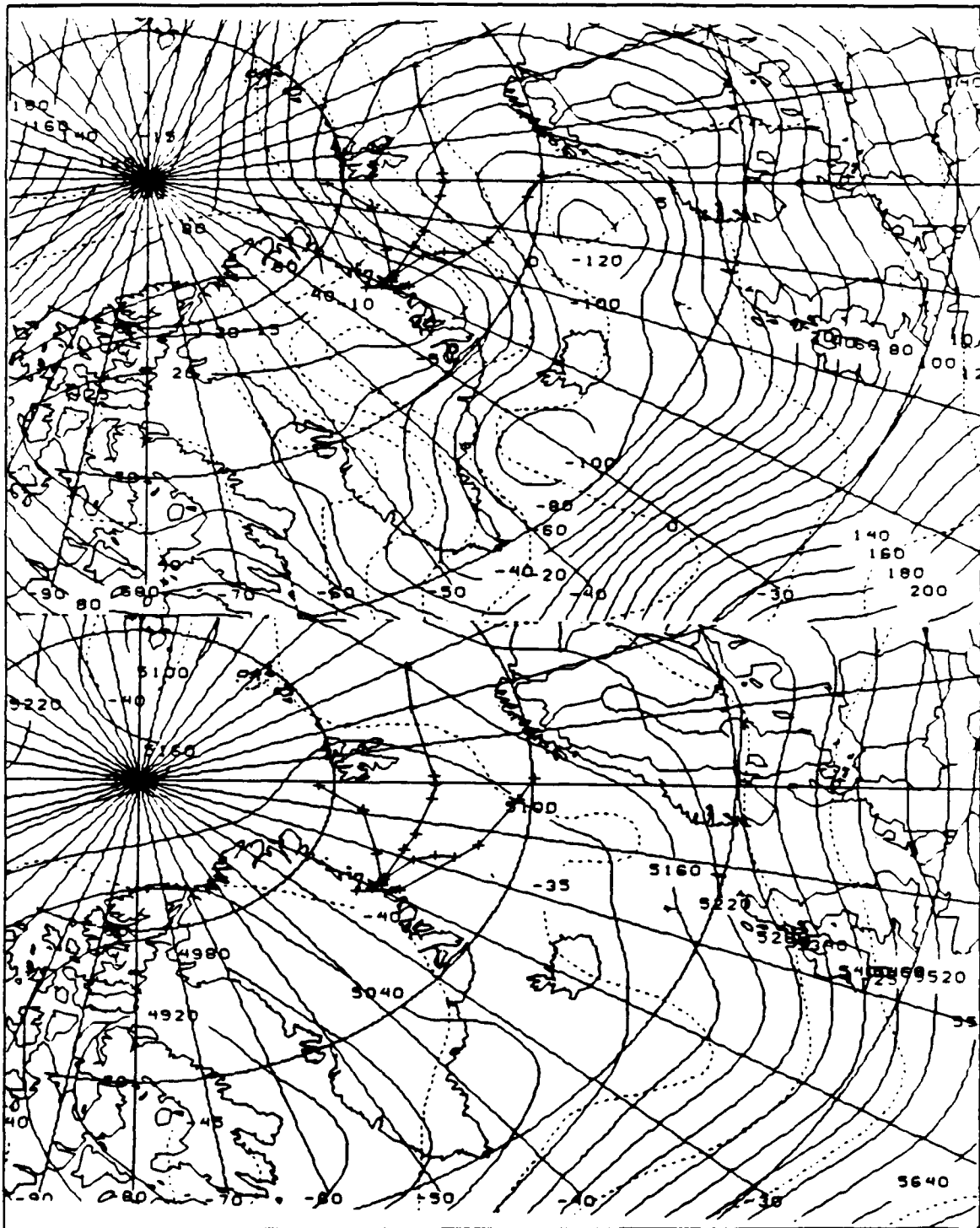


Figure 23b. March mean 1000 mb (upper) and 500 mb (lower) NOGAPS fields for polar lows detected over Northern Greenland.

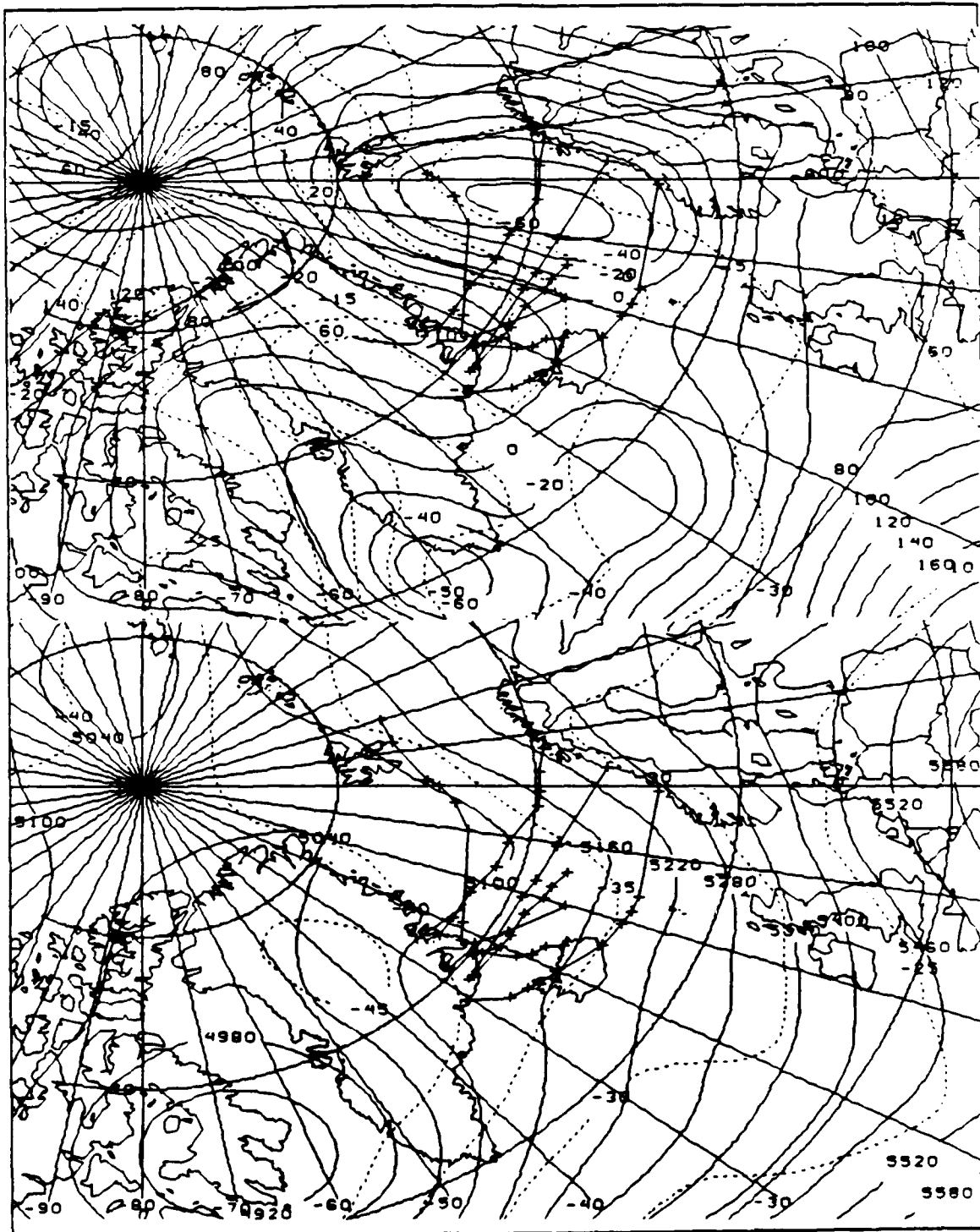


Figure 23c. March mean 1000 mb (upper) and 500 mb (lower) NOGAPS fields for polar lows detected over the Scoresby Sound region.

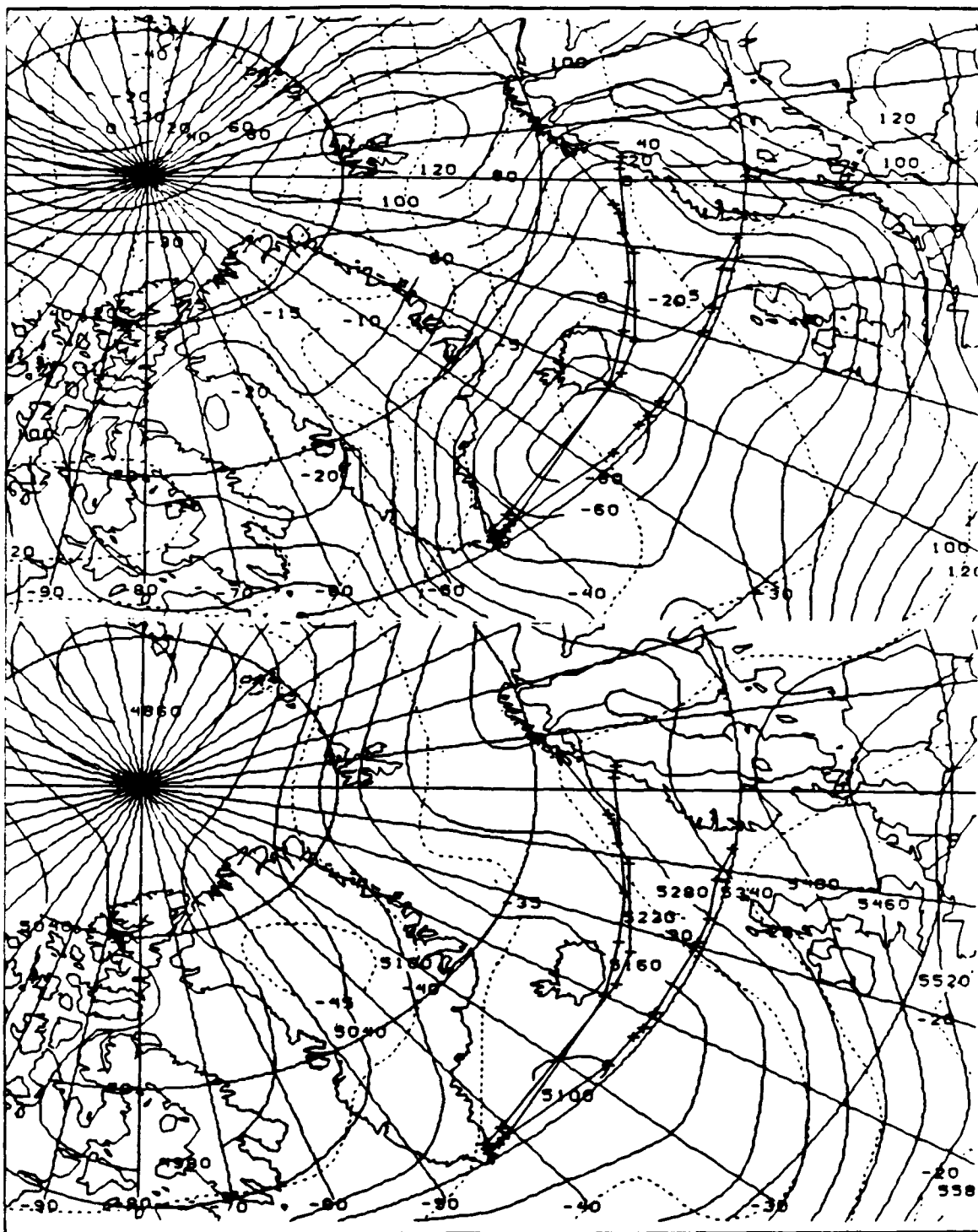


Figure 23d. March mean 1000 mb (upper) and 500 mb (lower) NOGAPS fields for polar lows detected over Southern Greenland.

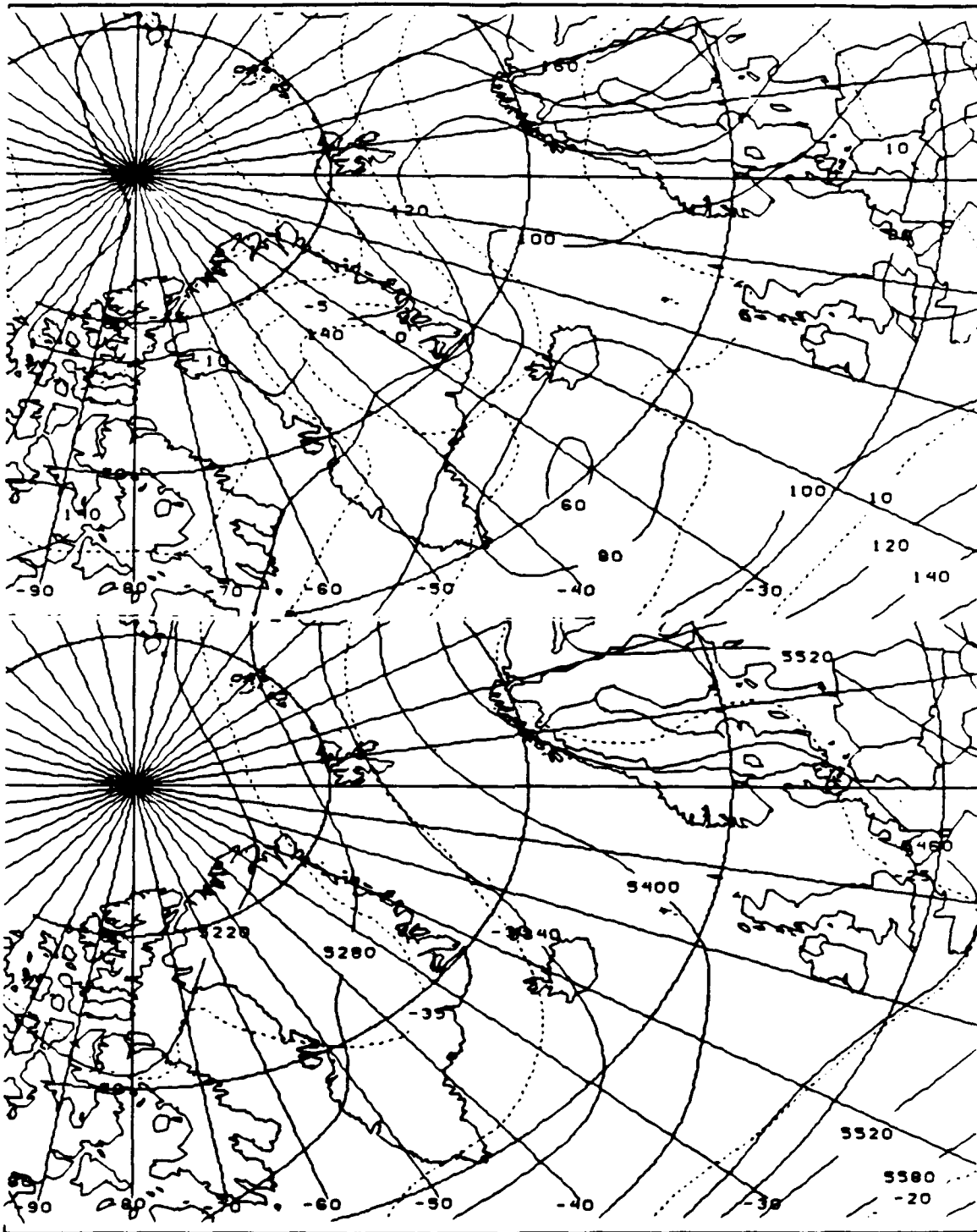


Figure 24a. April climatological NOGAPS fields for 1000 mb (upper) and 500 mb (lower).

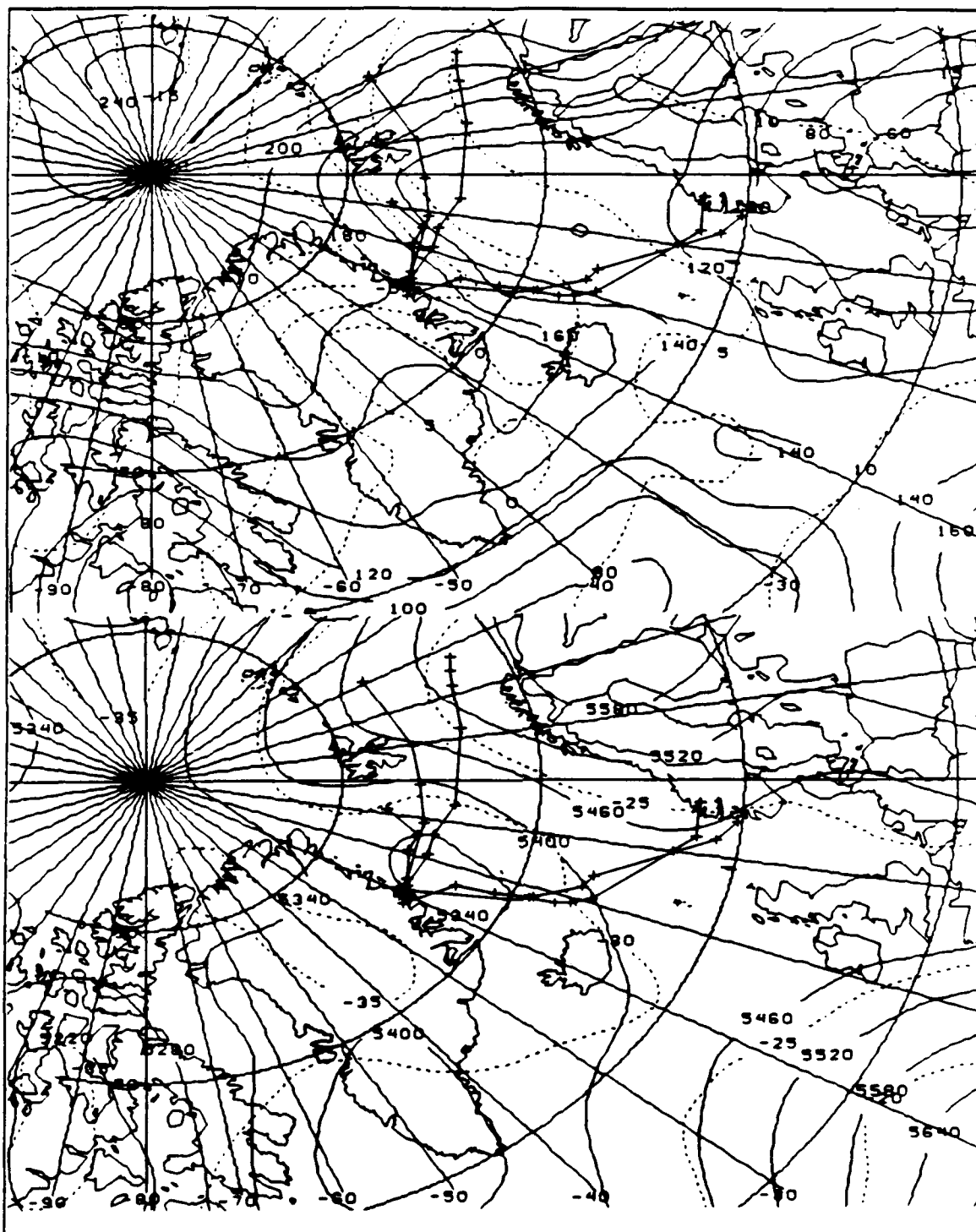


Figure 24b. April mean 1000 mb (upper) and 500 mb (lower) NOGAPS fields for polar lows detected over Northern Greenland.

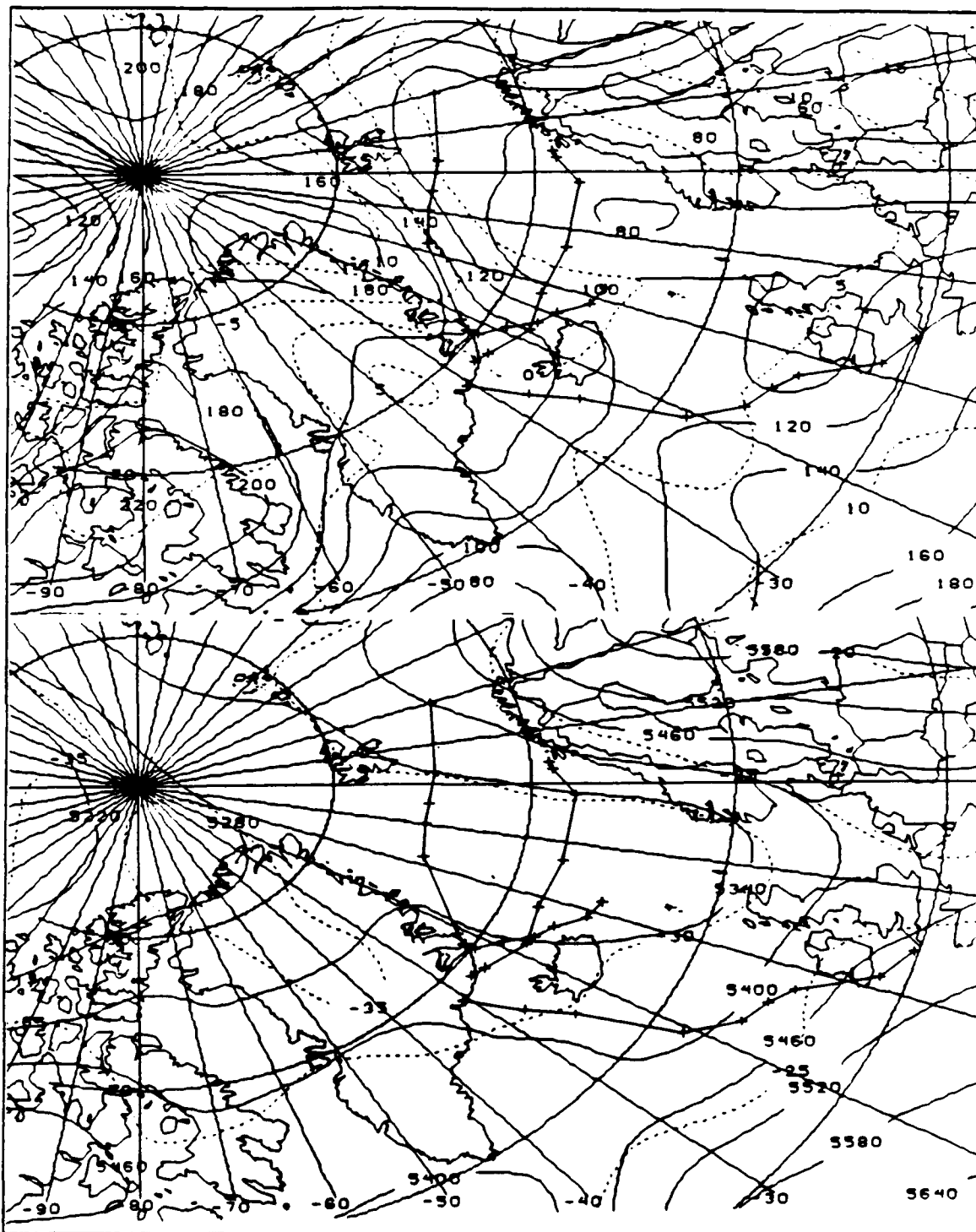


Figure 24c. April mean 1000 mb (upper) and 500 mb (lower) NOGAPS fields for polar lows detected over the Scoresby Sound region.

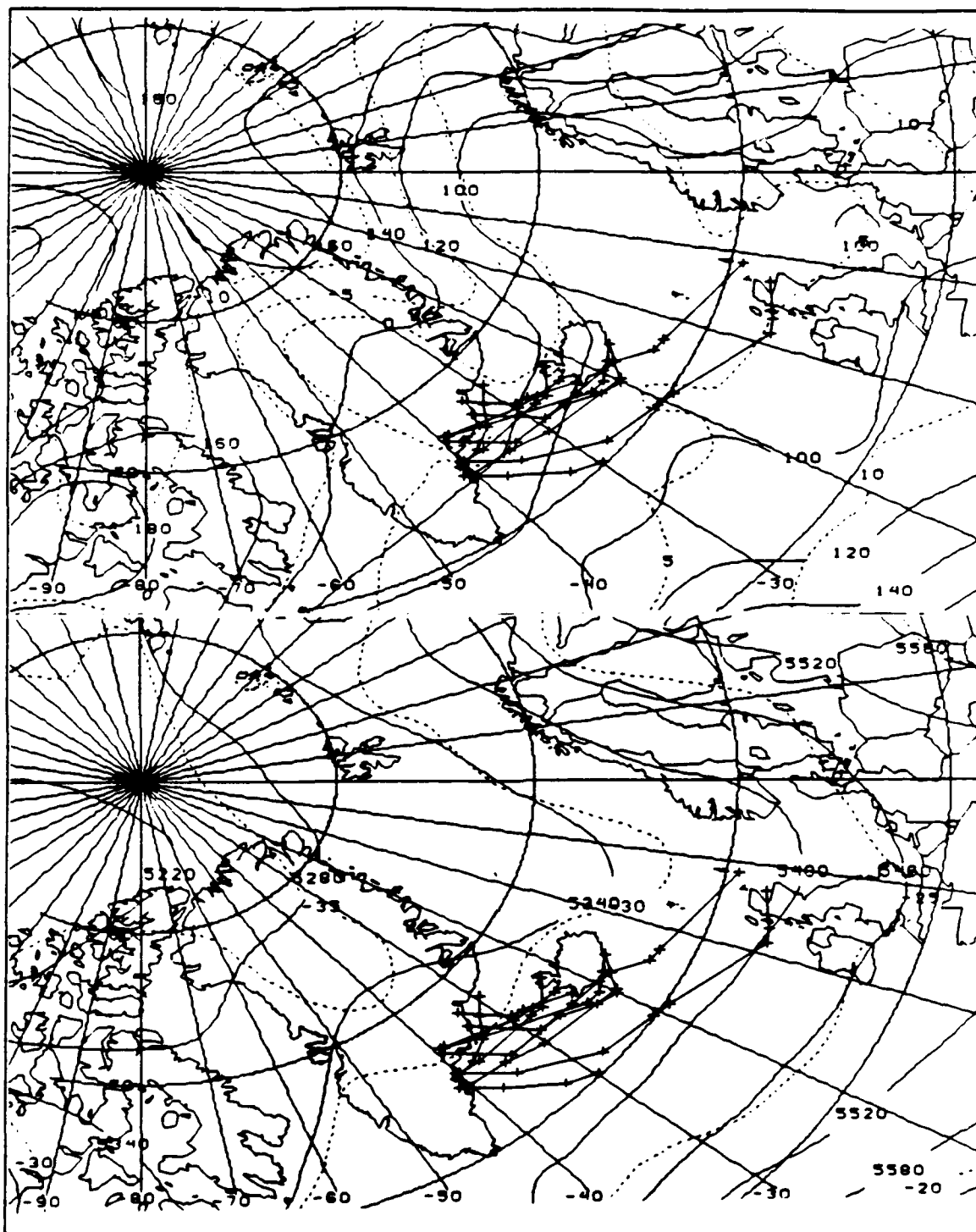


Figure 24d. April mean 1000 mb (upper) and 500 mb (lower) NOGAPS fields for polar lows detected over Southern Greenland.

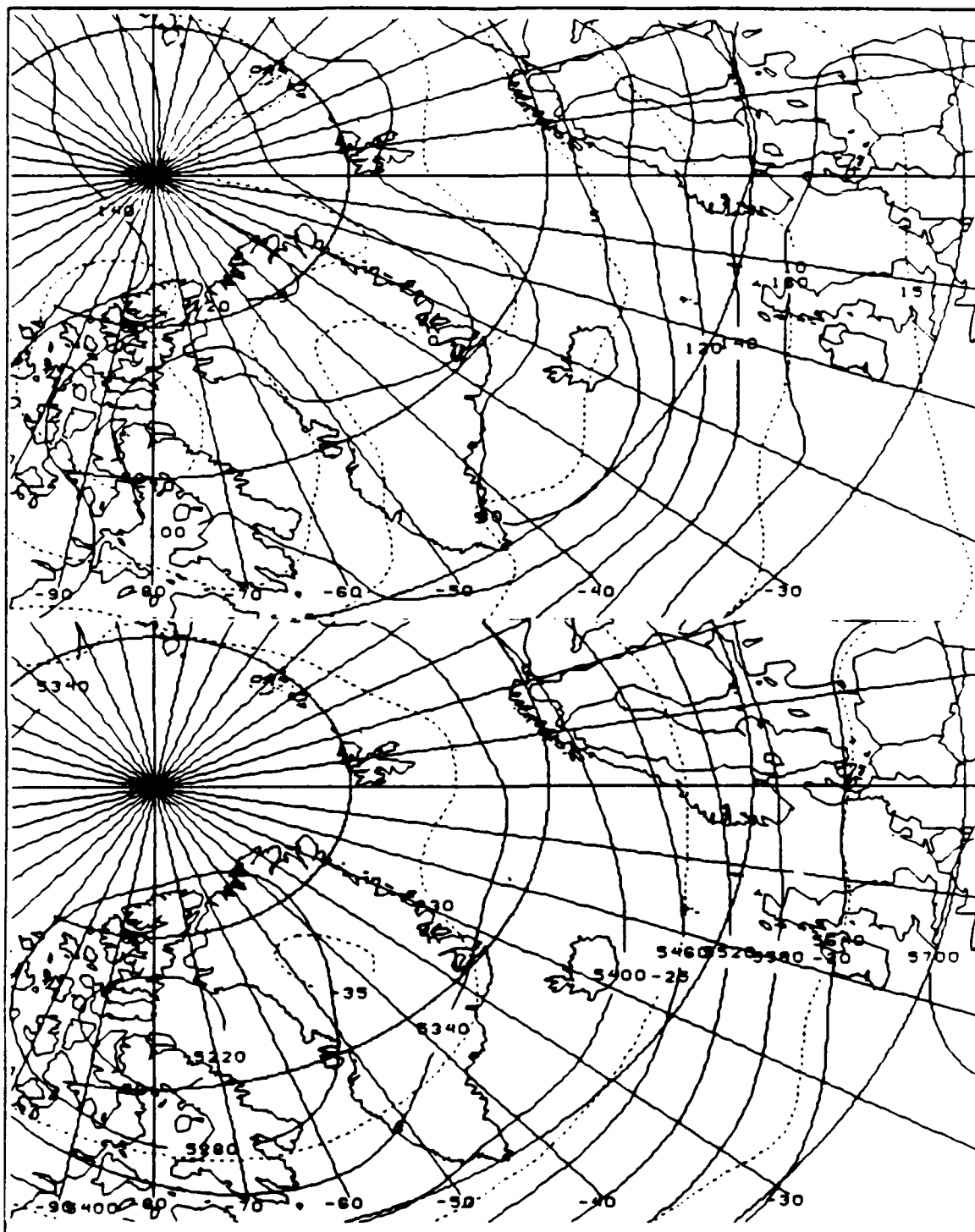


Figure 25a. May climatological NOGAPS fields for 1000 mb (upper) and 500 mb (lower).

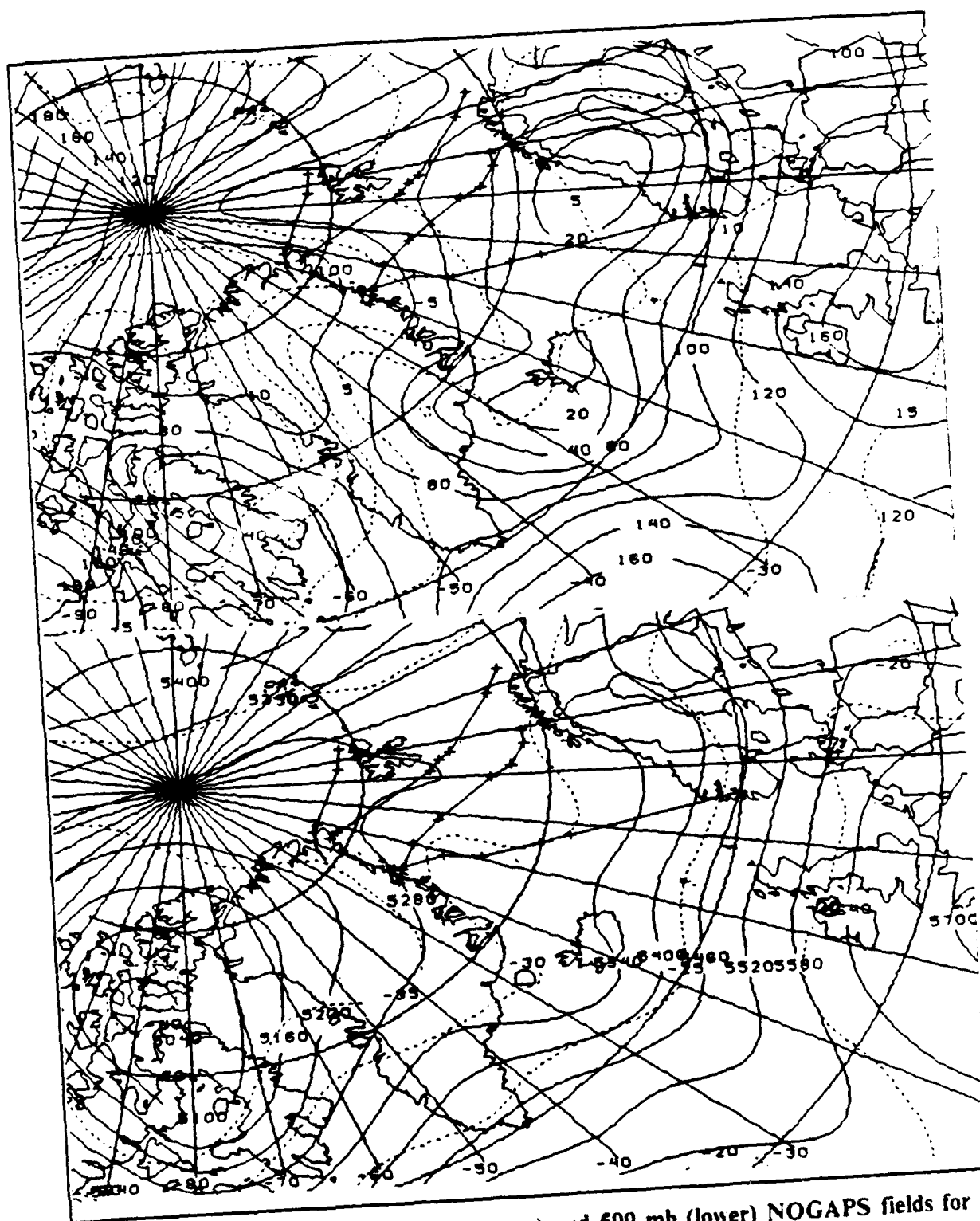


Figure 25b. May mean 1000 mb (upper) and 500 mb (lower) NOGAPS fields for polar lows detected over Northern Greenland.

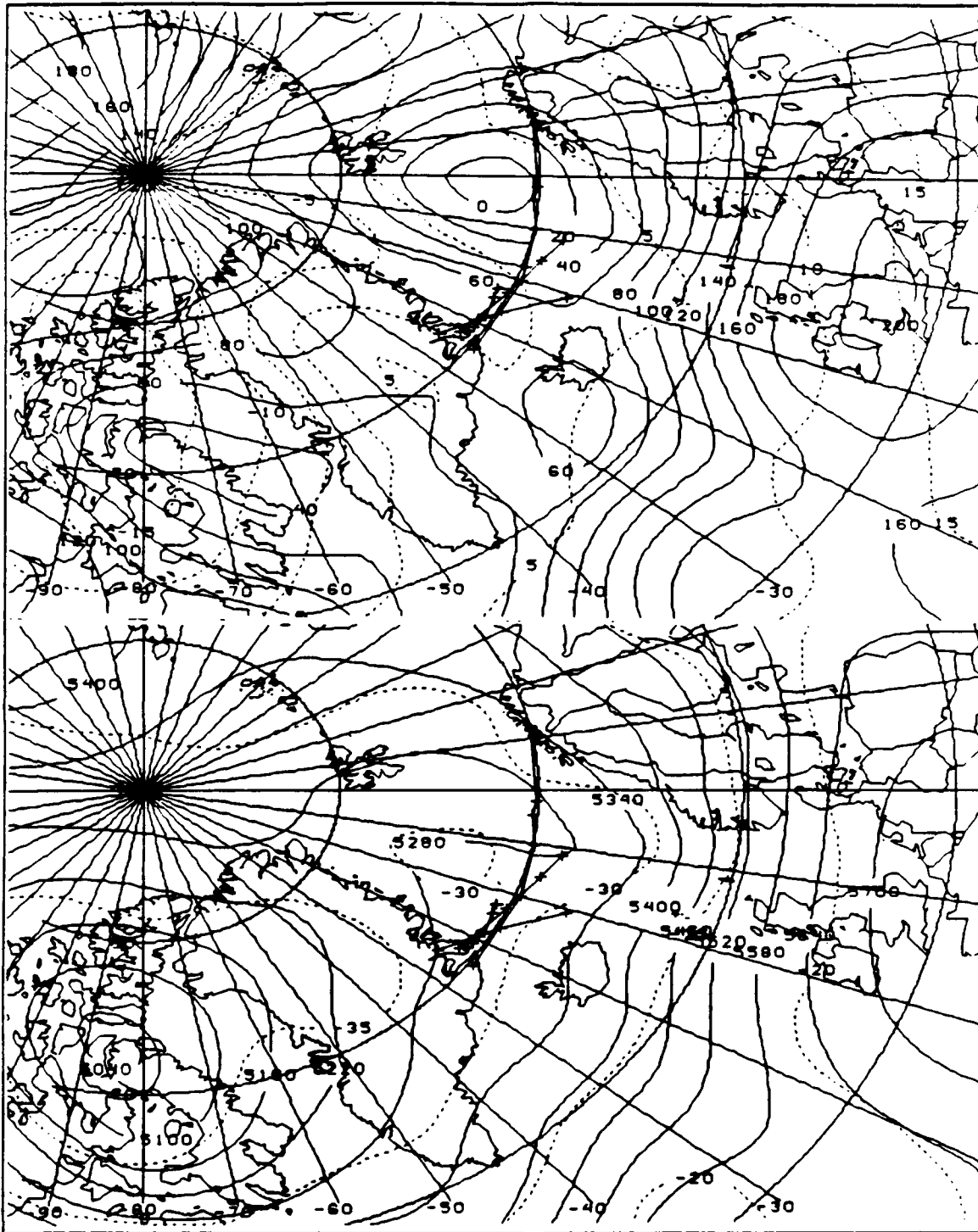


Figure 25c. May mean 1000 mb (upper) and 500 mb (lower) NOGAPS fields for polar lows detected over the Scoresby Sound region.

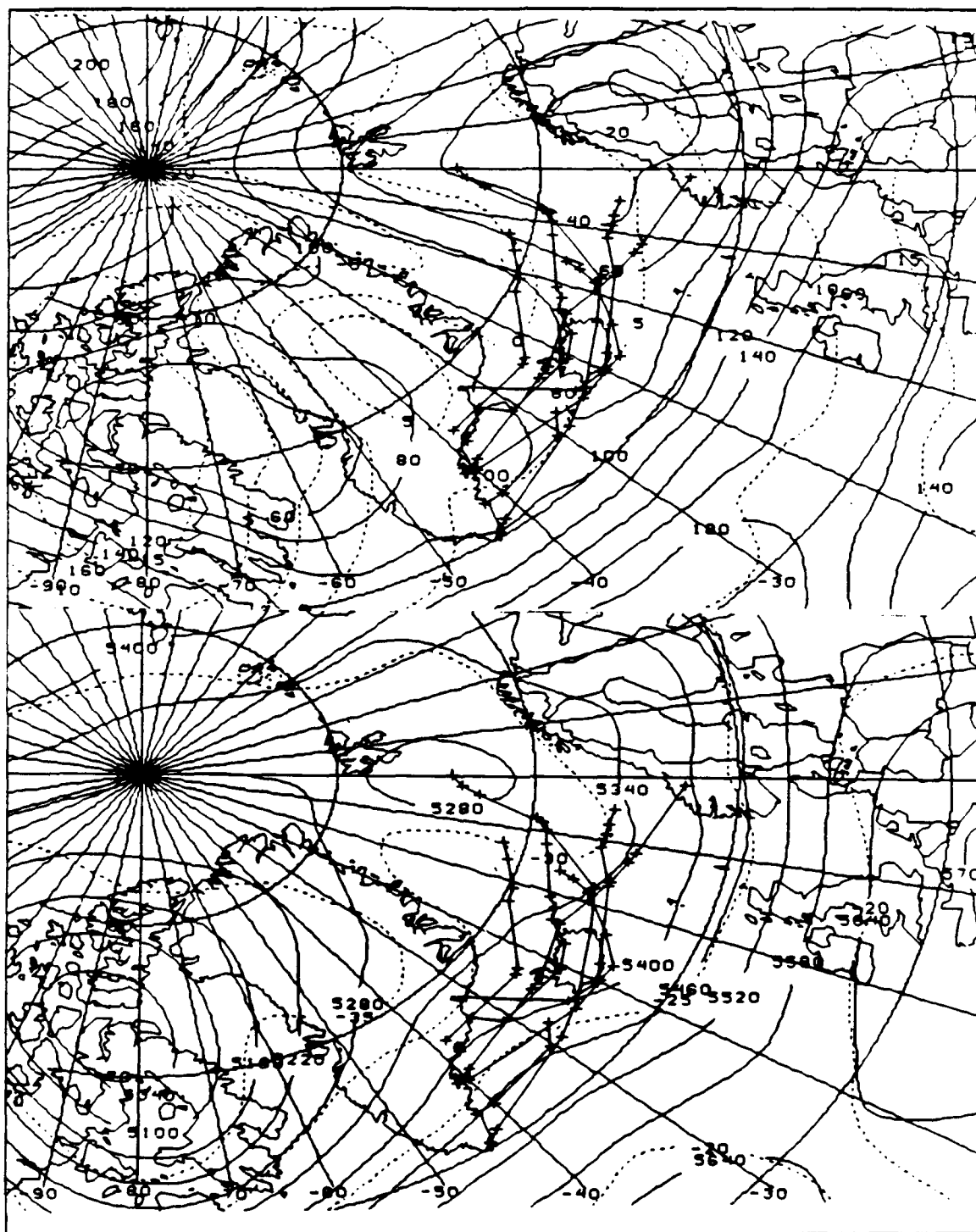


Figure 25d. May mean 1000 mb (upper) and 500 mb (lower) NOGAPS fields for polar lows detected over Southern Greenland.

Table 16. SOUTHERN GREENLAND HEIGHT GRADIENTS

Month	Detected	Back-tracked	Climatology
Sep	--	+ 60	+ 35
Oct	--	+ 15	+ 25
Nov	-(90)	+ 20	(-20)
Dec	+ 40	+ 40	+ 10
Jan	+ 100	+ 80	+ 50
Feb	+ 240	+ 90	+ 70
Mar	+ 60	+ 70	+ 100
Apr	+ 40	+ 90	+ 50
May	+ 60	+ 20	+ 20
Avg	+ 65	+ 55	+ 40

Table 17. STORMS BACKTRACKED TO SOUTHERN GREENLAND

Month	1000 mb				500 mb			
	ΔH	ΔT	Flow	Advection	ΔH	ΔT	Flow	Advection
Sep	20-40	-2-3	Under High (On)	WAA (CAA)	+ 30	-2	Ridge Conv (Neutral)	CAA (WAA)
Oct	-20	-2-4	On Off Shore (Cross)	CAA WAA (Neutral)	+ 60	-2-3	Ridge (Trough Div)	CAA
Nov	-40	-2-3	Cross-shore (On)	Neutral (WAA)	-60	-2	Trough (Ridge)	Neutral (WAA)
Dec	-60	-2-3	Cross-shore (On)	WAA CAA (WAA)	-60	-1-2	Trough	Neutral
Jan	-20	-3-5	On Off-shore	CAA (WAA CAA)	-60	-2	Trough	CAA
Feb	-20	-2-4	Cross-shore (On Off)	WAA (WAA CAA)	-60	-2	Trough	CAA (Neutral)
Mar	+ 40	-3	Cross-shore (On Off)	WAA CAA	-30	-2-3	Trough Div (Trough)	CAA
Apr	-20	--	Cross-shore (On)	Neutral (WAA)	+ 260	-2	Trough Div	WAA (Neutral)
May	-20	-3-5	On Off-shore	CAA	-60	-3-4	Trough (Div)	Neutral (WAA)

VI. CONCLUSIONS

This section presents the conclusions drawn from this study of Nordic Sea polar lows and presents recommendations for further research.

A. FORMATION FREQUENCY

Polar low formation is much more frequent than previously thought. Wilhelmsen identified 160 polar low over 12 years, but applied a minimum wind speed criterion of 15 m s and required that the storms be observed by Norwegian coastal stations or ships. Ese et al. observed that storm frequency doubled when polar lows were detected by satellite imagery.

The 941 mesoscale cyclonic circulations may, or may not be polar lows depending on the numerous definitions in use. The broadest definition was applied here: A mesoscale cyclonic circulation formed in the cold air north of the polar front. No wind speed was available through satellite imagery and formation mechanisms could not be identified. The 94 polar lows detected in January 1992 roughly agrees with the 106 storms detected by Carleton in January 1978 and 72 in January 1979.

B. LACK OF SENSIBLE HEAT SOURCE

A significant number of polar lows were detected over land areas of Greenland, Iceland and Svalbard. There was no apparent sensible heat source, which is a requirement for all existing polar low formation theories. It is possible that the detected circulation was very weak over land and only matured into a polar low when it encountered a moisture source.

C. POLAR LOW SYNOPTIC CONDITIONS

The overall synoptic conditions associated with polar low formation vary from month to month, but some common features are observed. Polar lows formed over Northern and Central Greenland form under 500 mb ridges, while storms south of 68 North form under cold 500 mb troughs. Polar lows tend to form in stronger than normal 1000 mb offshore height gradients with onshore flow. The overall onshore synoptic forcing advects relatively warm, moist air onto the pack-ice, establishing an over-ice baroclinic zone. The synoptic conditions for backtracked storms are similar to those for detected storms.

D. KATABATIC FLOW AS A TRIGGERING MECHANISM

There is only indirect evidence of katabatic flow as a polar low trigger mechanism. Both the detected and backtracked storms tended to form near glacial outflows through which the converging winds from the higher plateau converge. There were generally strong offshore height gradients, implying strong offshore pressure gradients which are necessary for katabatic flows. Overall flow was generally onshore, which advected moisture onto the pack-ice, establishing a boundary layer baroclinic zone. The presence of a strong offshore katabatic flow could distort the baroclinic zone (Fig. 10b) and initiate polar low formation as described by Bromwich (1991). There is usually a trough or low over the open water which acts as a low-level vorticity source. However, examining coastal wind observations for one month failed to relate katabatic winds to polar low formation.

E. RELATION TO CYCLOGENESIS THEORIES

Northern Greenland storms tend to form with ridging or divergence aloft, and a low-level offshore low or trough to provide cyclonic vorticity, conditions normally associated with Rasmussen's (1979) CISK theory. The generally onshore flow advects relatively warm, moist air over the short fetch of the ice-free Fram Strait. Southern Greenland storms tend to form with a trough aloft with a deep synoptic low in the Denmark Strait. Warm, moist advection onto the pack ice ahead of the low provides the large-scale low-level moisture source needed for Emanuel and Rotunno's (1989) ASI formation theory. The Central Greenland storms tend to form with elements of both processes. They tend to form under ridging aloft and with large-scale warm, moist advection, but with a fetch limited by the pack ice north of Iceland.

VII. RECOMMENDATIONS

A. POLAR LOW FORMATION FREQUENCY

Many storms were formed in the spring and fall transition seasons, implying that polar lows also occur during the summer months. A follow-on study should examine an entire year of satellite imagery to gauge the polar low formation frequency for the entire year.

B. POLAR LOW WIND SPEED

No attempt was made to assign wind speeds to the detected polar lows. A future project should attempt to assign wind speeds to the detected polar lows by examining regional surface synoptic, ship and buoy observations and compare those fitting the 15 m s minimum wind speed criteria with storms detected in earlier studies.

Polar lows form in remote areas and often dissipate before making landfall, or passing close to an observing station. A study could examine derived wind speeds from SSM I, Radar Altimeter, SAR and or Scatterometer.

C. DETECTION OF KATABATIC FLOW

Despite the indirect evidence, there was no firm link between katabatic flows and polar low formation. Following the example of studies in the Antarctic, a large-scale experiment could install a dense grid of automatic weather stations, with a satellite link to a base station, at the mouth of Greenland glacier valleys to detect katabatic flows and connect their existence to polar low formation.

D. REPEATABILITY

The number of polar lows detected in this study was far greater than previous studies. An attempt must be made to examine the satellite imagery from other years to determine if the numbers presented in this study are representative or anomalous.

APPENDIX CYCLOGENESIS MECHANISMS

Currently, three theories of polar low cyclogenesis are the cause of disagreement in the polar meteorology community. Baroclinic instability, Conditional Instability of the Second Kind (CISK) and Air-Sea Interaction (ASI) Instability may each contribute to polar low development, but the exact driving force may vary between the type of storm, location of formation, and time of year. Additionally, thermal and barotropic instability may each contribute to a lesser extent to polar low cyclogenesis. The exact cyclogenesis mechanism cannot be determined through satellite imagery or by surface and upper air observations. Thus far, aircraft observations have provided the most detailed, although infrequent, analyses of polar lows.

A. THERMAL INSTABILITY

Polar lows have been studied for decades by the Scandinavians and British. Formation was originally thought to be due to thermal instability, a form of small-scale convection. As cold air masses flow over warmer water (Harrold and Browning 1969), sensible heat flux warms the lower boundary layer. This reduces the stability of the existing low-level inversion, and initiates the convection and shower-type precipitation. Polar lows were thought to form through the merging of numerous convective cells into a single storm.

B. BAROCLINIC INSTABILITY

A baroclinic atmosphere exists where the geostrophic wind changes with height. This vertical wind shear is related to the horizontal temperature gradient through the thermal wind equation:

$$\vec{V}_T = \vec{V}_g(p_1) - \vec{V}_g(p_0) = - \frac{R}{f} \int_{p_0}^{p_1} (\vec{k} \times \nabla T) d \ln p. \quad (Eq. 2)$$

Strong horizontal temperature gradients lead to strong vertical wind shears which result in baroclinic instability (Holton 1979). Baroclinic instability exists where the potential energy of the basic state flow is converted to the kinetic energy of a developing perturbation. Not all potential energy is converted to kinetic energy. Only Available

Potential Energy (APE), or the difference between the total potential energy and the minimum potential energy that would result from an adiabatic redistribution of mass.

Harrold and Browning (1969), who first described polar lows in detail, examined a short-wave type storm with a pronounced comma shape (Fig. 26) crossing Britain and believed that the formation mechanism was large-scale, organized convection. They analyzed constant wet bulb potential temperature (θ_w) surfaces through dense rawinsonde observations and found a cold pool of air and strong low-level potential instability behind the polar low. Clouds formed and precipitation was observed where air flowed upward along constant θ_w surfaces. Vertical motions of 10-20 cm s were derived from Doppler radar, which closely corresponded to motion along the θ_w surfaces. The three-dimensional air flow pattern (Fig. 27) closely resembles the warm and cold conveyor belts and dry subsiding jet described by Carlson (1980) for synoptic systems.

Although small-scale convection was present along the trough axis, the major precipitation was due to slantwise convection, not to small-scale convective overturning as predicted by thermal instability theory. Furthermore, in the formation areas, a strong inversion at 800 mb prevented deep convection from being a formation source.

The observed temperature gradient was 10 C over 150 km. If the storm was in geostrophic balance, a temperature gradient of 10 C over 15 km would be required to account for winds derived from observations and conventional radar, which also argues against thermal instability as an energy source.

The presence of a baroclinic zone with a strong horizontal θ_w gradient in the low- and mid-troposphere was detected in the observed pool of cold air aloft (Fig. 26). Vertical wind shear exceeding 4 m/s over 250 meters was observed in the baroclinic zone, which indicated that low-level baroclinic instability was a cyclogenesis mechanism. The storm was steered by the average 850 mb wind, not the upper-level jet. Harrold and Browning also felt that upper-level baroclinity contributed to the development of more vigorous polar lows.

C. CONVECTIVE INSTABILITY OF THE SECOND KIND

Rasmussen (1979) viewed polar lows as thermal instability phenomena, as was originally believed. He acknowledged that baroclinic processes were important and could be the cyclogenesis mechanism for some polar lows, while CISK dominated in others. CISK theory states that an initial low-level cyclonic vorticity disturbance triggers low level convergence, which leads to convection and latent heat release and upper-level divergence. Subsidence at a distance from the initial disturbance leads to further low-level

convergence, which increases the vorticity of the initial disturbance and results in a positive feedback loop (Fig. 28).

In high latitudes, the atmospheric boundary layer is normally conditionally stable. A requirement for CISK development is high equivalent potential temperature (θ_e) in the boundary layer. This is due to higher humidities caused by large-scale evaporation or low-level moisture advection. During cold air outbreaks, sensible heat is transferred from the warm sea water into the cold air, destabilizing the boundary layer and enhancing convection.

The low-level vorticity source for the initial polar low triggering mechanism may be strong baroclinic instability above the SST gradients near the ice edge, which drives latent heat release by cumulus convection. Sensible heat transfer is also necessary to destabilize the lower layers, in contrast to the tropics where there is limited sensible heat transfer.

Rasmussen tested his theory with a quasi-geostrophic model and found that the advection of heat and moisture from the areas surrounding the storm were as important as direct latent and sensible heat transfer. This advection mechanism could be a synoptic-scale occlusion that enters the Norwegian Sea from the south and forces warm, moist air over the Marginal Ice Zone (MIZ). Upon landfall, storms quickly dissipate when the low-level heat and moisture sources are removed.

Rasmussen expected to find a weak high over the surface low to correspond to CISK theory, but often did not, possibly due to sparse upper air data. He theorized that a deep, cold pool of air aloft was responsible for the upper-level subsidence important for the CISK feedback loop.

D. AIR-SEA INTERACTION INSTABILITY

Emanuel and Rotunno (1989) believe that ASI instability rather than CISK is the dominant formation mechanism, but also admit that many forces may combine to form polar lows. They feel that polar lows form in baroclinic environments preceded by upper level precursors, while CISK only maintains nearly moist adiabatic lapse rates and does not store available potential energy. They find polar low formation to be a two-stage process. A triggering disturbance forms first and then it intensifies into a polar low.

Emanuel and Rotunno claim that some polar lows are arctic hurricanes with a warm θ_e core, a clear eye surrounded by deep convective clouds and rapid pressure changes near the center. Clear eyes have been observed in satellite imagery. Strong vertical entropy gradients from sensible heat flux resulting from the strong air-sea temperature

differences can support extreme pressure falls of up to 70 mb. Similar to Rasmussen, they conclude sensible heat flux is important to polar low formation, which is not true in tropical cyclones.

The driving source of ASI instability is warm moist air advected from surrounding areas toward the storm center (Fig. 29). The advected air then ascends in the convective eye wall where the parcels release latent heat through precipitation. The warm-air advection and latent heat release increases upward motion and cause an increase in wind speeds. Air at the top of the storm is carried away from the existing upper-level disturbance and descends back to the surface at a distance away from the storm. The parcels, which are now at higher wind speeds, are warmed again, re-acquire moisture at a faster rate and are returned to the polar low.

Using their axisymmetric, nonhydrostatic primitive equation model that eliminates barotropic and baroclinic instabilities, Emanuel and Rotunno found that a dynamic mechanism, such as a strong upper-level disturbance, is required to initiate ASI instability for polar low development. In the atmosphere, this could be the baroclinic instability that was not included in the model.

Emanuel and Rotunno observed that polar lows often form under upper-level, cold-core cut off lows. When modeled, this results in a very concentrated surface low. Cold air aloft does not inhibit polar low formation, but some energy may be diverted to enhance the upper-level cyclone rather than intensify the polar low at the surface.

E. BAROTROPIC INSTABILITY

Barotropic instability may also contribute to polar low development, but its forcing is not sufficient to cause the necessary rapid deepening. In the large scale, barotropically unstable cases have maximum height falls at jet stream levels while barotropically damped cases have maximum height falls near the surface (Businger and Reed 1989). A barotropic atmosphere is indicated by the absence of horizontal temperature or thickness gradients, so there is no change of the geostrophic wind with height.

Businger (1985) indicates that the atmospheric is nearly equivalent barotropic in the vicinity of mature polar lows. In an equivalent barotropic atmosphere, horizontal temperature gradients do exist, but thickness contours are parallel to height contours (Wallace and Hobbs 1977). If the geostrophic winds increase with height, warm highs and cold lows are formed. If the geostrophic winds decrease with height, cold highs and warm lows (Fig. 30) develop. Polar lows are generally of the second type, with warm cores and maximum winds at the surface which decrease with height.

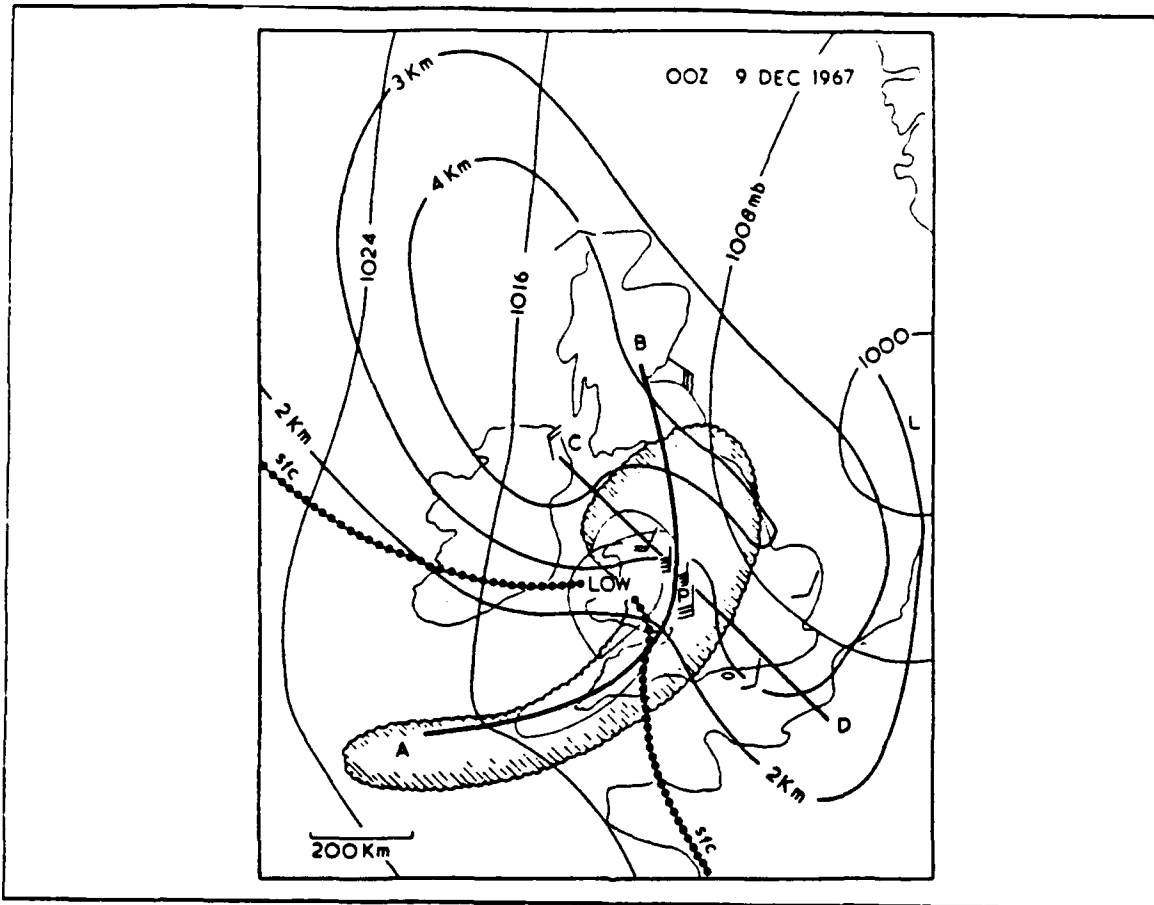


Figure 26. Topography of polar low potential wetbulb temperature surfaces in km (Harrold and Browning 1969).

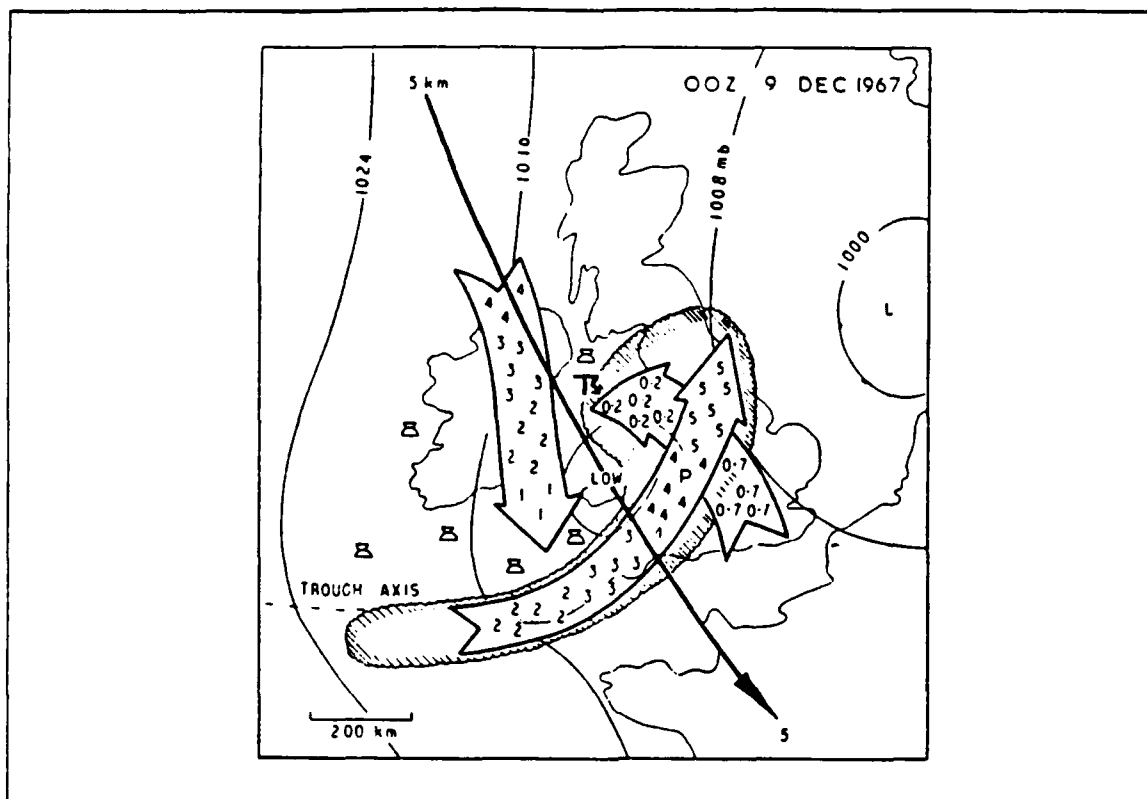


Figure 27. Flow relative to a polar low (numbers in arrows are in km) (Harrold and Browning 1969).

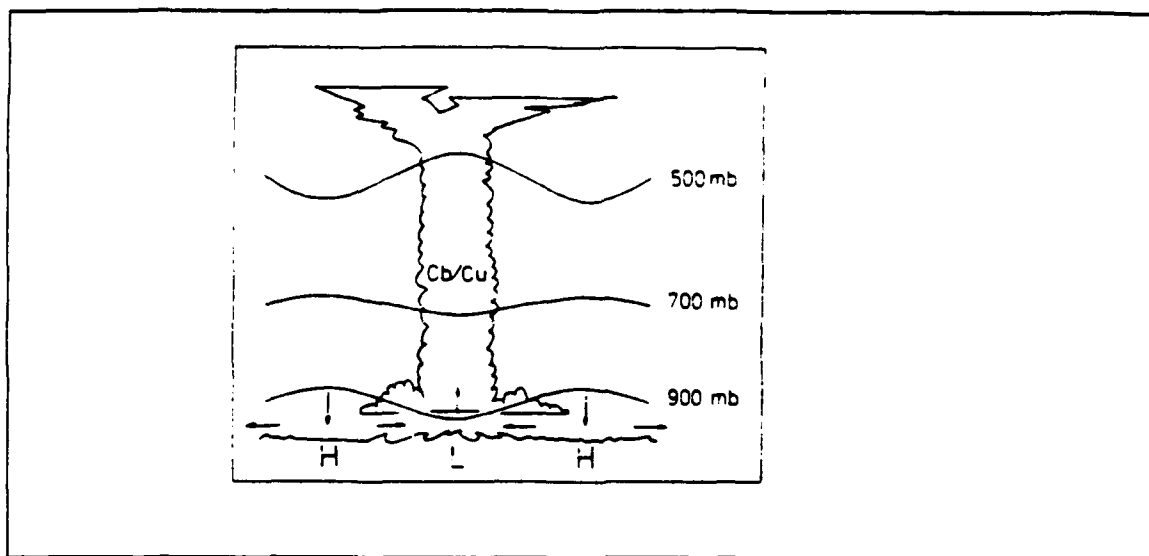


Figure 28. Vertical cross section of a CISK feedback loop (Rasmussen 1979).

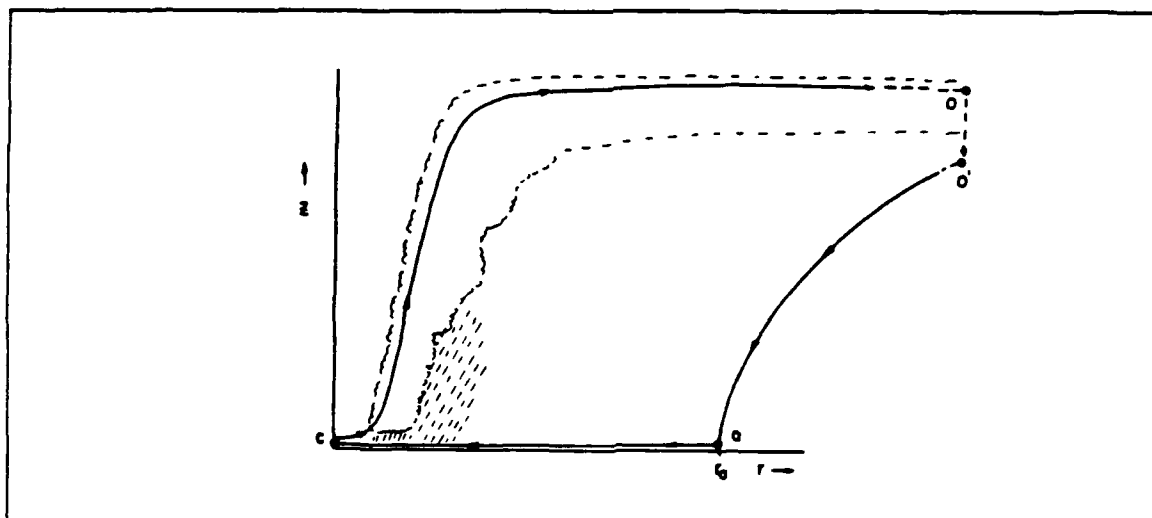


Figure 29. Integrated parcel path for ASI moisture advection (Emanuel and Rotunno 1989).

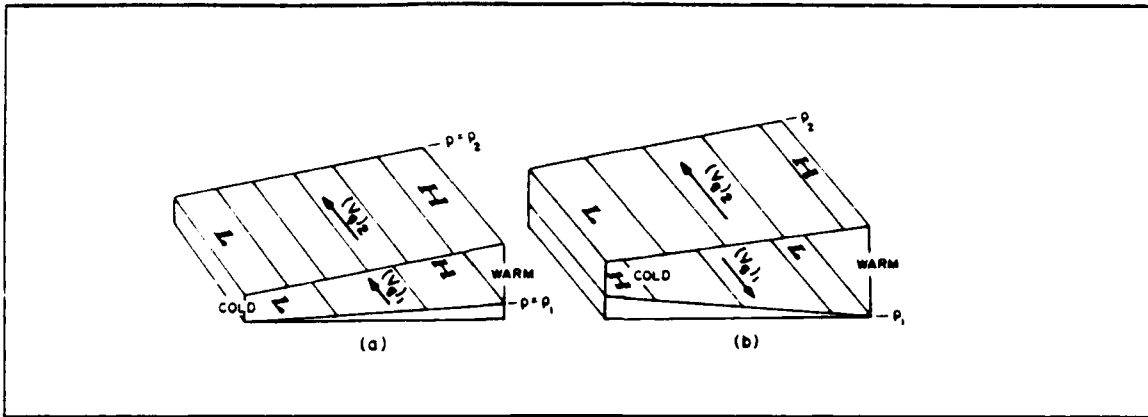


Figure 30. Equivalent barotropic atmosphere with geostrophic wind a) increasing and b) decreasing with height (Wallace and Hobbs 1977).

REFERENCES

- Atkinson, B. W., 1981: *Mesoscale Atmospheric Circulations*. Academic Press, New York, 495 pp.
- Bindschadler, R. A., et al, 1989: *Surface Topography of the Greenland Ice Sheet From Satellite Radar Topography*. NASA Special Report SP-503, 105 pp.
- Broeke, M. R. van den, et al, 1992: *Katabatic wind regime in the ablation zone of the Greenland Ice Sheet during the GIMEX-90 and 91 Expeditions: Influence of turbulent fluxes near the surface*. Third Conference on polar meteorology and oceanography, 29 Sep - 2 Oct, Portland, OR, J133-136.
- Bromwich, D. H., 1991: Mesoscale cyclogenesis over the southwest Ross Sea linked to strong katabatic winds. *Mon. Wea. Rev.*, 119, 1736-1752.
- Bromwich, D. H., J. F. Carrasco and Z. Liu, 1992b: *Katabatic surges across the Ross Ice Shelf, Antarctica: Atmospheric circulation changes and oceanographic impacts*. Third Conference on Polar Meteorology and Oceanography, 29 Sep - 2 Oct, Portland, OR, 29-32.
- Bromwich, D. H., Y. Du and T. R. Parish, 1992a: *Numerical simulation of katabatic winds crossing the Siple Coast area of West Antarctica*. Third conference on Polar Meteorology and Oceanography, 29 - 2 Oct. Portland, OR, 137-140.
- Bromwich, D. H. and S. N. Ganobcik, 1992: *Katabatic wind dynamics at Terra Nova Bay, Antarctica from the satellite image perspective*. Third Conference on Polar Meteorology and Oceanography, 29 Sep - 2 Oct, Portland, OR, 125-128.
- Bromwich, D. H., et al, 1992: Modeled variations of precipitation over the Greenland Ice Sheet. Submitted to *J. Climate*.
- Businger, S., 1985: The synoptic climatology of polar low outbreaks. *Tellus*, 37A, 419-432.
- _____, 1991: Arctic hurricanes. *Am. Scientist*, 79, 18-33.
- Businger, S., and R. J. Reed, 1989: Polar Lows. In *Polar and Arctic Lows*, P. F. Twitchell, E. A. Rasmussen and K. L. Davidson (Eds.), A Deepak Publishing, Hampton, VA, 3-46.
- Carleton, A. M., 1985: Satellite climatological aspects of the "polar low" and "instant occlusion". *Tellus*, 37A, 433-450.

Carleton, A. M. and D. A. Carpenter, 1989: Satellite climatology of "polar air" vortices in the southern hemisphere winter. In *Polar and Arctic Lows*, P. F. Twitchell, E. A. Rasmussen and K. L. Davidson (Eds.), A. Deepak Publishing, Hampton, VA, 401-414.

Carlson, T. N., 1980: Airflow through midlatitude cyclones and the comma cloud pattern. *Mon. Wea. Rev.*, 108, 1498-1509.

Carrasco, J. F., 1992: *A Mesoscale Cyclogenesis Study Adjacent to the Pacific Coast of Antarctica*. MS Thesis, Ohio State University, Columbus, OH, 187pp.

Carrasco, J. F., and D. H. Bromwich, 1992: Mesoscale cyclogenesis over the South West Ross Sea, Antarctica. Submitted to *J. Geos. Res.*

Claud, C., N. M. Mognard, K. B. Katsaros, A. Chedin and N. A. Scott, 1991: *Satellite observations of polar lows by SSM I, GEOSAT and TOVS*. Proceedings of IGARSS '91, Helsinki, 3-7 June, vol 4, 2081-2085.

Emanuel, K. A., and R. Rotunno, 1989: Polar lows as arctic hurricanes. *Tellus*, 41A, 1-17.

Ese, T., I. Kanestrom and K. Pederson, 1988: Climatology of polar lows over the Norwegian and Barents Seas. *Tellus*, 40A, 248-255.

Fett, R. W., 1989: Polar low development associated with boundary layer fronts in the Greenland, Norwegian and Barents Seas. In *Polar and Arctic Lows*, P. F. Twitchell, E. A. Rasmussen and K. L. Davidson (Eds.), A. Deepak Publishing, Hampton, VA, 313-322.

Fitch, M. and A. M. Carleton, 1991: Antarctic mesocyclone regimes from satellite and conventional data. *Tellus*, 44A, 180-196.

Fristrup, B., 1966: *The Greenland Icecap*. Univ. of Washington Press, Seattle, WA, 312 pp.

Harrold, T. W., and K. A. Browning, 1969: The polar low as a baroclinic disturbance. *Quart. J. Roy. Meteor. Soc.*, 95, 710-723.

Holton, J. R., 1979: *An Introduction to Dynamic Meteorology*, 2nd Ed., Academic Press, New York, 391pp.

Kanestrom, I., K. Pederson and T. Ese, 1988: Forecasting polar lows. *Zeitschrift fur Meteorologie*, 88, 337-341.

Lystad, M., 1986: *Polar lows in the Norwegian, Greenland and Barents Seas*. Final Rep., Polar Lows Project, The Norwegian Meteorological Institute, Oslo, 196pp.

Macklin, S. A., G. M. Lackmann and J. Gray, 1988: Offshore-directed winds in the vicinity of Prince William Sound. *Mon. Wea. Rev.*, 116, 1289-1301.

- Mahrt, L., 1982: Momentum balance of gravity flows. *J. Atm. Sci.*, 39, 2701-2711.
- Munzenberg, A., R. Engels and H.-D. Schilling, 1992: *Numerical studies on the formation of Antarctic mesoscale vortices in the Weddel Sea region*. Polar Low Workshop, Hvanneyri, Iceland, 23-26 June 1992, 21-28.
- Naval Polar Oceanography Center, Suitland, MD. *Eastern - Western Arctic Sea Ice Analysis*, 1988 - 89.
- Parish, T. R., P. Pettre, and G. Wendler, 1992: *On the interaction between the katabatic wind regime and large-scale tropospheric forcing near Adelie Land, Antarctica*. Third Conference on Polar Meteorology and Oceanography, 29 Sep - 2 Oct, Portland, OR, 141-144.
- Rasmussen, E. A., 1979: The polar low as an extratropical CISK disturbance. *Quart. J. Roy. Meteor. Soc.*, 105, 531-549.
- _____, 1985: *A Polar Low Development Over the Barents Sea*. Polar Low Project, Tech. Rep. No. 7, Norwegian Meteorological Institute, Oslo, Norway, 42pp.
- _____, 1989: A comparative study of tropical cyclones and polar lows. In *Polar and Arctic Lows*, P. F. Twitchell, E. A. Rasmussen and K. L. Davidson (Eds.), A. Deepak Publishing, Hampton, VA, 47-80.
- _____, 1991: Personal communication.
- _____, 1992: *On the definition and classification of polar lows*. Polar Low Workshop, Hvanneyri, Iceland 23-26 June 1992, 21-28.
- Reed, R. J., 1979: Cyclogenesis in polar airstreams. *Mon. Wea. Rev.*, 107, 38-52.
- Reed, R. J., 1988: Polar lows. In *the nature and prediction of extratropical weather systems, 7-11 September 1987*. Seminar Proceedings, vol 1, ECMWF, 213-236, 280 pp.
- Sardie, J. M., and T. T. Warner, 1985: A numerical study of the development mechanism of polar lows. *Tellus*, 37A, 460-477.
- Schwerdtfeger, W., 1984: *Weather and Climate of the Antarctic*. Elsevier Science Publishers B. V., Amsterdam, The Netherlands, 261pp.
- Shapiro, M. A., and L. S. Fedor, 1989: A case study of an ice-edge boundary layer front and polar low development over the Norwegian and Barents Sea. In *Polar and Arctic Lows*, P. F. Twitchell, E. A. Rasmussen and K. L. Davidson (Eds.), A. Deepak Publishing, Hampton, VA, 257-277.
- Shapiro, M. A., L. S. Fedor and T. Hampel, 1987: Research aircraft measurements over the Norwegian Sea. *Tellus*, 39A, 272-306
- Shuchman, R., 1992: Personal communication.

Streten, N. A., 1963: Some observations of Antarctic katabatic winds. *Aust. Met. Mag.*, 42, 1-23.

Turner, J., T. Lachlan-Cope and E. A. Rasmussen, 1991: Polar lows. *Weather*, 46, 107-114.

Wallace, J. M. and P. V. Hobbs, 1979: *Atmospheric Science: An Introductory Survey*. Academic Press, New York, 467pp.

Wilhelmsen, K., 1985: Climatological study of gale producing polar lows near Norway. *Tellus*, 37A, 451-459.

Yarnel, J. B and K. G. Henderson, 1989: A climatology of polar low cyclogenetic regions over the North Pacific Ocean. *J. Climate*, 2, 1476-1491.

INITIAL DISTRIBUTION LIST

	No. Copies
1. Defense Technical Information Center Cameron Station Alexandria, VA 22304-6145	2
2. Library, Code 52 Naval Postgraduate School Monterey, CA 93943-5002	2
3. Chairman (Code OC Co) Department of Oceanography Naval Postgraduate School Monterey, CA 93943-5000	1
4. Chairman (Code MR Hy) Department of Meteorology Naval Postgraduate School Monterey CA 93943-5000	1
5. Professor K. L. Davidson (Code MR Ds) Department of Meteorology Naval Postgraduate School Monterey, CA 93943-5000	2
6. LCDR Kenneth A. Wos COMUSNAVCENT Attn: Oceanographer FPO AE 09501-6008	1
7. Dr. Peter Guest Department of Meteorology Naval Postgraduate School Monterey, CA 93943-5000	1
8. Dr. S. Burk Naval Research Laboratory NPS Annex, Code 7500 Monterey, CA 93943-5006	1
9. Office of Naval Research Attn: Dr. T. Curtin, Code 1125 800 N. Quincy Street Arlington, VA 22217	1

10. Dr. James E. Overland 1
7600 Sand Point Way NE
Building 3
Seattle, WA 98115
11. Commanding Officer 1
Naval Oceanography Command Facility
Box 26
FPO NY 09571-0926
12. Prof. E. A. Rasmussen 1
Department of Meteorology
Geophysical Institute
University of Copenhagen
Haraldsgade 6, DK-2200, Denmark